

2018



**25th Congress of
International Federation for
Heat Treatment and Surface Engineering**

11-14 September 2018 | Xi'an China

PROCEEDINGS



Organized by Chinese Heat Treatment Society (CHTS)

25th IFHTSE CONGRESS PROCEEDINGS

11-14 September 2018

Xi'an China



Chinese Heat Treatment Society

Tel: +86 (0) 10 6292 0613 • Email: chts@chts.org.cn • Web: www.chts.org.cn

Add: 18 Xueqing Rd., Beijing, China

on AZ31 magnesium alloy and its mechanism.....	364
Effect of electrolyte composition on protective properties of PEO coating on zirconium alloy Zr-1Nb.....	365
Effects of phosphate on structure and thermal shock resistance of PEO ceramic coatings on Ti6Al4V alloy.....	366
Lotus leaf clusters-like organic-free super-hydrophobic Al ₂ O ₃ coating prepared by one-step plasma electrolytic oxidation.....	367
Thermophysical features of anode heating.....	368
First-principles calculations and narrow band gap energy of WO ₃ /TiO ₂ composite films on titanium prepared by microarc oxidation.....	369
Degradation mechanisms of micro-arc oxidation composite coatings on biomedical Mg-(Li)-Ca alloys for orthopaedic implants.....	370
Promising orthopedic implant material with enhanced osteogenic and antibacterial activity: Al ₂ O ₃ -coated aluminum alloy.....	371
Formation and properties of Ca-doped barium titanate based coatings produced by plasma electrolytic oxidation.....	371
Investigation on electrochemical behavior of TA2 alloy treated by micro-arc oxidation.....	372
Corrosion behavior of plasma electrolytic oxidation coatings on Mg alloy produced in an electrolyte containing SiO ₂ particles.....	372
Thermal damage of magnesium alloys ceramic coating by micro arc oxidation surface treatment.....	373
Effect of electrolyte system on the structure and corrosion resistance of plasma electrolyte oxidation (PEO) coating on 1060 aluminum alloy.....	373
The cavitation stripping mechanism of micro-arc oxidation system and the follow-up finishing design of 3D titanium alloy parts.....	374
Influence of circular workpieces configurations on temperature field of vacuum heating process.....	374
A novel energy management method for micro-arc oxidation.....	375
Anti-corrosive microarc oxidation film modified with layered double hydroxide on 6061 Al alloy.....	375
Quasi two-dimensional CePO ₄ and its self-lubrication in Al ₂ O ₃ coatings prepared by one-step plasma electrolytic oxidation.....	376
Plasma electrolytic polishing of steel after diffusion saturation.....	376

Functional Surfaces and Coatings

Nanocomposite WS ₂ /a-C coatings: self-adaptive and self healing triboactivity.....	377
Stable electrochromic polyamide films containing flexible chains: preparation, electrochemical, fluorescence and memory properties.....	378
Corrosion and wear properties of biomedical Ti-Zr-based alloys.....	380
Nano-structured silica as non-chromate anti-corrosion film for metal protection.....	382
In-situ grown MgO-ZnO ceramic coating with high thermal emittance on Mg alloy	

by plasma electrolytic oxidation.....	383
Corrosion resistance of DLC films-coated titanium and stainless steel prepared by ion beam enhanced deposition.....	384
One step electrodeposition of $\text{Cu}_2\text{ZnSnS}_4$ thin film for solar cells and their properties.....	385
Ion beam surface modification of alloys and ceramics using accelerators.....	386
TiAlN/MoN superhard and self-lubrication.....	387
The change of magnetism triggered by external bias voltage in $\text{CoFe}_2\text{O}_4/\text{PMN-PT}$ multiferroic heterostructures.....	388
Intrinsic and Ti, Sr doped MoS_2 thin films design and performance study.....	390
Multilayered thermal barrier coatings.....	391
Effect of heat treatment on bonding strength of nanostructured 8YSZ thermal barrier coatings deposited onto NiCrAlY(Ce) bond coat.....	391
Surface modification of biomedical titanium using plasma immersion ion implantation.....	392
The tribological properties of graphene modified $n\text{-Al}_2\text{O}_3/\text{TiO}_2$ coatings.....	392
Enhancing magnetron sputtered protective coatings via hierarchical structuring.....	393
Chemical vapor deposition growth of large-area ReS_2 monolayer films for optoelectronic applications.....	393
Morphological and microstructural characterization of nanostructured $\text{Al}_2\text{O}_3/\text{ZrO}_2$ eutectic layer induced by laser beam irradiation.....	394
Material-genome perspective towards robust T/EBC materials.....	394
Elevate the photoelectrochemical anticorrosion effect of corrosion product layers on electrogalvanized steel in simulated seawater through nanoelectrodeposition.....	395
$\text{La}_2\text{O}_3\text{-ZrO}_2\text{-CeO}_2$ thermal barrier coatings by EB-PVD: feathery nanostructure, thermal conductivity and thermal cycling life.....	395
Fabrication and characteration of layered double hydroxide films by conversion of MAO coatings on magnesium alloys.....	396
Effect of sputtering power on microstructure and photoelectrical properties of Al-doped ZnO films deposited by RF magnetron sputtering.....	396
High-rate deposition of structure controllable Al/Cu films by highpower density magnetron sputtering.....	397
Effect of diffusion characteristics of Pt in $\beta\text{-NiAl}/\gamma'\text{-Ni}_3\text{Al}$ within NiCoCrAl alloy on alumina growth behaviour.....	397
Surface and interface engineering of hybrid perovskite films for perovskite solar cells with highly improved efficiency and stability.....	398
The effect of micro-textured surface on tribological properties of nanostructured $\text{ZrO}_2(\text{Y}_2\text{O}_3)\text{-Al}_2\text{O}_3$ ceramics under dry sliding against Al_2O_3 and 304L steel.....	398
Prediction of the critical rupture and failure modes of the plasmasprayed yttria stabilized zirconia thermal barrier coatings under the burner rig test via acoustic emission technique.....	399
Enhancing the tribological and mechanical properties of epoxy coatings by graphene	

nanoparticle encapsulation.....	399
Preparation and toughening of a-CuZrc-ZrN nano-multilayer hard coating.....	400
The mechanical integrity of a MAO/PLGA composite coated magnesium alloy for biodegradable material.....	400
Surface engineering design of ceramics to improve tribological properties.....	401
Microstructure and high temperature oxidation resistance property of packing Al cementation on TA15 alloy.....	401
The effect of ladder region on the atom adsorption of Si (111) substrate.....	402
Effect of temperature on hot-dip galvanized Zn-0.05%Al coating with the application of the ammonium-free fluxing process.....	402
Preparation of surface TaC layer reinforced Ta-10W alloy by in situ solid-phase.....	403
Alumina growth behavior on surface-modified NiCoCrAl alloy by Pt and Hf at high temperature.....	403
Microstructure and corrosion behavior of different cladding regions of multi-track laser cladding Ni-based alloy coating.....	404
Effects of MTMS water content on morphology and corrosion resistance of non-chromium Zn-Al coatings.....	404
Comparative study on corrosion behavior of Mg-Zn-Ca metallic glass in deionized water, simulated seawater and simulated body fluids.....	405
Effect of N ₂ flow rate and annealing holding time on microstructure and properties of Ti ₂ AlN thin films.....	406
The study on preparation and antioxidant properties of FeCrAlY coatings by magnetron sputtering.....	407
Effect of different phase structures caused by Mo content on corrosion behavior of Al-Mo alloy thin films.....	408
Corrosion behavior of plasma electrolytic oxidation coated AZ31 and AZ91 Mg alloys: the influence of laser surface melting pretreatment.....	409
The preparation and characterization of different crystal of PbO ₂ in methylsulfonic acid.....	410
Effect of carbon-foam composite coating electrode on the power storage performance of lead-acid flow battery.....	411
Effect of plating flow rate on microstructure and properties of jet-electrodeposited Co-Ni alloy coating.....	412
Wear behavior of ceramic coatings formed by microarc oxidation on 7N01 aluminium alloy.....	414
Seed-mediated growth of the conductive yet transparent anatase Nb-TiO ₂ films.....	415
Increasing recoverable energy storage in PZT films using low dielectric constant layer.....	416
Preparation of nanocrystalline coating on Ti alloy by cathodic plasma electrolytic deposition and its catalytic activity toward oxygen evolution reaction.....	418
Spontaneous escape behavior of silver from carbon and titanium nitride coating and its inhibition mechanism.....	420

Photocatalytic water decomposition for hydrogen production on TiO ₂ loaded on foam nickel.....	421
Rapid preparation of alumina thin films by high-power density reaction magnetron sputtering.....	422
Effects of anodization-assisted electrodeposition conditions on the fabrication of Cu coatings on nanoporous stainless steel.....	424
Fabrication and characterization of dense Cr ₂ O ₃ -Al ₂ O ₃ double coatings by electrochemical technique.....	425
Wear resistance of Al ₂ O ₃ /WC-Co/epoxy coatings on TC18(Ti-5Al-5Mo-5V-1Cr-1Fe) alloy.....	426
A combined experimental and first-principle study on the oxidation behavior of plasma surface Ta-W alloyed γ -TiAl.....	426
Erosion behaviour of laser clad FeCoCrNiTi high-entropy alloy coating at elevated temperature.....	427
Influence of current density at glow-arc discharge transitional section on microstructure and properties of TiN films.....	427
The structure and properties of TiN films deposited using dc, modulated pulse power magnetron sputtering and arc ion plating.....	428
Effect of target power density on tribological properties of graphite-like carbon films deposited by pulsed dc magnetron sputtering.....	428
The effect of N ion implantation on the properties of W18Cr4V based TiAlN/Al ₂ O ₃ coatings.....	429
Corrosion properties of steel sheet with zinc-base alloyed coatings.....	429
Influence of different nanoparticles for the wear resistance on the surface of anodized AZ31.....	430
Friction and wear characteristics of TiN coatings in ethanol.....	430
Study on corrosion resistance of a DLC film coated titanium and stainless steel by magnetron sputtering.....	431
Effects of additives on the corrosion resistance of chromium-free zinc-aluminum coatings.....	431
Fabrication and characterization of HVOF sprayed NiCoCrAlYCe coatings on K417G nickel-based superalloy.....	432
Preparation and characterization of tetrahedral amorphous carbon thin films with high strength and high toughness on YG6 cemented carbide.....	432
Melt expulsion and ablation effects of the laser nanocrystallization on the surface of Al ₂ O ₃ /ZrO ₂ eutectic ceramic.....	433
The corrosion resistance of hot dip galvanized steel pretreated with silanes modified with nano silicon carbide.....	433
Hydrogen permeation resistance property and characterization of zircon coatings on the surface of zirconium hydride alloy.....	434
Research on the correlation between corrosion properties and electron work function of the Al ₂ O ₃ /TiO ₂ coatings modified by nano graphite.....	434
Solidification and epitaxial growth of nanostructured Al ₂ O ₃ /ZrO ₂ eutectic surface layers formed by high energy laser or oxyacetylene flame.....	435
Effects of vacuum heat treatment on composition, microstructure and thermal cycling life	

of thermal barrier coatings by EB-PVD.....	435
Effect of graphene on the properties of plasma electrolytic oxidation coating on the biodegradable ZK60 magnesium alloy.....	436
Effect of W coating on the microstructure and corrosion properties of NiTi alloys deposited by SLM.....	436
Surface modification of tools by application of tungsten compounds coatings in high-frequency discharge.....	437
Current advances in solid lubricant coatings.....	437
Microstructure and tribological properties of low-pressure plasmasprayed Mo-Cu-WC coatings at elevated temperatures.....	438
Effect of different working layer on wear and cutting performance of AlCrSiN coatings.....	438
Fabrication and high temperature properties of plasma-sprayed nanostructured yttria stabilized zirconia thermal barrier coatings.....	439
Improved adhesion of TiAlSiN nanocomposite coatings on cemented carbide substrate by pre-implantation.....	439
Influence of Al ₂ O ₃ addition in NaAlO ₂ electrolyte on microstructure and high-temperature properties of plasma electrolytic oxidation ceramic coatings formed on Ti ₂ AlNb alloy.....	440
Influence of thermo-hydrogen treatment on microstructure and superplastic properties of Ti6Al4V alloy.....	440
Microstructure evolution and impedance analysis of 7YSZ thermal barrier coating during gas thermal-shock.....	441
Plasma etching pretreatment effect on adhesion of carbon-based film.....	441
Stable electrochromic polyamide films containing flexible chains: preparation, electrochemical, fluorescence and memory properties.....	442
Controllable electrodeposition and mechanism research of nanostructured Bi ₂ Te ₃ thin films with high thermoelectric properties.....	442

Thermal Spray

Fabrication of Al matrix composites via cold spraying-process, structure and properties.....	443
Robust corrosion protection of magnesium alloys via in-situ microforging assisted cold spray.....	444
Evolution of anisotropy of cold-sprayed Cu during post-spray heat treatment.....	445
Influence of impinging angle, particle shape and tamping on splats deformation and interface bond of cold sprayed Ti particles.....	446
Comparative investigation on the electrical properties of plasma sprayed TiO ₂ and TiO ₂ -Al ₂ O ₃ coatings.....	447
Effect of heat-treated on the microstructure of micro-plasma sprayed hydroxyapatite coatings.....	448
Fabrication and characteristics of heating coatings by atmospheric plasma spraying.....	449
Microstructures, phase compositions and properties of warm sprayed HATi composite coatings.....	450
Thickness measurement and interface morphology characterization of thermal barrier coatings	

Nanocomposite WS₂/a-C coatings: self-adaptive and self-healing triboactivity

Y. T. Pei

(Department of Advanced Production Engineering, Engineering and Technology Institute Groningen,
Faculty of Science and Engineering, University of Groningen, 9747 AG Groningen, The Netherlands)

y.pei@rug.nl

Abstract: Layered transition metal dichalcogenides (TMD) such as WS₂ are materials well-known for their solid lubrication properties in vacuum^[1]. However, their lubricating property degrades through oxidation in moisture. In addition the material is limited by its low hardness and low load-bearing capacity particularly in high temperature applications. WS₂/a-C nanocomposite coatings, namely WS₂ lamellae embedded in amorphous diamond-like carbon (DLC) matrix, are reported having excellent tribological characteristics with both low coefficient of friction (CoF) and low wear rate and also imparting environmental robustness^[2-4]. WS₂/DLC nanocomposite coatings are produced by magnetron co-sputtering WS₂ and graphite targets. Surface chemistry, structure and mechanical properties of these coatings reversibly change with applied load and environment, providing the best wear protection and self-healing capability. The coating microstructure and self-adaptive and self-healing triboactivity are scrutinized by microscopy (SEM, FIB and EF/HR-TEM), spectroscopy (GIXRD, micro-Raman and XPS) and pin-on-disc tribotests (varied in dry air to humid air, room temperature to 500 °C). Experimental observations show that the CoF falls to 0.02 in dry air and reaches 0.10 in humid environment, and reverses as testing atmosphere cycled from dry to humid air, while the CoF can even remain at 0.02 with temperature rising from 100 to 500 °C. The excellent tribological properties are attributed to the formation of a thin WS₂ film on the top of the wear track of the coating and on the counterpart surface, which yields self-healing mechanism on damage. WS₂/a-C coatings exhibit favorable self-adaptation and self-healing over a wide range of humidities and temperatures, and thus potentials for tribo-applications in diverse environmental and loading conditions.

Keywords: WS₂, self-adaptation, self-healing, tribology, magnetron sputtering, coating

Reference:

- [1] S. Prasad, J. Zabinski. Super slippery solids, *Nature* 387, 761-763(1997).
- [2] A.A. Voevodin, J.S. Zabinski, *Thin Solid Films* 370, 223-231(2000).
- [3] T. Polcar, M. Evaristo, R. Colaço, C. Silviu Sandu, A. Cavaleiro, *Acta Materialia* 56 (2008) 5101.
- [4] H.T. Cao, J.Th.M De Hosson, Y.T. Pei, *Surf. Coat. Technol.* 332 (2017) 142-152.

Stable electrochromic polyamide films containing flexible chains: preparation, electrochemical, fluorescence and memory properties

Rongrong Zheng¹, Xu Zhang¹, Zhipeng Zhang¹, Haijun Niu¹, Cheng Wang¹, Wen Wang²

(1. Key Laboratory of Functional Inorganic Material Chemistry, Ministry of Education, Department of Macromolecular Science and Engineering, School of Chemical, Chemical Engineering and Materials, Heilongjiang University, Harbin, China;

2. School of Materials Science and Engineering, Harbin Institute of Technology, Harbin, China)
haijunniu@hotmail.com, wangc_93@163.com

Abstract: Electrochromic materials, which can be used in displays, optical switching devices, antiglare rear-view mirrors, smart windows for car or buildings, data storage, electronic papers and adaptive camouflage has been focused on at present. Conjugated polymers are the most studied materials, but they always have color in neutral state. Except conjugated polymers, wholly aromatic polyamides are characterized as highly thermally stable polymers with a favorable balance of physical and chemical properties, which can be used as excellent electrochromic materials. However, rigidity of the backbone and strong hydrogen bonding results in high melting or glass-transition temperatures (T_{gs}) and limited solubility in most organic solvents.

The main method to enhance the solubility of PAs is to introduce the flexible side chains or insert bulky groups into the main chain.

So, a series of electroactive polyamides (PAs) containing alkyl chains and triarylamine unit serving as functional group were synthesized via polymer condensation reaction of N1-(2-Amino-ethyl)-N1-(4-carbazol-9-yl-phenyl)-ethane-1,2-diamine, with various cyclohexane binary acids.

The structures of monomers and polymers were confirmed by fourier transform infrared (FT-IR), the nuclear magnetic resonance (NMR) techniques, and mass spectrometry (GC-MS). All polymers are readily soluble in polar organic solvents and the thermal properties of the polymers were investigated by thermogravimetric analysis (TGA) indicating high thermal stability which could be solution cast into tough and flexible films in solvent of dimethyl formamide (DMF), dimethylsulfoxide (DMSO), tetrahydrofuran (THF), N-methyl-2-pyrrolidinone (NMP) or N, N-dimethylacetamide (DMAc). Thus they were coated film on ITO glass. The PAs show high thermal stability with decomposition temperatures in excess of 300 °C. Cyclic voltammograms of the PAs exhibited well defined and reversible redox couples at 0.80 and 1.54 V. Electrochromic characteristics of the PAs films revealed excellent stability together with multielectrochromic behaviors, which changed from the almost colorless neutral form to dark green oxidized forms at applied potentials. And the optical and electrochemical properties of PAs were investigated by using ultraviolet visible (UV-vis) absorption spectroscopy, photoluminescence (PL) spectroscopy, transient photocurrent responses and cyclic voltammetry (CV).

The main absorption peak of PAs appeared at $\lambda_{max}=345$ nm in the NMP and exhibited strong photoluminescence. The simulation results of the highest occupied molecular orbital (HOMO), lowest unoccupied molecular orbital (LUMO) and energy band gap are -5.21 – -4.73 , -2.16 – -0.96 and 2.86 – 4.25 eV, respectively. PAs also showed memory property. A non-volatile rewritable flash memory device based on the active layer of PAs was fabricated with the sandwich structure ITO/PAs (102 nm)/Al. The memory device exhibited good electrical bistable resistive switching behavior, with low threshold voltage (VSET about -1.6 V and VRESET about 4.2 V), high ON/OFF current ratio in excess of 10^3 . The optical transmittance change ($D_{%T}$) at 1110 nm between the neutral state and the fully oxidized state is up to 90%. Hence, in this study we want to share our experiences of the polymerization of PAs with alkyl chains and triarylamine unit and effects of this donor unit on the electrochemical and optical properties in detail, for the first time.

Keywords: electrochromic, electrochemical, memory property, fluorescence, alkyl chains, triphenylamine

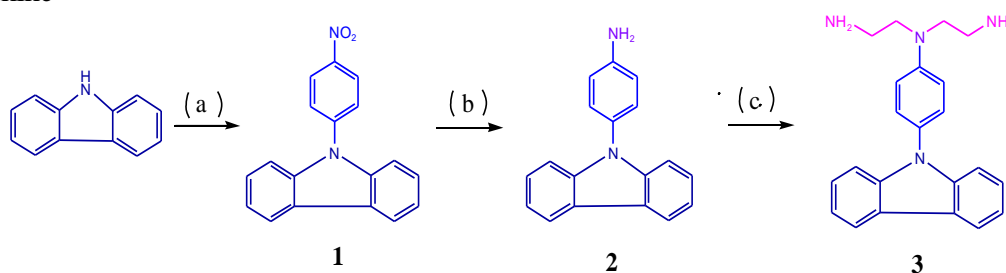


Fig.1 Synthetic routes to the target diamine compound 3

(a) p-fluoronitrobenzene, K_2CO_3 , DMF, 120 °C, 24 h; (b) hydrazine, 10wt% Pd/C, EtOH, 80 °C, 48 h; (c) bromoethylaminehydrobromide, methyl alcohol, 70 °C, 24 h

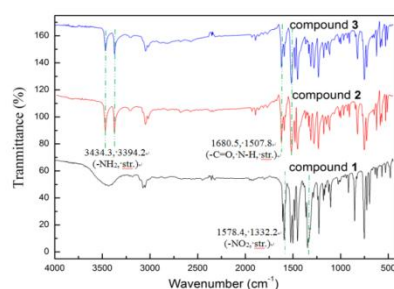


Fig.2 IR spectrum (a) spectrum (b) of monomers in DMSO-d6

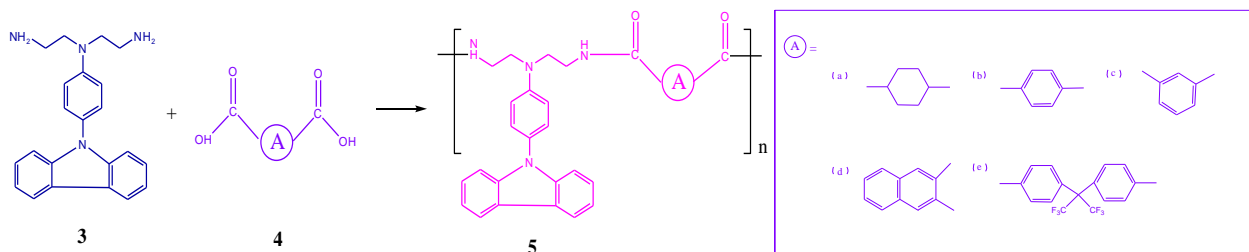


Fig.3 Synthetic route to the target PAs (5a-5e)

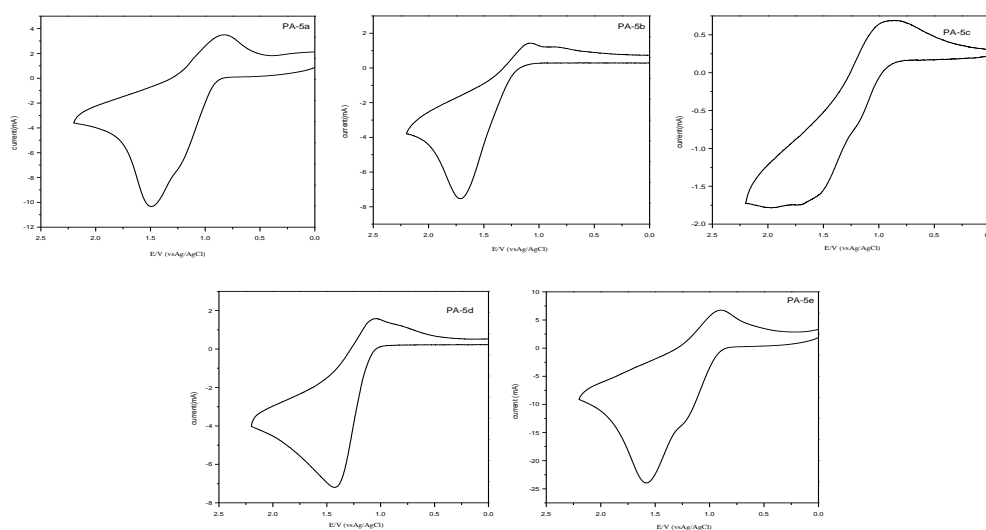


Fig.4 CV curves for PAs in CH_3CN containing 0.1 mol/L NH_4ClO_4 , at the scan rate of 50 mV/s

Corrosion and wear properties of biomedical Ti-Zr-based alloys

Jiaojiao Zhang¹, Hefeng Wang¹, Shangyu Yang¹, Xuegang Xing¹, Xuefeng Shu², Xiaomin Jin¹

(1. College of Mechanics, Taiyuan University of Technology, Taiyuan 030024, China;

2. Institute of Applied Mechanics and Biomedical Engineering, Taiyuan University of Technology, Taiyuan 030024, China)

wanghefeng@tyut.edu.cn

Abstract: Titanium (Ti) and titanium alloys have played important role in aerospace, chemical and biomedical industries owing to high corrosion resistance, perfect mechanical properties and excellent thermal stability, known as “space metals” and “marine metals”. In particular, Ti alloys are considered as one of the main alloys for biomedical applications due to its high corrosion resistance and biocompatibility. Zirconium (Zr) is generally known as a good biocompatible ideal element. Moreover, Zr and Ti belong to the same group, numerous properties of Zr are similar to those of Ti, such as high mechanical properties, low density, excellent corrosion resistance and biocompatibility. More important, Zr is non-toxic element and Zr helps to improve blood compatibility. Thus, it is constantly added for improving mechanical and corrosion properties. Hence, Ti-Zr alloy have obtained extensive attention. In the human body, the corrosion and wear resistance of alloy play a vital role as implant material. It has been proven that the released ions resulting from the corrosion and debris particles resulting from the wear of alloy can affect health. Therefore, the wear and corrosion properties of Ti-Zr alloy are well worth investigating. Assessment of Zr content in improving or reducing the effect of Ti-Zr alloy in biological engineering is conducted according to the Zr content. Meanwhile, the corrosion and friction properties of commercially pure titanium (cp Ti) have been explored in the same environment. Scanning electron microscope (SEM, TESCAN-MIRA 3) with energy dispersive spectrometer (EDS) was used to analyze the surface morphologies and microstructures. The phase compositions of the samples were detected by using X-ray diffraction (XRD) instrument (DX-2700) with 0.154 nm Cu K α radiation. Electrochemical tests were investigated with a conventional three-electrode configuration, which has a sample working electrode, a saturated calomel reference electrode and a platinum counter electrode. The specimens were packed with 704 silicon rubber, leaving 1 cm² immersed in the Hank's solution. Electrochemical experiment, including potentiodynamic polarization and electrochemical impedance spectrum (EIS) test, was tested by using an electrochemical workstation (CHI600E) at 37 °C in the Hank's solution. When open circuit potential of the samples reached their stable state, EIS curves were experimented at amplitude of 10 mV and a frequency range from 0.01 Hz to 100 kHz. Then the polarization behaviors were experimented at a scan rate of 0.001 V/s and potential range from -1 V to +1 V. The wear tests were measured on WTM-2E wear test machine. The ball was Si₃N₄ ball with a diameter of 5 mm and the sliding speed was 120 r/min. In all ball-on-disc tests, the sliding distance was fixed at 120 m and the specimens were carried out by applying load of 2 N. The tribological experiments were conducted in Hank's solution. The wear volumes of the specimens were measured by using an optical interferometer (WIVS). The electrochemical tests results show that Ti-2Zr alloy exhibits highest corrosion potential and lowest corrosion current density in comparison with other alloys. The corrosion resistance of the four materials changes in the following order: Ti-2Zr>Ti-1Zr>Ti-16Zr>cp Ti. The result have been obtained by the wear test shows wear mechanism of Ti-Zr alloy is abrasive, delamination, oxidation and adhesion wear and cp Ti is adhesion, abrasive and oxidation wear. In addition, the wear volume losses of Ti-Zr alloy decreases with the increasing contend of Zr. However, the wear volume loss of cp Ti is similar to Ti-16Zr alloy.

Keywords: corrosion, wear, Ti-Zr-based alloys

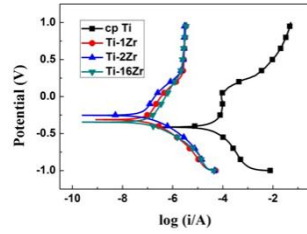


Fig.1

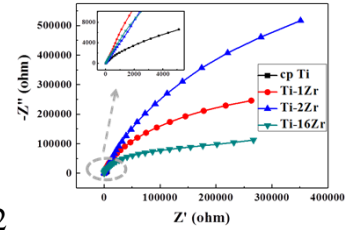


Fig.2

Fig.1 Polarization curves of the specimens in Hank's solution

Fig.2 Nyquist plots of the specimens

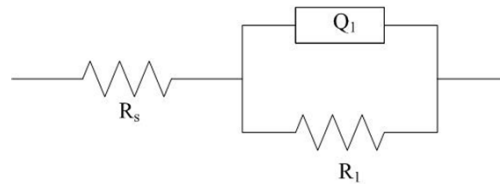


Fig.3 Equivalent circuit model of impedance spectra

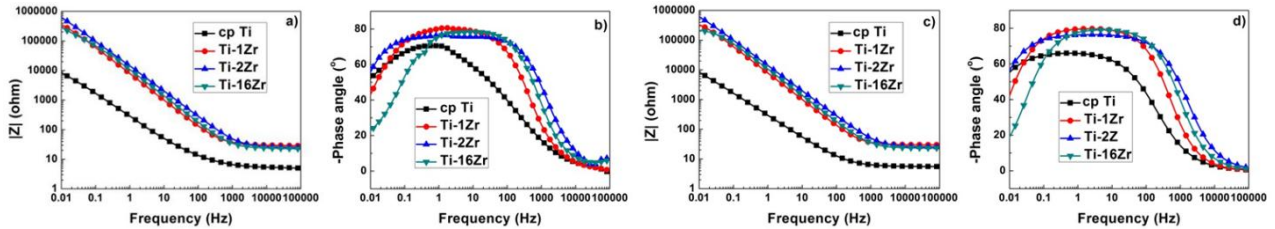


Fig.4 Bode plots of the samples in Hank's solution: (a, b) the original values, (c, d) the fitted values

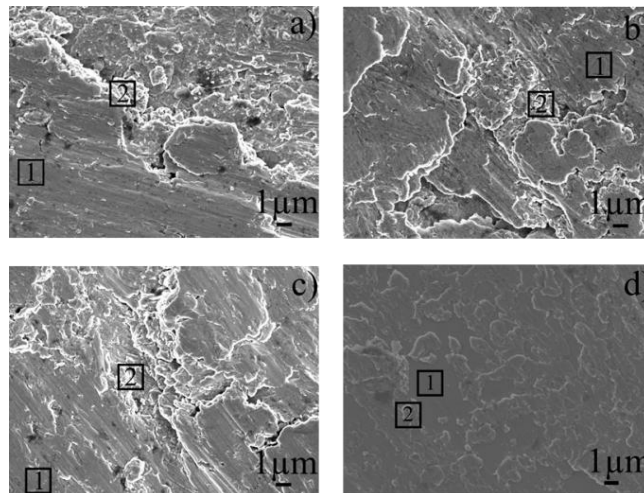


Fig.5 SEM images of the wear tracks of all samples after the wear test in the Hank's solution: (a) Ti-1Zr; (b) Ti-2Zr; (c) Ti-16Zr; (d) cp Ti

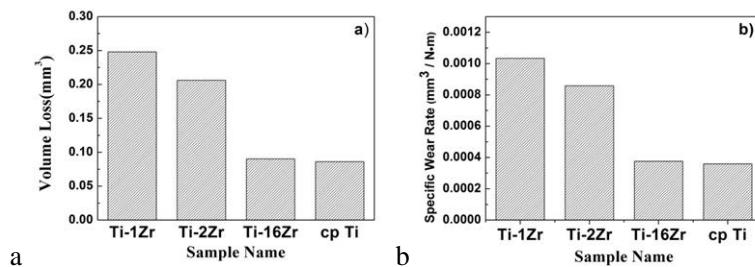


Fig.6 Variations of (a) volume loss and (b) specific wear rate of samples after the wear test in the Hank's solution

Nano-structured silica as non-chromate anti-corrosion film for metal protection

Shang-Tien Tsai¹, WenChyuan ChangJean¹, Pei-Hsiun Chao¹, Tseng-Chang Tsai²
(1. Hawing GemS Technology Corporation; 2. National University of Kaohsiung)
tctsai@nuk.edu.tw

Abstract: Different strategies were devised for the preparation of silica anti-corrosion coating. Nanostructured silica film was proven having strong protection capability from corrosion in NaCl, H₂SO₄ and NaOH solution for metal substrate. While amorphous silica coating could form a barrier shielding the penetration of aggressive species, the ordered mesoporous silica (MS) and crystalline zeolite films showed strongly enhanced anti-corrosion capability. In general, the anti-corrosion capability of nano-structured silica film depends mainly on film resistance, which is governed by film density and thickness as well as hydrophobicity. Dry-gel conversion (DGC) method was developed for the growth of silica coating on metal surface. MS film grown on aluminium alloy AA6061 was converted by hydrothermal process from the solid gel consisting of tetra-orthosilicate and cetyltrimethylammonium bromide (CTAB). The as-synthesized MS film containing CTAB showed strong corrosion protection property for AA6061 in NaCl solution. The strong corrosion protection property of the MS film is attributed to its blocked porous structure and hydrophobic nature. On the other hand, the encapsulated CTAB in MS film could be removed to open up high mesoporous pore volume which could be used as nano-vessel for replenishing corrosion inhibitor. The corrosion protection capability of the CTAB-replenished MS film is stronger than the benzotriazole (the most applied corrosion inhibitor)-replenished one. As such, the corrosion protection capability of the as-synthesized MS film is repairable due to loss of CTAB over long term service by replenishing CTAB to extend its service life.

In the preparation of zeolite MFI coating, in-situ crystallization (InC) or DGC protocols were developed. Zeolitic micro-pores could be blocked by the structure directing agent, tetrapropyl-ammonium bromide, during zeolite crystallization; the inter-crystalline voidage could be minimized by reduction of crystal size and formation of structure packing. While the InC protocol generated loosely packed film (MFI-InC) made of large zeolite crystal, the DGC protocol prepared dense film (MFI-DGC) comprising of nano particles. Superior protection ability of DGC-grown film is attributed to the increased film resistance associated with a dense and impermeable zeolite layer. As such, the DGC-grown film with thinner film thickness performed stronger anti-corrosion function than the InC-grown film. Furthermore, a very thin structured film exhibited satisfactory protection for AA6061 substrate during salt spray test over 1000 h. The MFI film also exhibited strong protection capability against the corrosion of H₂SO₄ and NaOH solution. The nano-structured silica could reduce the corrosion current of bare AA6061 substrate by five orders of magnitude, ranking in the order of MFI-DGC - MS > MFI-InC » silica. Their applications for carbon steel and stainless steel substrates were also examined.

Keywords: anti-corrosion, silica

In-situ grown MgO-ZnO ceramic coating with high thermal emittance on Mg alloy by plasma electrolytic oxidation

Songtao Lu, Yang Li, Wei Qin, Xiaohong Wu
(Harbin Institute of Technology)
wuxiaohong@hit.edu.cn

Abstract: Orbital spacecraft suffers the extreme temperature cycling owing to direct sun load on one side and deep cold space on the other, which reduces the component lifetime. As a result, effective thermal prevention measures are very necessary to ensure the normal operation of devices and instruments in the spacecraft. A common passive method is the thermal control coating, which provides the radiative pathway to dissipate heat without energy consumption. Mostly, exposure components in the spacecraft are made of Al alloy, which normally employed the white coating with a low solar absorptance (α_s) and a high infrared emittance (ϵ) for a purpose of thermal control. With the rapid development of science and technology, light-weight materials are in great demand for the spacecraft application for the purpose of increasing the payload ratio and reducing energy consumption. Mg alloy has been considered as a promising material for the spacecraft owing to its low density, high specific strength and excellent electromagnetic shielding. Recently, more certain components in this type light-weight engine are made of Mg alloy rather than Al alloy, e.g. the engine block, oil pan and front engine cover. However, an important disadvantage of Mg alloy is the high chemical activity which seriously hinders its future application. Thermal control coatings prepared on Mg alloy using the anodizing and painting are easily led to the property degradation in the space environment and show relatively weak adhesion with the substrate. Therefore, it is of great significance to develop a novel technique for thermal control coating to increase the adhesive strength. Herein, a novel ceramic coating with high thermal emittance and good adhesion was directly prepared on the Mg substrate using an economical process of controlled plasma electrolytic oxidation (PEO) in the electrolyte containing $\text{Na}_5\text{P}_3\text{O}_{10}$, NaOH and ZnSO_4 . XRD and XPS results revealed that the PEO coating was mainly composed of ZnO and MgO. A pull-off test showed that all coatings possess an excellent adhesive strength. After the incorporation of ZnO in the PEO coating, the infrared emittance improved from 0.68 to 0.88. The thickness and roughness of the coating were mostly influenced by the concentration of Zn^{2+} ions. When the concentration of Zn^{2+} ions was 4 g/L, the PEO coating showed the strongest adhesive strength of 9.2 MPa, and its infrared emittance and solar absorptance reached 0.88 (2-16 μm) and 0.35 (200-2500 nm), respectively. The results indicated that the ceramic coating can be used as the promising thermal control coating. It is believed that this technique may open a new approach to expand the application of Mg alloy.

Keywords: Mg alloy, thermal control coating

Corrosion resistance of DLC films-coated titanium and stainless steel prepared by ion beam enhanced deposition

Beibei Han¹, Huijun Zhao², Dongying Ju³, Maorong Chai⁴, Susumu Sato¹

(1. Saitama Institute of Technology; 2. Hangzhou Dianzi University;

3. Advanced Science Institute, Saitama Institute of Technology, Ningbo Institute of Materials Industry Innovation, Hangzhou Dianzi University;

4. Advanced Science Institute, Saitama Institute of Technology)

dyju@sit.ac.jp

Abstract: Among the components of proton exchange membrane fuel cell (PEMFC) the bipolar plates play important roles. The traditional bipolar plates were made from non-porous graphite with the disadvantage of its low toughness, gas permeability and the difficulties in machining gas flow channels. In lieu of this, considerable effort has been made into the development of metallic bipolar plates from materials such as stainless steel and titanium alloys. To improve the corrosion resistance of titanium and stainless steel used for bipolar plates in PEMFC, an amorphous hydrogenated carbon (a-C:H) film, also known as diamond-like carbon (DLC) was deposited on the titanium or stainless steel substrate using Ion beam enhanced deposition (IBED) technique. The characterizations and corrosion behaviors of the DLC coated titanium and stainless steel deposited with different CH₄/H₂ ratios and deposition times were investigated and evaluated. The chemical bonding structure and composition of the DLC coatings were confirmed by Raman spectroscopy and X-ray photoelectron spectroscopy (XPS). The micromorphology and surface roughness of the films were observed and analyzed by scanning electron microscope (SEM) and atomic force microscopy (AFM). The DLC coated titanium and stainless steel were corroded by potentiostatic polarizations in a 0.5 mol/L sulfuric acid solution at 90 °C for 168 h. The metal ions in sulfuric acid corrosion solution were detected by inductively coupled plasma (ICP) atomic emission spectroscopy. The results indicate that the DLC coatings have been successfully deposited on the titanium and stainless steel substrates. A higher CH₄/H₂ ratio and a shorter deposition time can result in a decreasing ID/IG ratio, low root mean square (RMS) of the surface morphology and low concentration of metal ions in corrosion solution. The ID/IG ratio of corroded DLC coating on titanium with a minimum of 0.5 is lower than that of corroded DLC coating on stainless steel with a minimum of 1.17. The significant improvement in the corrosion resistance of DLC film was mainly attributed to the increased sp³ bond element. The metal ions concentration of a DLC coating on titanium with a minimum of 0.3459 ppm is obviously lower than that of a DLC coating on stainless steel with a minimum of 16.6017 ppm. As a result, the DLC film deposited on the titanium substrate is more promising in the applications with the superior anti-corrosion properties.

Keywords: diamond-like carbon, titanium, stainless steel, corrosion resistance

One step electrodeposition of Cu₂ZnSnS₄ thin film for solar cells and their properties

Aiyue Tang, Jingyu Guan, Meiling Dou, Jingjun Liu, Jing Ji, Ye Song, Zhilin Li, Feng Wang
(State Key Laboratory of Chemical Resource Engineering, Beijing Key Laboratory of Electrochemical Process and Technology for Materials, Beijing University of Chemical Technology, Beijing, China)
lizl@mail.buct.edu.cn, wangf@mail.buct.edu.cn

Abstract: The solar cells of CdTe and Cu(In, Ga)Se₂ thin films have high efficiency, but Cd, Te and Se are toxic and In and Ga are scarce. Cu₂ZnSnS₄ (CZTS) is promising for solar cells because of its optimal direct band gap of 1.5 eV and high absorption coefficient, and it is comprised of non-toxic and earth abundant elements only, so it is considered as substitution for Cu(In, Ga)Se₂. However, conventional vacuum based preparations with high costs and complicated apparatus confined its large scale application. Electrodeposition is regarded as a feasible synthesizing method for various functional nanostructured materials in industry scale. But the co-deposition of the four elements of CZTS is difficult and the composition control arouses another challenge. In this article, we developed a one-step electrodeposition method of CZTS thin films and proposed an electrolyte design principle based on the co-deposition mechanism research. We developed a novel electrolyte and obtained the CZTS thin films with both high carrier concentrations and high carrier mobility. The main achievements were as follows:

We prepared the targeted off-stoichiometry CZTS thin films by one-step electrodeposition. The chemical composition was successfully controlled based on the adjustment of different kinetics of the metallic ion reduction. The Cu/(Zn+Sn) and Zn/Sn ratios of the thin films were precisely controlled. After annealing, pure kesterite structure was obtained with hole as majority carrier. The grain size was in the range of 20-30 nm and the band gap was in the range of 1.43-1.52 eV. The carrier mobility reached 28.20 cm²/V·s with carrier concentration of 2.09×10¹⁸ cm⁻³. The high carrier mobility was attributed to the electronic interactions between Cu and Sn.

Electrochemical studies indicated that trisodium citrate and tartaric acid could narrow the co-deposition potential range of the four elements to -0.8- -1.2 V (vs SCE). The cause was the synergetic effect that trisodium citrate inhibited the reduction of Cu²⁺ and Sn²⁺ and tartaric acid promoted the reduction of Zn²⁺. The reduction of S₂O₃²⁻ was mainly attributed to the induction effect of the metallic ions. Such mechanism indicates that complexing agent and organic acid should be added in the electrolyte to narrow the potential gaps among the main salts and achieve co-deposition.

Potassium pyrophosphate and sulfosalicylic acid were chosen as additives in the novel bath for synthesizing CZTS thin films with high S content of 43.15at%. The obtained CZTS thin films had pure kesterite structure and suitable band gap after a sulfurization free annealing. Potassium pyrophosphate and sulfosalicylic acid were verified to have synergetic effect to narrow the potential gaps among the main salts. They also promoted the reduction of S₂O₃²⁻ to ensure the stoichiometry. The sulfurization free annealing process can promote the commercialization of CZTS films and the successful design principle of environmental friendly electrolytes could be applied in other electrodeposition systems.

The heat treatment of the thin films was optimized by the controlling of Ar flow rate and multi-step annealing. Long and narrow particles and the preferential orientation of the grain boundaries were obtained. With such structure, the direct transportation of the holes along the vicinity of the grain boundaries increased carrier mobility to 19.8 cm²/V s in the circumstance of high carrier concentration of 3.10×10²⁰ cm⁻³.

Keywords: Cu₂ZnSnS₄ thin film, one-step electrodeposition, sulfurization free annealing, carrier concentration, carrier mobility

Ion beam surface modification of alloys and ceramics using accelerators

Tao Wei, Mihail Ionescu

(Australian Nuclear Science and Technology Organisation)

tao@ansto.gov.au

Abstract: The reliability and reproduction of ion beam implantation using accelerators make it highly desirable for material modification in many industrial applications to improve friction, wear and corrosion of industrial components and to enhance the performance of bio-medical implants. There are vast range of ions could be selected to conduct the implantation by using different ions in the ion sources and the profile of the implanted ions could be precisely controlled by the accelerated beam energy. Additional advantage of ion beams is to control the stress in the affected layer. Recently ion beam implantation has also been used to simulate the neutron radiation effects, corrosion effects in the materials for the future fusion and fission nuclear reactors ^[1].

Ion beam implantation capability using accelerators has been developed at Australian Nuclear Science and Technology Organisation (ANSTO), Australia. Various ion beams, such as He, Au, Ni, Si, Fe, Ta, and Te, were implanted on different targets^[1-2]. The irradiated target materials include titanium aluminide, nickel-based alloy, oxide dispersion-strengthened steels and glass-ceramics waste forms.

An energy degrader was employed in front of the targets and a uniformly distributed helium ions was produced up to 17 m. The profile of the implanted ions and the defects in the target induced by high energy ion beam were investigated by transmission electron microscopy (TEM) and scanning electron microscope (SEM). The TEM specimens were prepared by a crossbeam focused ion beam and scanning electron microscope (FIB-SEM) system at ANSTO.

To evaluate the changes of mechanical properties in the affected surface layer, nanoindentation was employed to measure the hardness of the implanted samples. Furthermore, the micro-mechanical testing capability was developed at ANSTO. Using FIB the micro-size mechanical test specimens could be fabricated from the implanted samples along different orientations in the grain and the in situ micromechanical compressive and tensile testings were carried out in an SEM. The results demonstrated the hardening effects in the implantation layer, which gained a better understanding of the irradiation effects on the mechanical property in those alloys for the design of future reactors.

This presentation will report the recent developments of the ion beam implantation at ANSTO and in situ micro-mechanical testing to characterize the change of mechanical property.

Keywords: surface modification, ion beam, mechanical property

Reference:

- [1] G.S. Was, R.S. Averback, 1.07-Radiation Damage Using Ion Beams, in J.M.K. Rudy, (Editor), Comprehensive Nuclear Materials, Elsevier, Oxford, (2012): p. 195-221.
- [2] T. Wei, H. Zhu, M. Ionescu, P. Dayal, D. G. Carr, R. P. Harrison, and L. Edwards, Journal of Nuclear Materials, (2015) 459: p. 284-290.
- [3] T. Wei, A. Xu, H. Zhu, M. Ionescu, and D. Bhattacharyya, Nuclear Instruments and Methods in Physics Research B, (2017) 409: p. 288-292.

TiAlN/MoN superhard and self-lubrication

Wang Zhen, Zhang Guojun

(School of Materials Science & Engineering, Xi'an University of Technology)

zhangguojun@xaut.edu.cn

Abstract: The metal nitride films, such as TiN, have been widely used as a protection of cutting and forming tools for their excellent wear and corrosion resistance. As the fast development of high speed precision finishing, especially the improvement of high speed and dry cutting, lower coefficient of friction (COF) were required to prolong the lifetime of these nitride films. The studies about metal nitride films with both high hardness and low COF have become current research focuses. Meanwhile, molybdenum nitride films have exhibit lower COF because of the lubricious molybdenum Magnēi oxides formed in frictions process. Hence, studies on Mo₂N based metal nitride films would be helpful on fabricating metal nitride films with both high hardness and low COF. The microstructure, mechanical and tribological properties of TiAlN/MoN films deposited by magnetron sputtering were investigated. The hardening mechanisms, wear mechanisms and the relationship between the mechanical properties, oxidation behavior and tribological peoperties were discussed. Preparation and characterization of TiAlN/MoN nano-multilayer films: by reactive magnetron sputtering, using Mo target and TiAl target on the mirror polished steel disks and the Si wafers deposits TiAlN/MoN nano-multilayer films, thickness about 2.5 microns, modulation period constant 5 nm, modulation ratio for TiAlN:MoN ranging from 1 to 10. Meanwhile, TiAlN films with the same thickness were prepared for comparison. The microstructure, mechanical and tribological properties of TiAlN/MoN films deposited by magnetron sputtering were investigated ultimately.

It was found that different modulation ratio TiAlN/MoN nano-multilayer l ms exhibited fcc structure similar to B1-NaCl and formed isostructural superlattice with well dened interfaces between TiAlN and MoN layers. The studies about TiAlN/MoN nano-multilayer films showed that the COF were influence by values of H and H/E. TiAlN/Mo₂N nano-multilayer films were composed by TiAlN and Mo₂N phase and formed a superlattice structure. The layer interfaces bwtween TiAlN layers and Mo₂N layers were abrupt. TiAlN/MoN films exhibited super hardness, the values of which are about 46 GPa. The hardness enhancement of TiAlN/MoN films was mainly determined by the altering-stress strengthening theory.

Keywords: TiAlN/MoN nano-multilayer films, hardness

The change of magnetism triggered by external bias voltage in CoFe₂O₄/PMN-PT multiferroic heterostructures

Aopei Wang¹, Wen Wang¹, Ming Feng²

(1. Harbin Institute of Technology; 2. Jilin Normal University)

wangaopei@sina.com

Abstract: Multiferroic materials exhibit ferroelectric (FE) and ferromagnetic (FM) properties simultaneously. However, the selectivity of single-phase multiferroic materials presenting coexistence of powerful ferroelectricity and ferromagnetism is limited, which restricts the actual application. Multiferroic composite thin films, by contrast, possess particular superiority for reducing the interface loss and fusion, and it is in favor of the research of magnetoelectric coupling mechanism. With the in-depth research of theory and experiment, the interface interaction of multilayer film still seems to be very weak mainly caused by the clamping of substrate which is ferroically inactive. An effective way to solve this issue is building the multiferroic system by means of FE/FM single crystal substrate, and in the meanwhile inplane elastic coupling can be strengthened. In this work, Multiferroic CoFe₂O₄/0.65Pb(Mg_{1/3}Nb_{2/3})O₃-0.35PbTiO₃ (CFO/PMN-PT) heterostructures were fabricated by growing CFO films on PMN-PT single crystal substrates using pulse laser deposition.

The magnetism modulation of CFO films grown on PMN-PT substrates has been performed by a series of measurements. The magnetic hysteresis loops test by SQUID displayed the distinct temperature dependence and in-plane anisotropy of as-produced CFO films which possessed fine surface quality and highly preferential orientation. To further study the coercive field distribution of the CFO film, the angle-dependent measurement under the in plane magnetic field was performed through the magneto-optical Kerr effect (MOKE) test system by rotating the substrate. The result shows that the coercive field reaches to the maximum when the magnetic field along PMN-PT^[1-10] and reaches to the minimum at the perpendicular direction. The coercive field increases by the angle from 0° to 90°. This noteworthy in plane anisotropy of coercive field for the CFO film indicates a strong stress deriving from the PMN-PT substrate. Here we investigated the converse magnetoelectric (ME) effect through the MOKE test system containing both direct current (DC) mode and alternating current (AC) mode. By applying a sequence of DC voltage (0 V→200 V→0 V→-200 V→0 V) on the heterostructure under the magnetic field along PMNPT^[1-10], the coercive field of CFO films changes with the voltage and the curves exhibits butterfly-shaped definitely, which just resembles the strain loop. By measuring the magnetic hysteresis loops under a sequence of DC voltage and the magnetic field along the PMN-PT [001], we can see that an absolutely opposite tendency is acquired contrast to that of 90°. This result indicates that the electric field can modulate the coercive field and the in plane anisotropy of CFO films through the strain transfer. Besides, regardless of the external magnetic field, AC mode MOKE test shows that ΔKerr-V curve also behaves to be the similar butterfly-shaped, revealing the mechanism of strain mediated ME coupling. The strain generated from the PMN-PT substrate by applied an electric field was transmitted to the CFO films, which changed the magnetization and the coercive field of the films. This result demonstrated that the strain mediated ME coupling mechanism played the dominative role in CFO/PMN-PT multiferroic heterostructures. This work illustrates that the coercive field and magnetization of CFO films grown on PMN-PT single crystal substrates can be modulated by external electric field, which indicates a wide application prospect of multiferroic heterostructure on novel electric field assisted recording medium.

Keywords: magnetic anisotropy, multiferroic heterostructure, magneto-optical kerr effect

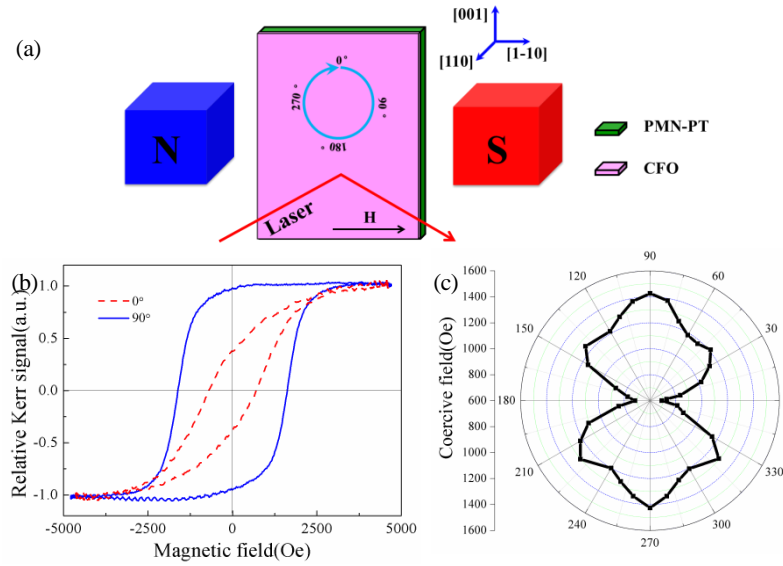


Fig.1 (a) Schematic diagram of the magneto-optical Kerr measure system. (b) In plane MOKE hysteresis loops of CFO films while the magnetic field parallels to [001] and [1-10] orientation of the substrates respectively. (c) In plane angular dependence of the coercive field of CFO films under the applied magnetic field (i.e. 5000 Oe) measured by rotating the samples

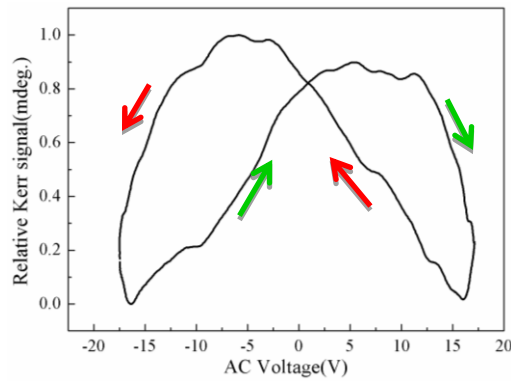


Fig.2 The relative Kerr signals as a function of AC voltage

Intrinsic and Ti, Sr doped MoS₂ thin films design and performance study

Yudong Fu¹, Yang Song², Huanzheng Sun²

(1. Chinese Heat Treatment Society; 2. Harbin Engineering University)

2406808423@qq.com, fuyudong@hrbeu.edu.cn

Abstract: Since graphene materials were successfully separated from graphite in 2004, twodimensional nanomaterials represented by graphene have become one of the research hotspots in materials science today. Transition metal sulfides (TMSs) are novel graphenelike materials. As a representative material in TMSs, Molybdenum disulfide is a hexagonal layered material with a direct band gap. Its bandgap is adjustable. It has good lubrication, catalytic and optoelectronic properties, and it has a promising outlook. Its excellent photoelectric properties make it even expected to replace graphene. Nowadays, people have made some achievements in the preparation of molybdenum disulfide films. However, the study of doped molybdenum disulfide films is still rare. In this paper, we prepared and characterized the intrinsic and multi-element doped molybdenum disulfide films and characterized, and then carried out theoretical studies based on the first-principles calculations. We used monocrystalline silicon as a base material, and prepared molybdenum disulfide films doped with different elements by electrodeposition. Then we analyzed the effect of deposition time on film thickness by observing the thickness of the film. We analyzed the influence of deposition current on the films by observing the surface morphology of the film. We analyzed the influence of deposition time on the film thickness by observing the thickness of the films. We used XRD, SEM, EDS, XPS, and UV-Vis to characterize the films doped with different elements. We observed the morphology of the films and analyzed the elemental composition and content difference of the films doped with different elements. We used the test results to analyze the effect of doping elements on the surface modification of the films. We measured the UV-visible absorption spectra and analyzed the material composition. We used Material Studio software to analyze the energy band structure, density of states and differential charge density of molybdenum disulfide films basing on the first-principle principle. We calculated the electronic structures of intrinsic and doped molybdenum disulfide films by establishing a model separately, and then analyzed and compared the properties of the two films.

It has been calculated that the intrinsic molybdenum disulfide film has a direct bandgap energy band structure with a band gap width of about 1.876 eV. The doped molybdenum disulfide thin film produces a new energy level, which leads to the generation of new transitional modes, and thus has a greater change in the photoelectric properties of the intrinsic molybdenum disulfide film. Comparing the density of electron states before and after doping, the d orbital of the molybdenum atom and the p orbital of the sulfur atom may produce strong covalent bonds, acting like π bonds. Then we analyzed the strength of the interatomic bond by differential charge density. After doping, the chemical bonds formed between the dopant atom and the sulfur atom became stronger, while the optical properties of the molybdenum disulfide film were changed. We analyzed the optical properties of the molybdenum disulfide film by the dielectric function, absorption coefficient and reflection spectrum of the molybdenum disulfide film. The absorption coefficient spectrum shows a strong absorption peak around 2.85 eV, which explains the reason why the molybdenum disulfide film is blue-violet. After doping, the absorption of light in the visible range decreases, new absorption peaks appear in the ultraviolet range, the absorption range in the infrared range increases, and new absorption peaks are generated at the same time.

Keywords: molybdenum disulfide film, electrodeposition, doping, first-principles

Multilayered thermal barrier coatings

Xueqiang Cao

(State Key Laboratory of Silicate Materials, Wuhan University of Technology, Luoshi Road 122, Wuhan 430070, China)

xcao@whut.edu.cn

Abstract: Thermal barrier coatings (TBCs) are finding increasing applications in gas turbines to provide thermal, corrosion and erosion protections for the metallic hot-section components in order to achieve higher gas temperature capability, improved efficiency and durability. YSZ has large thermal expansion coefficient and extremely high fracture toughness, but the high thermal conductivity and phase transformation below 1200 °C are its intrinsic shortcomings. Currently, the long-term application temperature of YSZ coating is below 1200 °C, which cannot match the requirements of the next generation gas turbine operated at a higher gas temperature. We have successfully developed the multilayered TBCs based on rare earth composite oxides and YSZ. LMA/YSZ, LZ7C3/YSZ and LZ/YSZ double-layered or functionally graded TBCs have outstanding thermal cycling lives which are much longer than that of single layered YSZ coating due to the thermal stress relief.

A novel non-destructive inspection technique was developed to measure the residual stresses in TBCs by using Eu^{3+} photoluminescence piezo-spectroscopy. The relationship between the strongest peak of $^5\text{D}_0 \rightarrow ^7\text{F}_2$ and stress was determined by the high-pressure experiments and used to evaluate the residual stresses. When the top ceramic coat LZ7C3 in the double-layered coating LZ7C3/YSZ:Eu spalled, the inner YSZ:Eu could produce visible luminescence under UV illumination, providing an indication of the spallation location. The LZ7C3/YSZ:Eu coating spalled bit by bit from LZ7C3 to YSZ:Eu during thermal cycling. The similar thermal expansions of LZ7C3 and YSZ:Eu prolonged the thermal cycling life of the coating.

Keywords: multilayered TBCs, YSZ

Effect of heat treatment on bonding strength of nanostructured 8YSZ thermal barrier coatings deposited onto NiCrAlY(Ce) bond coat

Zhenguo Zhang¹, Feifei Zhou¹, Junfeng Gou¹, Qiwen Zhang¹, Saiyue Liu¹, Lan Wang¹,
You Wang¹, Ruiqing Chu²

(1. Department of Materials Science, School of Materials Science and Engineering, Harbin Institute of Technology; 2. School of Environmental and Materials, Yantai University)

wangyou@hit.edu.cn

Abstract: The effect of rare earth element Ce in NiCrAlY bonding coating and heat treatment on the bonding strength of nanostructured 8YSZ thermal barrier coatings (TBCs) was studied. The TBCs were prepared by atmospheric plasma spraying (APS) and heated in air. The results show that the bonding strength of the TBCs with NiCrAlYCe bond coatings (BC) is greatly improved by heat treatment. Especially after the TBCs with NiCrAlYCe BC were heated at 800 °C for 6 h or at 900 °C for 2 h, the bonding strength of the coating can be up to 48.9 MPa or 45.2 MPa at least, which were 48.6% or 37.4% more than of TBCs with NiCrAlY BC at the same conditions. The SEM and XRD analysis indicate that the processes of air heat treatment mainly refer to element diffusion and oxidation. The formation of Al_2O_3 film is advantage for increasing the bonding strength of the TBCs while the formation of the spinel oxide is disadvantage. The rare earth element Ce promotes the preferential oxidation of Al to form Al_2O_3 film, which is conducive to improving the bonding strength of the TBCs.

Keywords: bonding strength, heat treatment, Ce, APS, nanostructured TBCs

Surface modification of biomedical titanium using plasma immersion ion implantation

Xuanyong Liu

(State Key Laboratory of High Performance Ceramics and Superfine Microstructure, Shanghai Institute of Ceramics, Chinese Academy of Sciences, Shanghai 200050, China)

xyliu@mail.sic.ac.cn

Abstract: The implant for hard tissue replacement should possess various attributes, including appropriate mechanical properties, good biocompatibility, high corrosion and wear resistance, well osseointegration and antibacterial property. Titanium-based implantable devices such as joint prostheses, fracture fixation devices and dental implants, are important to human lives and improvement of the life quality of patients. However, biomedical titanium is lack of osseointegration and antibacterium ability, therefore many works were conducted to improve the osseointegration and antibacterium ability in our group. Plasma immersion ion implantation (PIII) is a novel physical technique which can enhance the multi-functionality, mechanical and chemical properties as well as biological activities of artificial implants and biomedical devices. Silver (Ag) as a non-specific biocidal agent is able to act strongly against a broad spectrum of bacterial and fungal species, including antibiotic resistant strains. Calcium (Ca), magnesium, (Mg) and zinc (Zn) can stimulate bone formation, increase osteogenetic function in osteoblasts through exciting cell proliferation, alkaline phosphatase activity, collagen synthesis and protein synthesis. Here, we introduce the current progress of silver plasma immersion ion implantation into biomedical titanium in our group. Silver nanoparticles (Ag NPs) embedded titanium surfaces possesses efficient micro-galvanic effect controlled antibacterial activity and excellent cytocompatibility was fabricated via a single step silver plasma immersion ion implantation (Ag-PIII) process. The Ag-PIII samples inhibit the growth of both *S. aureus* and *E. coli* while enhancing proliferation of the osteoblast-like cell line MG63. Silver accompanied with calcium, magnesium and zinc dual ions were sequentially implanted into titanium. The obtained results suggest that the Ag/(Ca, Mg and Zn) dual ions co-implanted process is the efficient way to obtain the titanium implant with high antibacterial activity and bone formation ability.

Keywords: plasma immersion ion implantation, surface modification, biomedical titanium

The tribological properties of graphene modified $n\text{-Al}_2\text{O}_3/\text{TiO}_2$ coatings

Lan Wang¹, Saiyue Liu¹, Junfeng Gou¹, Qiwen Zhang¹, Feifei Zhou¹, You Wang¹, Ruiqing Chu²

(1. Harbin Institute of Technology; 2. Yantai University)

wangyou@hit.edu.cn

Abstract: Graphene modified $n\text{-Al}_2\text{O}_3/\text{TiO}_2$ coatings were prepared on 316L stainless steel by plasma spraying. The microstructure of feedstocks and coatings was characterized using X-ray diffractometer and scanning electron microscope. The bonding strength of the coating were studied by the dual tensile testing. The Vickers hardness of the coatings were used in this paper. The tribological behavior of the coatings were demonstrated by sliding wear testing. The coatings containing 6wt% graphene shows the best performance, of which the porosity is 35% lower, the bonding strength is 62% higher, and the wear rate is 20%-25% lower than that of the non-graphene coatings. In addition, there is no obvious effect on the hardness of the coatings with the addition of graphene.

Keywords: plasma spraying, $n\text{-Al}_2\text{O}_3/\text{TiO}_2$ coating, tribological properties, graphene

Enhancing magnetron sputtered protective coatings via hierarchical structuring

Feng Huang

(Ningbo Institute of Materials Technology and Engineering, Chinese Academy of Science)

HuangFeng@nimte.ac.cn

Abstract: Rapid development of protective coatings for targeted applications typically requires a proper combination of structural tuning, over many length scales, and coating chemistry. Examples will be provided to highlight the effectiveness of this approach, based on our results, to developing magnetron sputtered coating with enhanced properties for various applications. They include extremely wear-resistant superhard V-Si-N coatings, hardness-independent wear-resistant Cr-Si-N coatings over a wide range of hardness (13-35 GPa), self-lubricating hard W-S-N coatings, damage-tolerant amorphous TiB coatings, and self-healing corrosion-resistant Al-Al₂O₃ nanocomposite coatings. The phase formation, critical to forming the hierarchical structures, are interpreted in terms of equilibrium and metastable phase diagrams. These examples demonstrate that coatings with selected chemistry, combined with proper process development to obtain hierarchical structures, could exhibit improved performance in many situations. Furthermore, it appears that simultaneous top-down and bottom-up considerations could be an effective strategy worthy of further investigation.

Keywords: coating selection, hierarchical structuring, magnetron sputtering, phase formation

Chemical vapor deposition growth of large-area ReS₂ monolayer films for optoelectronic applications

Chengyan Xu, Jingkai Qin, Yang Li, Dandan Ren, Liang Zhen

(Harbin Institute of Technology)

cy_xu@hit.edu.cn

Abstract: Transition metal dichalcogenide (TMDs) are among the most studied two-dimensional (2D) materials because of their unique properties and promising applications in nanoelectronics, optoelectronics, photonics, sensing, electrocatalysis and energy storage. Rhenium disulfide (ReS₂) maintain a direct bandgap as transitioning from monolayer to bulk due to its very weak interlayer coupling effect, which is different from other TMD materials such as MoS₂ and WS₂. In addition, the distorted 1T anisotropic in-plane structure in ReS₂ would induce anisotropic electrical behavior with the layer plane. Here, we report the epitaxial growth of large-area, continuous ReS₂ monolayer films on mica substrate by chemical vapor deposition. By prolonging the growth duration, continuous ReS₂ multilayer films can be also obtained. We also realized substitutional doping of monolayer RS₂ with Mo, leading to the degenerate p-type semiconducting behavior in Mo-doped ReS₂ field effect transistors, in agreement with density functional calculations. The p-n diode device based on a doped ReS₂ and ReS₂ homojunction exhibited gate-tunable current rectification behavior, and the maximum rectification ratio could reach up to 150 at $V_d = -2/+2$ V. In addition, we demonstrate the performance enhancement of ReS₂-based phototransistor by coupling CdSe-CdS-ZnS core-shell quantum dots. Under 589 nm laser irradiation, the responsivity of the ReS₂ phototransistor decorated with quantum dots could be enhanced by more than 25 times (up to 654 A/W) and the rising and recovery time can be also reduced to 3.2 and 2.8 s, respectively. The excellent optoelectronic performance is originated from the coupling effect of quantum dots light absorber and cross-linker ligands 1,2ethanedithiol. Photoexcited electron-hole pairs in quantum dots can separate and transfer efficiently due to the type-II band alignment and charge exchange process at the interface.

Keywords: chemical vapor deposition, two-dimensional (2D) materials, ReS₂, optoelectronics

Morphological and microstructural characterization of nanostructured

Al₂O₃/ZrO₂ eutectic layer induced by laser beam irradiation

Zhigang Wang¹, Jiahu Ouyang^{1,2}, Yonghui Ma¹, Lingyun Xie¹, Yujin Wang¹, Zhanguo Liu¹, Yang Wang³
(1. Key Laboratory of Advanced Structural-Functional Integration Materials & Green Manufacturing Technology, School of Materials Science and Engineering, Harbin Institute of Technology, Harbin 150001, China; 2. National Key Laboratory for Precision Hot Processing of Metals, Harbin Institute of Technology, Harbin 150001, China; 3. School of Mechatronics Engineering, Harbin Institute of Technology, Harbin 150001, China)
ouyangjh@hit.edu.cn

Abstract: In the present work, nanostructured surface layers of eutectic oxide ceramic with a thickness of approximate 1000 μm , free of micro-cracks delamination and pores, were produced on the surfaces of conventionally sintered Al₂O₃/ZrO₂ ceramic via the laser beam induced rapid solidification process. The evolutions of molten pool profile, microstructure and phase composition were characterized by scanning electron microscopy (SEM) and Raman spectroscopy. The geometrical evolution map of the molten pool in response to laser power, scanning speed and input energy density is established, where the molten pool has a circular shape at low velocities and tends to lengthen at high velocities. It is noted that the surface of remelted layer exhibits a spontaneously nucleated dendritic ZrO₂-cored eutectic colonies with a minimum diameter of 100-200 μm , in which the average interphase spacing is ranging from about 190 to 280 nm. Furthermore, the variations of eutectic spacing versus growth rate is essentially linear on the logarithmic scale, and the relationship is obtained by binary regression analysis as $\lambda = KV^{-0.4}$. The eutectic spacing is also consistent with the inverse-square-root dependence on the growth rate, and the constant of proportionality is 3.5. Independent colonies are composed of α -Al₂O₃, m -ZrO₂ and t -ZrO₂ phases, where t -ZrO₂ is the dominant phase and the m -ZrO₂ phase increases with the decrease of scanning speed. Besides, the peaks corresponding to α -Al₂O₃ phase become much weaker and far less than the nominal composition compared to the t -ZrO₂ phase.

Keywords: surface nano-structuring, nanoeutectic, Al₂O₃-ZrO₂, laser remelted layer

Material-genome perspective towards robust T/EBC materials

Jingyang Wang

(High-performance Ceramics Division, Shenyang National Laboratory for Materials Science, Institute of Metal Research, Chinese Academy of Sciences, Shenyang 110016, China)

jywang@imr.ac.cn

Abstract: SiCf/SiC ceramic matrix composites (CMCs) are the key high temperature structural materials in next generation gas turbines. Robust T/EBC is critically requested to protect CMC components from severe high temperature oxidation and corrosion in extreme combustion environments. Rare earth silicates, typically referring RE₂SiO₅ orthosilicates and RE₂Si₂O₇ pyrosilicates, are new T/EBC materials due to their low thermal conductivity and excellent stability in extreme environments. There are crucial challenges for the optimal choices of RE-silicate T/EBC candidates due to their complex and tunable crystal chemistry and performances. High-throughput screening of advanced T/EBC materials would be promoted based on material informatics of candidates. Strategic material-genome initiative would also prevail to disclose mechanisms of property diversity and to further adopt novel concepts on the design of robust T/EBC for advanced SiCf/SiC CMCs.

Keywords: material-genome, environmental barrier coating

Elevate the photoelectrochemical anticorrosion effect of corrosion product layers on electrogalvanized steel in simulated seawater through nanoelectrodeposition

Qingyang Li
(Jinan University)
qingyang@jnu.edu.cn

Abstract: Zinc electrodeposit is the most widely used sacrificial anode coating for protection iron and steel against corrosion, due to their many outstanding features, including non-toxicity, low cost, and easy fabrication. There is a strong consensus that the key to maximize its service life is the stability of oxides or corrosion product layers, e.g. a high-quality corrosion product layer could provide effective protection to zinc substrate over 10 year. Therefore, many efforts have been made to improve the performance of corrosion product layers on electrogalvanized steel. All of them only focused on the physical barrier effect of corrosion product layers in aggressive environments, but ignored the photogenerated cathode protection of the corrosion product layers (main ZnO) to zinc substrate. In our most recent work, we demonstrate that the oxides and corrosion product layers not only endured the attack from aggressive environments, but also provided an additional photogenerated cathode protection to electrogalvanized steel in simulated seawater under simulated sunlight illumination. The corrosion product layer, which is composed of ZnO, Zn(OH)₂, Zn₂(OH)₂CO₃ and Zn₅(OH)₈Cl₂·H₂O provided approximately 30% higher corrosion protection to zinc coating under sunlight illumination than the situation in darkness. The responsible mechanism is due to the fact that the ZnO layer could produce photoelectrons which are transferred directly to the substrate, thereby provide a cathodic protection to electrogalvanized steel under sunlight illumination. In the present study, we further elevate the photoelectrochemical corrosion protection of ZnO layer to electrogalvanized steel by controlling the grain size of zinc coating. Detailed analyses are also conducted to clarify the mechanism responsible for the improvements.

Keywords: photoelectrochemical corrosion, electrogalvanized steel

La₂O₃-ZrO₂-CeO₂ thermal barrier coatings by EB-PVD: feathery nanostructure, thermal conductivity and thermal cycling life

Zaoyu Shen, Limin He, Zhenhua Xu, Rende Mu
(Beijing Institute of Aeronautical Materials)
shenzaoyu@163.com

Abstract: Thermal barrier coatings (TBCs) with low thermal conductivity have triggered tremendous attention due to their promising application in the gas turbine engines. Recent studies have prepared pyrochlore (A₂B₂O₇) materials, which limit their element controllability and thermal performances. It still remains a big challenge for controlling element content in coatings and investigating the relationship between the complex hierarchical architectures and their thermal performances. Here we describe a La₂O₃-ZrO₂-CeO₂ (LZC) coating by electron beam-physical vapor deposition (EB-PVD). The complex hierarchical architectures are composited of spherical and elongated nanowires, exhibiting feathery nanostructure and intra-columnar pores. The coatings show an especially low thermal conductivity and relatively high thermal cycling life. The optimization of hierarchical architectures by different deposition energy can be extended to design other promising TBCs materials.

Keywords: thermal barrier coatings, EB-PVD

Fabrication and characteration of layered double hydroxide films by conversion of MAO coatings on magnesium alloys

Zeyu Zhang¹, Liang Wu², Fusheng Pan², Yu Xin Zhang¹, Aitao Tang², Lingjie Li³, Gen Zhang¹, Zhicheng Zheng¹, Andrej Atrens⁴

(1. College of Materials Science and Engineering, Chongqing University, China;

2. National Engineering Research Center for Magnesium Alloys, Chongqing University, China;

3. Chemistry and Chemical Engineering, Chongqing University, Chongqing 400044, China;

4. School of Mechanical and Mining Engineering, The University of Queensland, Australia)

wuliang@cqu.edu.cn

Abstract: Super-hydrophobic films were synthesized on the Mg alloy AZ31 by modifying in-situ grown Mg-Al layered double hydroxide (LDH) films with stearic acid (SA), sodium laurate (SL), myristic acid (MA) and 1H, 1H, 2H, 2H-Perfluorodecyltrimethoxysilane (PFDTMS). These films exhibited a static water contact angle of 150.6°, 153.7°, 152° and 145.5°, respectively. Mg-Al LDH-SA, Mg-Al LDH-SL and Mg-Al LDH-MA films were produced by the neutralization reaction of the fatty acid and Mg(OH)₂ whereas the Mg-Al LDH-PFDTMS film was produced by the hydrolysis reaction of PFDTMS along with the condensation polymerization reaction. The electrochemical impedance spectroscopy (EIS), the hydrogen evolution data as well as long-term immersion tests indicated that Mg-Al LDH-PFDTMS provided better barrier protection to improve the corrosion resistance of AZ31 Mg compared with the Mg-Al LDH-SA, Mg-Al LDH-SL and Mg-Al LDH-MA films, because the Si-OH groups and the hydroxyl groups on the surface of the film were combined to form CF₃(CF₂)₇(CH₂)₂Si(O-Surface)₃, which decreased the surface energy and improved the corrosion resistance.

Keywords: layered double hydroxides, superhydrophobicity, surface, corrosion resistance, magnesium alloy

Effect of sputtering power on microstructure and photoelectrical properties of Al-doped ZnO films deposited by RF magnetron sputtering

Xiaoxiao Qiu, Xiying Zhou

(Shanghai University of Engineering Science)

1511921567@qq.com

Abstract: Aluminum doped zinc oxide (AZO) films were deposited on glass substrate by radio frequency (RF) magnetron sputtering, and the RF power ranged from 40 to 150 W which applied to the target. The influence of sputtering power on deposition rate, crystalline structure, surface topography and photoelectric properties of the films were investigated by X-ray diffraction (XRD), scanning electron microscopy (SEM), atomic force microscopy (AFM), UV-visible spectroscopy, and electrical measurements. XRD patterns indicated that the films had a preferential growth orientation along (002) direction, and the (002) peak intensity increased with the increase of sputtering power. SEM and AFM results demonstrated that the films was more closed-packed with pyramid-like structure appeared on film surfaces in high power condition, the particle size and surface roughness were also increased with the sputtering power increasing. The resistivity of the films decreased from $21.8 \times 10^{-3} \Omega \cdot \text{cm}$ at 40 W to $5.4 \times 10^{-3} \Omega \cdot \text{cm}$ at 150 W when the sputtering power increased. The transmittance curves revealed that the optical transmittance deteriorated with the sputtering power increasing, the average transmittance of the AZO films were over 80% in the visible range, and the band gap shifted toward higher energy as sputtering power increasing.

Keywords: AZO, magnetron sputtering, photoelectric property

High-rate deposition of structure controllable Al/Cu films by highpower density magnetron sputtering

Tielei Shao, Zhongzhen Wu, Suihan Cui, Liangliang Liu, Xiaokai An, Shu Xiao
(School of Advanced Materials, Peking University Shenzhen Graduate School, Shenzhen, China)
wuzz@pkusz.edu.cn

Abstract: Magnetron sputtering has become the most popular deposition technology of a wide range of industrial coatings, such as hard coatings, self-lubricated coatings, corrosion resistant coatings, decorative coatings and coatings with specific optical or electrical properties. Although the basic sputtering process has been known and used for many years, there are many aspects such as deposition rate, ionization rate and structure control should be improved. This study develops a novel rectangular magnetron sputtering cathode with extra high power density (200 W/cm^2). And the discharge and deposition characteristics are studied as exemplified by pure metal targets (Al and Cu). The results show that both the ion current and deposition rate increase significantly and the structures of metal films evolve from dense to loose with increasing the power density. The emission spectral intensity of copper and aluminum ions are also significantly improved, indicating the increased ionization of the sputtered materials. For Al, the deposition rate arrives to $1.3 \mu\text{m/min}$ at the distance of 10 cm from the target to substrate when the power density is 140 W/cm^2 and the obtained dense Al films show a large average reflectivity of 92% at the wavelength of 350 nm to 900 nm. For Cu, the deposition rate reached $2.6 \mu\text{m/min}$ when the power density is 180 W/cm^2 at the distance of 10 cm from the target to substrate. More interestingly, a special nano-structured Cu film can be obtained by coating density and preferred orientation control and a super hydrophobic surface ($\text{CA}=152.5^\circ$) can be produced by further oxidation. Owing to the greatly increased deposition rate and structure controllable induced by high power density, it provides great potential in metallic films and foils fabrication industry to replace the electroplating that induces severe pollution to the environment.

Keywords: high power density magnetron sputtering, Al/Cu films, high-rate deposition, structure controllable

Effect of diffusion characteristics of Pt in $\beta\text{-NiAl}/\gamma'\text{-Ni}_3\text{Al}$ within NiCoCrAl alloy on alumina growth behaviour

Asim Khan, Peng Song, Chao Li, Jiansheng Lu
(Kunming University of Science and Technology)
songpengkm@163.com

Abstract: In recent years a lot of researches have been done on Ni base super alloy by adding REs to improve the oxidation resistance of Al_2O_3 . In this study a layer of platinum was fabricated through electroplating on the surface of NiCoCrAl model alloy. Pt diffusion characteristics and oxidation behavior of Pt-modified NiCoCrAl compared to conventional NiCoCrAl was investigated at 1050°C . The Pt inter diffusion layer within the alloy is obtained through heat treatment. The results indicate that Pt presented different diffusion ability in $\beta\text{-NiAl}$ and $\gamma'\text{-Ni}_3\text{Al}$ phases during the heat process due to different covalent bonding. The addition of Pt restrained the spallation of Ni-rich oxide on Pt-modified NiCoCrAl compared to conventional NiCoCrAl, hence the adhesion between the oxide layer and NiCoCrAl was improved.

Keywords: metal coatings, alumina, platinum, oxidation, interfaces

Surface and interface engineering of hybrid perovskite films for perovskite solar cells with highly improved efficiency and stability

Hongqiang Wang
(Northwestern Polytechnical University)
hongqiang.wang@nwpu.edu.cn

Abstract: Passivation of defects that exist at either surface or grain boundaries in hybrid perovskite film has been of significance to improve the photo-converse efficiency as well as the degradation of perovskite devices. We herein present a simple but effective strategy of copassivating surface & grain boundaries to achieve highly improved photo-conversion efficiencies and durabilities of perovskite solar cells (PSCs). The co-passivation agent of PFA was experimentally verified to be located at the surface and GBs of the perovskite layer, which was found much effective to achieve highly improved PCEs and durabilities of PSCs. A remarkable 53.3% enhancement in PCE was achieved within the archetypal MAPbI₃based perovskite solar cells, which demonstrated much improved moisture-durability owing to the hydrophobic CF₃- terminal groups in PFA. Based on the performance comparison between the PSCs with surface-only passivation and surface & GBs co-passivation, a conclusion can be drawn that GBs passivation plays equal importance with that of surface passivation. We further apply the co-passivation strategy to the construction of mixedcation lead mixed halide perovskite solar cell, which produced air stable PSCs with efficiencies above 20%. We thus believe that our study opens an avenue of accessing higher performance PSCs based on the simple passivation protocols.

Keywords: perovskite solar cell, surface engineering, interface engineering, defeces passivation, grain boundaries passivation

The effect of micro-textured surface on tribological properties of nanostructured ZrO₂(Y₂O₃)-Al₂O₃ ceramics under dry sliding against Al₂O₃ and 304L steel

Yufeng Li, Yi Kaiyang, Fu Rao

(School of Materials Science and Engineering, Shenzhen Graduate School, Harbin Institute of Technology)
yfli@hit.edu.cn

Abstract: Surface texturing with specific patterns is a well-known and effective approach for improving the tribological performance in sliding contact. In this article, three kind of regular micro-dimpled textures with different area densities were fabricated on the surfaces of sparkplasma-sintered nanostructured ZrO₂(Y₂O₃)-Al₂O₃ ceramics by laser-ablation method. In order to understand the influence of the surface texturing, the tribological testing of untextured and textured samples have been conducted by using a pin-on-disk tribometer in dry sliding against Al₂O₃ and 304L steel pin. The results exhibit that the surface texturing is helpful to improve the tribological properties of nanostructured ZrO₂(Y₂O₃)-Al₂O₃ ceramics. For the Al₂O₃ pin, the friction coefficients of samples decrease with increasing the texture area density from 0 to 33% under 4.9 N load, including a maximum friction reduction of 18%. However, the improvement of friction coefficients is not significant under 9.8 N load due to the destruction of the surface textures. For 304L steel pin, the lowest coefficients of friction were obtained with the highest texture area density of 33% under 4.9 N load and 9.8 N load, where the reduction in friction were 34% and 29% of that of the untextured samples.

Keywords: surface texturing, ZrO₂(Y₂O₃)-Al₂O₃ ceramics, friction, dry sliding

Prediction of the critical rupture and failure modes of the plasmasprayed yttria stabilized zirconia thermal barrier coatings under the burner rig test via acoustic emission technique

Liang Wang¹, Jinxing Ni¹, Xinghua Zhong¹, Fang Shao¹, Jiasheng Yang¹, Huayu Zhao¹, Shunyan Tao¹, You Wang²

(1. Shanghai Institute of Ceramics, Chinese Academy of Sciences; 2. Harbin Institute of Technology)
wang@mail.sic.ac.cn

Abstract: The yttria partially stabilized zirconia (YPSZ) thermal barrier coatings (TBCs) have been fabricated by atmospheric plasma spraying. The failure modes of the TBCs during burner rig test (BRT) have been investigated via in-situ acoustic emission (AE) technique systematically. The filtering technique has been used to exclude the disturbance of the noise in the process of BRT in order to capture the actual and effective AE signals. The propagation patterns of the cracks have been obtained based on the analysis of AE signals. Based on the characteristic waveform of effective AE signals, the Fast Fourier Transformation (FFT) and wavelet transformation has been adopted to analyze the key distribution range of the amplitude and frequency. The investigation results indicate that the acquired AE signals during BRT mainly include signals which came from plastic deformation of the substrate and creep of each layers, propagation of vertical cracks and interfacial cracks (horizontal cracks). During heating stage, propagation of vertical cracks at the inner of the ceramic-layer tend to occur, while during cooling stage, propagation of interfacial horizontal cracks tend to occur. The prediction of service lifetime of the TBCs can be obtained via the analysis of the accumulated energy of the AE signals.

Keywords: thermal barrier coatings, burner rig test, failure, finite element simulation, acoustic emission

Enhancing the tribological and mechanical properties of epoxy coatings by graphene nanoparticle encapsulation

Chao Xia, Boris Zhmud
(Applied Nano Surfaces)

chao.xia@appliednanosurfaces.com

Abstract: Polymer bonded solid lubricant coatings are used when application conditions prevent the use of conventional lubricants such as greases and oils. Such coatings help to protect machine elements exposed to high tribological stress against wear and corrosion, ease mounting of screw threaded connections, reduce stick-slip, etc. From the structural viewpoint, polymer bonded solid lubricant coatings comprise dispersions of solid lubricants – such as graphene, graphite, MoS₂, WS₂, or PTFE - in an organic polymer binder, usually of epoxy or polyurethane type. The choice of binder largely determines the coating properties such as operating temperature range, surface adhesion, hardness and abrasion resistance, chemical stability, etc. Polymer bonded coating systems lack the mechanical toughness of hard coatings, such as DLC or CrN, which limits the range of possible applications. In the present communication, we show that the mechanical properties of typical polymer bonded solid lubricant coatings can be significantly boosted by using nanoparticulate fillers – such as graphene platelets. The structural, mechanical and tribological properties of such nanoparticle-fortified coatings are studied.

Keywords: solid lubricant coating, nanoparticle encapsulation, graphene

Preparation and toughening of a-CuZr-c-ZrN nano-multilayer hard coating

Zhenyu Guo¹, Dayan Ma¹, Xiaomin Zhang²

(1. Xi'an Jiaotong University; 2. Xi'an University of Architecture and Technology)

madanyan@mail.xjtu.edu.cn, xmzhangxauat@vip.163.com

Abstract: Hard coatings are prone to crack and failure when subjected to large external impact loads due to poor toughness. In this paper, a-CuZr/c-ZrN nanomultilayers were designed to improve the toughness of ZrN coatings. Two groups of a-CuZr/c-ZrN nanomultilayers were prepared: CuZr (20 nm)/ZrN (40, 60, 100 nm) as Group 1 and CuZr (5, 10, 20, 30 nm)/ZrN (40 nm) as Group 2. The microstructures were analyzed by X-ray diffraction (XRD) and scanning electron microscopy (SEM). Hardness, elastic modulus were tested by nanoindentation; scratch tests and Vickers indentation methods were adopted to characterize the toughness. The relationship between parameters of layer structure and mechanical properties were analyzed, the toughening effect and related mechanism were investigated. The conclusions were: In Group 1, both of the hardness and fracture toughness of multilayer coatings increase with the decrease of ZrN layer thickness. In Group 2, the hardness decreases first and then increases with the CuZr thickness increases. The toughness increased with the CuZr thickness increases, especially the a-CuZr/c-ZrN=30/40 nm has the significant toughening effect, which toughness reached 0.5468 MPa m^{0.5} (about 43% higher than the ZrN single-layer film). This is mainly affected by the a-CuZr layer thickness of the multilayer film which alter the deformation mechanism.

Keywords: nanomultilayer film, toughening mechanism

The mechanical integrity of a MAO/PLGA composite coated magnesium alloy for biodegradable material

Lianxi Chen, Yinying Sheng, Xiaojian Wang, Xueyang Zhao, Hui Liu, Wei Li

(Jinan University)

xiaojian.wang@jnu.edu.cn, liweijn@aliyun.com

Abstract: In order to decrease the degradation rate and stress corrosion cracking susceptibility of the biodegradable magnesium alloy, a MAO/PLGA composite coating prepared on the ZKJ400 (Mg-4Zn-0.6Zr-0.4Sr) alloy was investigated. The stress immersion tests, the slow strain rate tensile tests and electrochemical technique were used. The pores on the MAO film were sealed by the PLGA, and the composite coatings were tightly bonded on the substrate. The surface coating has retarded the corrosion process of ZKJ400 substrate. Compared with that of the uncoated alloys, the corrosion current density of MAO coated alloys decreased by two orders of magnitude, while that of composite coating alloys decreased by three orders of magnitude. Our results showed that the applied stress could significantly accelerate the corrosion process of biodegradable ZKJ400 alloy. The tensile strength of the uncoated alloys decreased by 75% after 14 d immersion, and decreased by 90% under a stress of 20 MPa. After 28 d immersion under stress, the MAO coated samples were found broken, however, the tensile strength of the MAO/PLGA coated alloys decreased only by 10%. The stress corrosion cracking susceptibility of the MAO/PLGA composite coating alloy was the lower, and the fluctuation of the potential during the slow tensile process was smaller than the uncoated and MAO samples. The results indicated that the MAO/PLGA composite coating could greatly improve the corrosion resistance and slow down the decay process of mechanical properties of the ZKJ400 alloy, either static or under applied stress.

Keywords: composite coating, magnesium alloys, stress corrosion, mechanical integrity

Surface engineering design of ceramics to improve tribological properties

Yongsheng Zhang, Hengzhong Fan, Junjie Song, Yunfeng Su, Litian Hu
(State Key Laboratory of Solid Lubrication, Lanzhou Institute of Chemical Physics,
Chinese Academy of Sciences, Lanzhou 730000, China)
zhysh@licp.cas.cn

Abstract: The three-dimensional lubricating layer on ceramic surface realizes the integration of structure and lubricating function in ceramic materials, which can achieve the outstanding lubricating properties and keep the excellent mechanical properties of ceramic itself, thus solving special lubrication and wear failure in mechanical system under extreme conditions (e.g., corrosive environment, wide-temperature condition). In the present study, based on the experiment research and theoretical simulation, two kinds of self-lubricating structural ceramics with high-reliability were designed and prepared, which can achieve stable and effective lubrication under water environments and wide-temperature range conditions. Those are alumina/nickel and alumina/molybdenum laminated composites suitable for use in a water environment and wide-temperature range conditions, respectively. The relation between surface microstructure of the prepared materials and their properties was investigated. The results indicated that through bionic, surface micro-structure and three-dimensional lubricating design of the materials, which helped to realize the integration of structure and lubricating function of the ceramic composites and further improve their lubricating and practical properties. Through the systematic research on the tribological behavior under different environments and test conditions as well as the relation among the structure, composition and properties of these two kinds of materials, factors which can influence the tribological behavior and wear failure of the above materials were proposed and the theoretical models of the relation between structural parameters and performance of the materials were built. These provided theories and technologies for preparation and application of high performance lubricating materials that can be used in corrosive and wide-temperature range environments.

Keywords: ceramic, tribological properties

Microstructure and high temperature oxidation resistance property of packing Al cementation on TA15 alloy

Hong Tian¹, Chunyan Jiang², Yaming Wang², Guoliang Chen², Huai Cai², Xuewei Li¹
(1. Heilongjiang University of Science and Technology; 2. Harbin Institute of Technology)
tianhonghappy2008@163.com.cn

Abstract: The aluminized coating was prepared on TA15 titanium alloy by pack cementation to enhance the high temperature oxidation resistance for aerospace application. The microstructure and phase composition of the coating were characterized by SEM and XRD, respectively. The results show that the compact coating was composed of TiAl₃ with about 60 μm thick. High temperature oxidation behavior of packing cementation coated and uncoated TA15 alloy samples were comparatively investigated by isothermal oxidation at 800 °C and 900 °C in air. After oxidation at 800 °C for 100 h, the oxidation weight gain of the TA15 alloy sample was 3.20 mg cm⁻², while the oxidation weight gain of the aluminized coating sample was 1.29 mg cm⁻², registering as 1/3 of TA15 alloy. After oxidation at 900 °C for 100 h, the oxidation weight gain of the TA15 alloy sample increased up to 20.33 mg cm⁻², while the oxidation weight gain of the aluminized coating sample was only 4.06 mg cm⁻², about 1/5 of TA15 alloy. The aluminized coating exhibits potential application for improving oxidation resistance of TA15 alloy.

Keywords: titanium alloy, pack cementation, oxidation resistance, high temperature

The effect of ladder region on the atom adsorption of Si (111) substrate

Wenxin Li¹, Dongying Ju²

(1. Department of Electronic Engineering, Graduate School of Engineering, Saitama Institute of Technology;
2. Advanced Science Institute, Saitama Institute of Technology)

wwenxindiaolong@163.com

Abstract: STM results showed that different atoms were deposited on Si (111)-7×7 reconstructed surface, with or without ladder region. The latest progress of the dynamic phenomenon on solid surface is summarized, including 3 compound types in adsorption process: Strong compound, weak compound, and the new quasi-strong compound. Different compounds correspond to different surface potential energy, a newly formed surface is stabilized by a quasi-potential made by breaking, and adsorbed atoms or molecules can be stabilized by forming ‘quasi’ compounds. In this paper, the ladder region is an excellent perspective to compare and observe the mechanism of atomic adsorption. Through STM images and mass spectrometer, CH₃OH adsorption model was proved. Au and Fe atoms were steamed on the Si(111)-7×7-CH₃OH surface and were compared to the situation on the ladder region. In order to further improve the probability of linear structure, we have explored their formation process and compound models. With the intervention of methanol as an interlayer, the linear structure of metal atoms is disrupted. Under the influence of a relatively weak interaction, the gold atom cannot form a linear structure even in the ladder region. Unlike the previous strong compound Fe, the new quasi-strong compound Fe remained its linear structures after methanol isolation and weakening, especially in ladder region. These investigations are believed that there is a certain extent promotion to form metal linear compounds on restructured Si(111)-7×7 surface with CH₃OH, especially according to the coating and surface technology we adjusted.

Keywords: STM, CH₃OH, ladder region, quasi-compounds, linear

Effect of temperature on hot-dip galvanized Zn-0.05%Al coating with the application of the ammonium-free fluxing process

Dedong Wang, Shengmin Wang, Jingang Liu, Xiaojun Zhao, Mingyi He, Guoxiong Huang, Rong Tan
(Kunming University of Science and Technology)

wsmkm2000@sina.com

Abstract: With the application of the ammonium-free fluxing process, to examine the effect of bath temperature on the quality and the microstructure of Zn-0.05%Al coating, the surface quality, thickness and microstructure of the coating were characterized using the macro observation, scanning electron microscopy and energy-dispersive X-ray spectroscopy. The results showed that when the bath temperature of Zn-0.05%Al alloy is 430 °C to 470 °C, the temperature has no effect on the surface quality of the coating, in terms of the skip plating rate, surface particle adhesion, and glossiness. Moreover, the thickness of the coating increases parabolic with an increase of bath temperature. Aluminum has an inhibitory effect on the growth of the alloy layer, and the inhibition effect becomes weaker with the increase of bath temperature. The results showed that the alloy layer in the coating is incomplete and the microstructure is fine at low bath temperature, the thickness of the alloy layer increases and the microstructure becomes coarse with the increase of bath temperature.

Keywords: ammonium free fluxing progress, hot-dip galvanized aluminum alloy, coating quality, coating microstructure

Preparation of surface TaC layer reinforced Ta-10W alloy by in situ solid-phase

Haiqiang Bai¹, Lisheng Zhong¹, Zhao Shang¹, Yunhua Xu¹, Baowei Cao², Yingchun Ding³

(1. School of Material Science and Engineering, Xi'an University of Technology;

2. School of Chemistry and Chemical Engineering, Yulin University;

3. College of Optoelectronics Technology, Chengdu University of Information Technology)

zhonglisheng1984@163.com, xuyunhua0107@163.com

Abstract: A TaC layer with a thickness of about 15 μm was prepared by an in situ solid-phase diffusion reaction on the surface of Ta-10W alloy at 1130 $^{\circ}\text{C}$ for 10 h. The phase constitution, microstructure, nanoindentation hardness and elastic modulus of the carbide coating were investigated using X-ray diffraction (XRD), scanning electron microscopy (SEM), electron backscattered diffraction (EBSD) and nanoindentation testing. The results show that carbide layer, which is predominantly composed of TaC phase, exhibited a completely dense and pore-free microstructure with metallurgical adherence to the substrate. The TaC phase grows mainly along the {100} orientation and the average grain size of TaC is approximately 438 nm. Thermodynamic calculations show that TaC has lower Gibbs free energy than WC, so TaC is more stable and easier to form. When the cast iron and Ta-10W alloy contact at the atomic scales at 1130 $^{\circ}\text{C}$, the interstitial carbon atoms in the cast iron diffuse into the Ta-10W alloy to preferentially react with the Ta atoms to form the TaC layer, whereas the metallic W existed mainly in the elemental form in the layer. The inward growth of the TaC layer is controlled by the diffusion of carbon atoms. The nanoindentation hardness of TaC layer is 25.1-27.9 GPa, which is about 6 times of the Ta-10W alloy (4.4 GPa). The elastic modulus of TaC layer is 500.8-521.6 GPa, which is about 2 times of the Ta10W alloy (238.3 GPa). The enhancement of the mechanical properties may be due to the formation of the ultrafine TaC.

Keywords: tantalum carbide, solid-phase diffusion, microstructure, mechanical properties, EBSD

Alumina growth behavior on surface-modified NiCoCrAl alloy by

Pt and Hf at high temperature

Chao Li, Peng Song, Kunlun Chen, Asim Khan, Jiansheng Lu

(Faculty of Materials Science and Engineering, Kunming University of Science and Technology)

songpengkm@163.com

Abstract: At present, a lot of studies have been modified to MCrAlY alloy by adding REs to improving the oxidation resistance of alumina, but it is not clear when direct surface-modified NiCoCrAl alloy by Pt and Hf. In this study, alumina layer of NiCoCrAl alloy modified with magnetron sputtering, the growth behaviour of the surface-modified NiCoCrAl alloy by Pt and Hf at 1050 $^{\circ}\text{C}$ in air was investigated respectively. The cyclic oxidation resistance has been greatly improved when change the doping order of Pt and Hf. NiCoCrAl alloy had extremely serious oxide scale spallations. More Pt particles agglomerated over the NiCoCrAl + Hf + Pt alloys surface to constitute irregular polyhedron particles and a lower TGO growth has been observed for the NiCoCrAl+Hf+Pt alloys. The spinel (NiCr_2O_4) as second-phase in the oxide layer of NiCoCrAl + Hf alloys resulted in the internal diffusion of oxygen is accelerated. The volume of Al_2O_3 changed when metastable phase ($\delta\text{-Al}_2\text{O}_3, \theta\text{-Al}_2\text{O}_3$) transition to a stable phase ($\alpha\text{-Al}_2\text{O}_3$), it leads to formation of voids at NiCoCrAl + Pt alloys surface in the initial stage of oxidation.

Keywords: doping order, NiCoCrAl alloy, oxidation, diffusion

Microstructure and corrosion behavior of different cladding regions of multi-track laser cladding Ni-based alloy coating

Qinying Wang, Shuang Liu

(School of Materials Science and Engineering, Southwest Petroleum University)

wangqy0401@126.com, liushuang62@126.com

Abstract: region, microstructure, corrosion behavior, SKP Multi-track Ni-based alloy coatings were prepared on steel substrates by a high power diode continuous laser cladding technique. The microstructure and corrosion behavior of the overlapping (C1) and non-overlapping (C2) regions on the surface of the achieved coatings were investigated. The observation of the microstructure showed that a dendritic structure and an equiaxed cellular structure were dominant at regions C1 and C2, respectively. Meanwhile, both C1 and C2 were mainly composed of primary phase γ -nickel with the solution of Fe, W, and Cr. In addition, the electrochemical results indicated that C2 displayed a lower corrosion current density and a lower density of defects than C1, revealing a higher corrosion resistance. Meanwhile, a higher surface potential at the surface of C2 tested by using a scanning Kelvin probe was found compared with that at the surface of C1, indicating a lower corrosion tendency. Generally, overlapping and non-overlapping regions of the multi-track Ni-based alloy coating displayed differences in both microstructure and corrosion resistance, which will significantly influence the application of the laser cladded coatings.

Keywords: multi-track Ni-based alloy coating, laser cladding, cladding

Effects of MTMS water content on morphology and corrosion resistance of non-chromium Zn-Al coatings

Jiangjiang Huang, Guan Wang, Jiawei Liao

(Guangdong University of Technology)

178353218@qq.com

Abstract: In this paper, a non-chromium Zn-Al coating was prepared using methyltrimethoxysilane (MTMS) as binder at a sintering temperature of 250 °C. Investigations were carried out on three coatings containing 30%, 40% and 50% water content of MTMS. The morphologies, phases and compositions of the coatings prepared with 30%, 40% and 50% water content of MTMS were observed with scanning electron microscope; X-ray diffract meter and Fourier transform infrared spectroscopy. The effect of MTMS water content on the corrosion behavior of Zn-Al coating was investigated by potentiodynamic polarization test and immersion test. The coating with good surface quality can be fully formed under sintering temperature of 250 °C. XRD results indicated that Al_2O_3 and a small quantity of ZnO existed in the coating prepared with MTMS with 40% water. The coating prepared with MTMS hydrolysate with 40% water content had better corrosion resistance.

Keywords: non-chromium Zn-Al coating, surface morphology, sintering temperature, MTMS water content, corrosion resistance

Comparative study on corrosion behavior of Mg-Zn-Ca metallic glass in deionized water, simulated seawater and simulated body fluids

Xin Wang, Shuiqing Liu, Lichen Zhao, Peng Chen, Dongxu Jiang, Chunxiang Cui
(Hebei University of Technology)

ahaxin@hebut.edu.cn

Abstract: Mg-Zn-Ca metallic glasses (MGs) have been widely concerned due to their good mechanical properties, biodegradability and excellent capability to degrade azo dyes. In essence, functional applications in the fields of biomaterials and water treatments relate to the same basic chemical process on the surface, namely the degradable/corrosive behavior of Mg-Zn-Ca BMGs in the corrosive media involved. However, the corrosion behavior of MgZn-Ca BMGs in different corrosion mediums still is lacking in detailed experimental comparison. In the present work, we study the corrosion behavior of Mg₆₆Zn₃₀Ca₄ bulk metallic glass (BMG) in three typical corrosive medium solutions including deionized water (DW), 3.5wt% NaCl solution (ASW) and simulated body fluid (SBF) for the first time. The macroscopic corrosion behavior and microscopic morphology evolution on the surface of Mg₆₆Zn₃₀Ca₄ BMG in the above three corrosive mediums was examined and compared in detail. It has been found that corrosion process of Mg₆₆Zn₃₀Ca₄ BMG is sensitive to the ion concentration of corrosive medium solution and the presence of large amounts of chloride ions accelerates its corrosion and degradation processes. However, the chloride content is not the only factor that limits its corrosion rate. We also found that the abundant various ions in SBF also accelerate the corrosion of Mg₆₆Zn₃₀Ca₄ BMG, leading to faster degradation of the BMG in SBF than that in ASW. Although the corrosion rate is faster in SBF, the evolution of hydrogen is strongly inhibited in SBF by comparing with DW and ASW. We believe that the formation of ZnO-like whiskers which delays the cracking and shedding of the deposited Ca/P layer. Our work is of great significance for an in-depth understanding of the corrosion behavior and corrosion mechanism of amorphous Mg-ZnCa alloys. The main conclusions are as following:

- 1) The macroscopic mass loss of Mg₆₆Zn₃₀Ca₄ (MZC) BMG in the used corrosive medias gradually decreased in the order of SBF>ASW>DW. The short-term erosion mass loss of MZC in DW and ASW was not obvious, but in SBF, it has a wave-like curve caused by the crossover deposition and shedding of Ca/P layer.
- 2) The hydrogen evolution rate of MZC in different solutions gradually decreases in the order of ASW>DW>SBF, which is not proportional to the mass loss. Different kinds of ions in SBF have the coupling effect of inhibiting the precipitation of hydrogen.
- 3) The potentiodynamic polarization curve shows that the corrosion resistance of MZC in SBF is good and significantly higher than that of pure Mg. However, in ASW, MZC and Mg show closed corrosion resistance, due to the similar passivation behavior.
- 4) The corrosion behavior of MZC BMG in DW and ASW is similar and NaCl in ASW only accelerates the dissolution of Mg without changing the chemical reaction mechanism. However, it is significantly different in SBF that the formation of ZnO-like whiskers delays the cracking and shedding of the deposited Ca/P layer.

Keywords: Mg-Zn-Ca, corrosion, bulk metallic glass, surface morphology

Effect of N₂ flow rate and annealing holding time on microstructure and properties of Ti₂AlN thin films

Chen Zhe, Zhang Guojun

(School of Materials Science and Engineering, Xi'an University of Technology)

zhangguojun@xaut.edu.cn

Abstract: The material of Mn+1AX_n ($n=1,2,3$) is a kind of ternary layered new material and its crystal structure is hexagonal crystal system. It is widely concerned by many scholars for the performance of both metals and ceramics, such as good electrical-thermal conductivity, high melting point, excellent thermal shock resistance and machinability etc. The most prominent is high temperature oxidation resistance and high temperature corrosion resistance. There are more than 100 MAX phase materials found so far, and Ti₂AlN is a typical MAX phase.

The purpose of this research is to optimize the preparation technology of Ti₂AlN films by changing the N₂ flow rate and annealing time of heat preservation, and to study influence of N₂ flow and annealing time on the microstructure properties of the films. Ti-Al-N thin films were prepared by magnetron sputtering ion plating technology, and Ti₂AlN phase was prepared by vacuum annealing treatment. The microstructure of the film was observed and analyzed by X-ray diffraction, scanning electron microscope, atomic force microscope and transmission electron microscope. The hardness and elastic modulus of Ti₂AlN films were tested by nano indentation apparatus. The oxidation resistance of the film was analyzed by oxidation test.

The results show that the Ti, Al atom ratio of 2:1 Ti-Al compound target preparation of TiAl-N films are mainly in the form of amorphous, N₂ = 4, 5, and 6 sccm three sets of samples, after vacuum 700 °C annealing processing, The Ti₂AlN phase in the film is detected, only crystallization degree is different, The samples of N₂=5 sccm crystallization degree is better. And N₂=7 sccm, after 700 °C vacuum annealing, the Ti₂AlN phase is not detect, due to excessive N₂ is priority and Ti atoms to form TiN. The samples of N₂=5 sccm were successively maintained for 30, 60, 90 and 120 minutes. The results of Xrd show that the crystallization effect of Ti₂AlN is best when heat preserved for 60 min. With the increase of the holding time, the crystallization of Ti₂AlN phase is promoted, and the partial decomposition of Ti₂AlN phase occurs when prolongs the holding time. Therefore, N₂=5 sccm, 700 °C annealing, 60 min heat preservation, the optimum process of pure Ti₂AlN phase is obtained. The surface roughness of the sample is about 7.2 nm after atomic force microscope test. The hardness of the pure Ti₂AlN phase is about 33.2 GPa, and the elastic modulus is about 374.8 GPa. After being oxidized in air at 700, 800, 900, and 1000 °C for 2 h, the surface morphology of the sample was relatively flat. After oxidation at 700 °C and 800 °C, TiO₂ formed on the surface was attached to the surface of the film. And after oxidation at 900 °C and 1000 °C for 2 h, a dense Al₂O₃ oxide film was formed on the surface to prevent further reaction of oxygen, which acted as a protective film and made the film have good oxidation resistance.

Keywords: magnetron sputtering, heat treatment

The study on preparation and antioxidant properties of FeCrAlY coatings by magnetron sputtering

Qi Ji, Guojun Zhang

(School of Materials Science and Engineering, Xi'an University of Technology)

zhangguojun@xaut.edu.cn

Abstract: With the depletion of traditional energy sources and increasingly serious environmental problems, new types of clean energy are getting more and more attention. Nuclear power is not only continuous and stable, but also more economical and efficient compared with wind power and hydropower. Since the Fukushima nuclear accident in 2011, nuclear energy research and development have been focusing on improving the capacity of nuclear reactor accident from the conversion of nuclear fuel, among which, researching and developing accident tolerant fuel was one of the effective measures to prevent serious nuclear accidents.

Fuel cladding is one of the most important components in nuclear fuel system, and the choice of better performance of cladding material is the key to develop accident tolerant fuel. Molybdenum alloy can completely meet the requirements of new cladding material for the advantages of high melting point, good thermal shock resistance, high temperature stability, no reaction with hydrogen, etc. Thus, molybdenum alloy cladding is proposed one of the most promising new cladding materials in the world. However, molybdenum is easily oxidized to generate volatile MoO₃ at high temperature which make it necessary to prepare protective coating on the surface of molybdenum alloy in order to protect it from high temperature in case of good mechanical properties.

In this paper, using magnetron sputtering ion plating technology, different Al/Y content and different thickness FeCrAlY coatings were prepared on the molybdenum alloy substrate by changing the Al/Y inlay target current and deposition time. The microstructure, mechanical properties, high pressure corrosion resistance, and high temperature vapor corrosion resistance of the coating were analyzed and tested; the effect of Al/Y target current and deposition time on the microstructure and mechanical properties of the coating was revealed, and the coating was analyzed. The corrosion resistance mechanism.

With the increase of Al/Y target current, the Vickers microhardness of the film increased gradually and the coating was Fe/Cr solid solution and the bonding force was good. At the same time, the surface roughness of the film decreased gradually. The corrosion test of FeCrAlY coatings on Mo substrates were carried out under different test conditions. Under the condition of 360 °C\18.6 MPa\72 h, the corrosion rate of Mo substrate was 4.2 mg/dm² and the morphology was not changed after corrosion test.

Keywords: magnetron sputtering, molybdenum alloy, FeCrAlY coating, bonding strength, corrosion

Effect of different phase structures caused by Mo content on corrosion behavior of Al-Mo alloy thin films

Caixia Wang

(School of Materials Science & Engineering, Xi'an University of Technology)

wangcaixia520@126.com

Abstract: The aluminum-refractory transition metal (Al-RM) systems are particularly research focus in the metallic thin film area due to their particular structures and excellent performances. The research on their corrosion behavior is an important area. And the composition of alloy film is the main focus of previous studies. Recently, an intriguing observation arose from many researches was that the phase structure of alloy would have crystalline-amorphous transitions with variation of alloy composition. Hence, for a specific Al-RM system which is accompanied with phase transformation, the corrosion behavior is no longer dominated only by the composition of alloy, perhaps affected by the phase structure at the same time. However, this case has not been given attention in the present studies.

In this study we prepared Al-Mo thin films with fcc solid-solution, amorphous and bcc solid-solution phase structure respectively. Then the corrosion behavior of them was investigated via considering the synergy of composition and phase structure in the course of exposure to 3.5 M NaCl solution. The study found that, as a kind of “dissolution moderators” element, the addition of Mo improved the corrosion properties of Al alloy films dramatically. Whereas, this trend did not monotonously change with the increase of Mo content, but affected simultaneously by the phase structure. The amorphous alloy film displayed the homogeneous feature of composition and chemistry and exhibited tiny surface roughness. The passive film of it was continuous, uniform and compact, thus there was nearly no the formation of pitting nucleation on its surface until the potential rose to 0V. In addition, the homogeneity of amorphous phase and the enrichment of Mo were all conducive to enhance the corrosion resistance of alloy film. Thus, the film exhibited extremely excellent corrosion resistance with more positive potential, smaller corrosion current and large charge transfer resistance. The Mo base solid-solution alloy film with the highest Mo content grew up by the Stranski-Krastanov mode and exhibited three-dimensional heterogeneity. Meanwhile it displayed a large surface roughness. Both of them lead to the passive film was unstable and been attacked to form pitting nucleation. Whereas, the pitting nucleation was repaired subsequently via the formation of new passive film by the action of corrosion inhibition of sufficient Mo and the timely diffusion of O. Thus, the alloy film could maintain the stable passivity renewedly. Nevertheless, the existence of second-phase of Al would be a potential danger if the potential went up further. The Al base solid-solution alloy film had similar growth pattern with Mo base solid-solution alloy film and was inhomogeneous. The passivity of it was very unstable and the pitting was occurred easily on the surface of film. And that the pitting nucleation could not be repaired timely because of Mo content was so little that not insufficient to impede the Cl⁻ diffusion. Furthermore, the presence of a small amount of amorphous phase and the relatively small crystalline size all played a role to accelerate the corrosion process. So, the corrosion resistance of it was the worst.

Keywords: phase structure, corrosion behavior

Corrosion behavior of plasma electrolytic oxidation coated AZ31 and AZ91

Mg alloys: the influence of laser surface melting pretreatment

Can Liu¹, Bailing Jiang², Jun Liang³

(1. NanJing Tech University; 2. Corrosion resistance; 3. Lanzhou Institute of Chemical Physics)

liucan9933@163.com

Abstract: In recent years, magnesium (Mg) alloys are attractive for the automotive, electronics and aerospace industries due to their low density and adequate strength to weight ratio. However, the practical application of Mg alloys is often limited by their high susceptibility to corrosion, which is primarily attributed to the high chemical activity of Mg and to the unstable imperfect natural oxide film on its surface. Plasma electrolytic oxidation (PEO) is one of the most effective methods for corrosion protection of Mg alloys, because it can produce a relatively thick, dense and well adherent ceramic-like coating. Many works have proved that the PEO coatings can significantly enhance the corrosion resistance of Mg alloys in short term. Unfortunately, there exist many inherent defects including micro-pores and micro-cracks in the PEO coating, which resulted from the continual intense sparking discharge and gas evolution on the substrate surface, as well as the low Pilling-Bedworth ratio of Mg oxide to metal substrate. A number of attempts have been made to enhance the long-term corrosion performance of PEO coatings on Mg alloys. One solution is to optimize preparation parameters of PEO coating including electrolyte and power supply to reduce the generation of defects and increase the content of stable compounds. However, this solution usually requires precise control of preparation parameters, which increases the difficulties in production of PEO coatings. Another solution is to seal the micro-pores and micro-cracks of the PEO coatings by post treatments. Nevertheless, the inherent properties of the PEO coatings such as porosity, insulativity and scratch/wear resistance, may thus be deteriorated or even shielded. So, it is important to develop new methods that can improve long-term corrosion performance of PEO coatings on Mg alloys under common preparation conditions. Studies indicated that the corrosion properties of PEO coated Mg alloys not only depend on the microstructure and composition of PEO coating, but also on microstructure characteristics of the substrate. In this work, top ceramic coatings were fabricated on the laser surface melting (LSM) modified AZ31 and AZ91 Mg alloys by PEO in phosphate electrolyte. The microstructure, composition and corrosion behavior of the LSM, PEO and LSM-PEO treated AZ31 and AZ91 Mg alloys as well as the as-received alloys were investigated, respectively. Especially, the effect of LSM pre-treatment on the longterm corrosion resistance of the PEO coated Mg alloys was evaluated. Results showed that the LSM treatment had no obvious influence on the phase composition and microstructure of the PEO coatings on AZ31 and AZ91 alloys, whereas the corrosion properties of the PEO coated Mg alloys after LSM treatment revealed large enhancement. The improvement of corrosion resistance of LSM-PEO coated AZ31/AZ91 Mg alloys was closely related to the changed microstructure characteristics and improved corrosion resistance of the substrates. Moreover, LSM pre-treatment led to larger changes to corrosion resistance of PEO coated AZ91 alloy compared to PEO coated AZ31 alloy. This phenomenon was clearly related to relatively large change of microstructural characteristics of AZ91 alloy before and after LSM treatment, indicating that the corrosion properties of substrates played a key role in the corrosion resistance of PEO coated Mg alloys.

Keywords: magnesium alloy, plasma electrolytic oxidation, laser surface melting, corrosion resistance

The preparation and characterization of different crystal of

PbO₂ in methanesulfonic acid

Xiaofei Luo

(Xi'an University of Technology)

luoxiaofff@163.com

Abstract: In this paper, the influence of H⁺ concentration, temperature and sedimentary current density on the crystal form of PbO₂ in the methanesulfonic acid was studied, and the α -PbO₂, β -PbO₂ and mixed sediments with specific crystal proportion were prepared by controlling the deposition conditions to investigate the discharge capacity, conductivity as well as intergranular stress of different sediments as positive active materials. Meanwhile the effect of these properties on the discharge capacity and intergranular bonding force of the active sedimentary layer were compared, and optimizing the best crystal ratio of PbO₂ as the active material of positive electrode in order to improve the coulombic efficiency and energy efficiency of the lead methanesulfonic flow battery.

The results showed that: 1) By controlling the concentration of H⁺, temperature and current density of the solution in the electrodeposition conditions, α -PbO₂, β -PbO₂ and different ratios of two-phase mixed sediments can be obtained. The increase of H⁺ concentration and current density all improve the overpotential of the electrodeposition, which lead a transition of the sediments from the single phase of α -PbO₂ to the mixed phase of α -PbO₂ and β -PbO₂, and the increase of temperature accelerates the mass transfer process and promotes the formation of β -PbO₂. 2) The discharge capacity of β -PbO₂ is two times that of α -PbO₂. While during thirty times of cyclic charge and discharge process, the stability of coulombic efficiency of α -PbO₂ is higher than that of β -PbO₂. Compared to the other three kinds of positive active material of PbO₂, the discharge capacity reaches the highest when the mass ratio of α -PbO₂ and β -PbO₂ in the mixture is 2:8, and at this time, the coulombic efficiency of cyclic charge and discharge as well as energy efficiency also reach the highest of 95% and 76% respectively with a good cyclic stability as well. 3) The charge-transfer resistance of β -PbO₂ is the minimum which is easier to be dissolved electrochemically, the mixture of α -PbO₂ and β -PbO₂ with a mass ratio of 2:8 takes the second place and that of α -PbO₂ is the maximum. However, the oxygen exchange current density of the mixture is the least which is hard for oxygen evolution, β -PbO₂ takes the second place and that of α -PbO₂ reaches the highest. 4) The mixed deposition layer with a mass ratio of 2:8 of α -PbO₂ and β -PbO₂ is no crack, small internal stress and tight bonding between grains, and the loss of active substances in the discharge process is the least.

Keywords: PbO₂, lead methanesulfonic

Effect of carbon-foam composite coating electrode on the power storage performance of lead-acid flow battery

Dongdong Ji
(Xi'an University of Technology)
895943309@qq.com

Abstract: The lead-acid flow battery is expected to be applied to large scale distributed energy storage power station to solve the problems of non steady state of renewable energy and the dilemma of remote districts that are not accessible to the State Grid, etc. The core of distributed energy storage power station is to develop large capacity, high performance and low cost energy storage system. According to that the permanence of reversible conversion that Pb^{2+} in solution store electricity with the form of solid PbO_2 and Pb ; the low cost of single fluid flow without membrane; the flexibility of power and capacity can be adjusted by the logarithm of electrode and the concentration of Pb^{2+} ; the environmental protection of the residual storage layer can be recovered by H_2O_2 and reach no pollution, the lead-acid flow battery have caused the high attention of the field of distributed energy storage power station. Electrode is an important part of lead-acid flow battery, and the physical and chemical characteristics of that determine the storage property of the battery directly. The conventional graphite plate electrode showed the poor conductivity, low specific surface area and lower hydrogen evolution potential. So the battery showed severe negative dendrite, the lower and unstable charge-discharge efficiency, etc.

Based on this, the paper seeks to study the effect of porous composite coating material on the charge/discharge performance and positive-negative active sedimentary layer of leadacid flow battery compared with traditional graphite plate(graphite plate).The carbon foam matrix was prepared by direct foaming method using mesophase pitch as matrix. The carbon foam after compound with copper/lead coatings has the properties that open porous structure, the larger specific surface area, excellent conductivity, low hydrogen overpotential after composite lead coating and higher bond strength with the storage electric lead layer based on homogenous lead binding, etc. Carbon foam composite coating used as negative electrode of lead-acid flow battery can effectively disperse charge and inhibit dendritic growth in negative Pb deposition, and the negative active deposition Pb layer particles is uniform and delicate. Moreover, maybe due to the uniform and dense distribution of the electric field influence on distribution of Hydroxyl radical on positive electrode, the PbO_2 particles on the corresponding positive electrodes are fine and compact. The common effect of many excellent characteristics reduces the difference between charge/discharge voltage, improves battery cycle efficiency and charging capacity. The charging voltage is low (low voltage 1.7436 V) and rises slowly, the discharge platform is higher (1.6059 V) and the stability is good. Cycle efficiency is higher that coulombic efficiency 93%-95%, voltage efficiency 89%-90%, energy efficiency 83%-85%. The electrode surface capacity can be increased to 50 mAh/cm² and the coulombic efficiency will be stable at about 96%. Meanwhile, the carbon foam composite coating electrode can improve the fast charge/discharge performance of the battery effectively.

Keywords: carbon-foam composite coating, active sedimentary layer, power storage performance

Effect of plating flow rate on microstructure and properties of jet-electrodeposited Co-Ni alloy coating

Jun Tan, Xiong Ye

(Science and Technology on Remanufacturing Laboratory, Army Academy of Armored Forces)

tanjuncn@sina.com

Abstract: In order to investigate the effect of plating solution flow rate on the composition, microstructure and performance stability of Co-Ni alloy coating, Co-Ni alloy coating was prepared by jet-electrodeposition on the surface of brass substrate with the current density kept at 40 A/dm² and the nozzle moving speed kept at 1.2 mm/s. The plating solution flow rate is 2, 2.5, 3, 3.5, 4, 4.5 L/min, and the Co²⁺/Ni²⁺ ratio in plating solution is 2:1, 1:1, 1:2, 1:3. The surface morphology of the coating was observed by scanning electron microscopy (SEM). The content of elements in the coating was determined by EDS, and the influence mechanism of plating solution flow rate on the composition and morphology of the coating was discussed. The phase structure of the coating was analyzed by X-ray diffraction (XRD). The hardness and wear resistance of the coating were measured using a microhardness tester and a friction and wear tester. The results show that with increasing the flow rate of the plating solution, the Co content in the coating increases, the crystal grains on the surface of the plating layer are significantly refined, and the hardness increases. However, the flow rate of the plating solution does not affect the grain growth orientation, and the phase structure is determined by the element content of the plating layer. When the Co content is more than 80%, the coating is a single hcp phase. When the Co content is less than 80%, the hcp phase and the fcc phase coexist. When the Co²⁺:Ni²⁺ in the bath is 2:1 and 1:1, the microstructure of the coating is stable and all of them are single hcp phases. The variation range of the Co content is 0.63% and 1.67% respectively, and the microhardness of the coating changes, of which the variation range is 6 HV and 14 HV respectively, and the change in wear volume was 0.016 mm³ and 0.02 mm³ respectively. When the plating solution of Co²⁺:Ni²⁺ is 1:2 and 1:3, the fluctuations of the Co content in the coating are 6.75% and 8.54% respectively. The microstructure of the coating both appear to change from a mixed fcc+hcp phase to a single hcp phase. The variation range of the microhardness of the coating was 28.7 HV and 106 HV respectively, and the variation range of the wear volume was 0.02 mm³ and 0.135 mm³ respectively. The mechanism study indicates that the Co-Ni co-deposition process is an abnormal co-deposition. Co deposition is mainly controlled by the mass transfer of Co²⁺, and Ni deposition is controlled by the reaction activation. Increasing the flow rate of the plating solution reduces the concentration polarization near the cathode, and leads to the increasing of Co content in the plating layer. At the same time, increasing the flow rate of the plating solution reduces the thickness of the cathode diffusion layer, and the grain of the plating layer is significantly refined.

Keywords: Co-Ni alloy, flow rate, jet-electrodeposition

Table 1 Composition of the bath

Components	bath 1	bath 2	bath 3	bath 4
NiSO ₄ · 6H ₂ O/(g L ⁻¹)	100	150	200	225
CoSO ₄ · 7H ₂ O/(g L ⁻¹)	200	150	100	75
NaCl/(g L ⁻¹)	20	20	20	20
HBO ₃ /(g L ⁻¹)	30	30	30	30

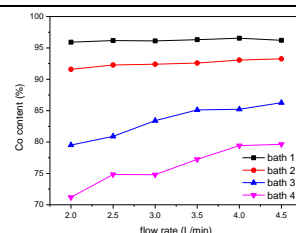


Fig.1 Co content in the plating layer varies with the flow rate of the plating solution

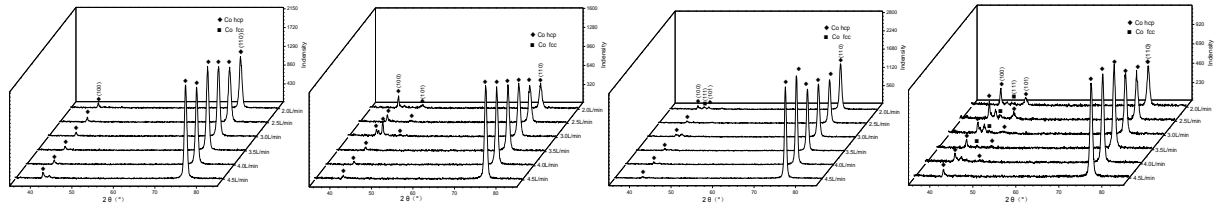


Fig.2 Effect on phase structure: bath1, bath2, bath3, bath4

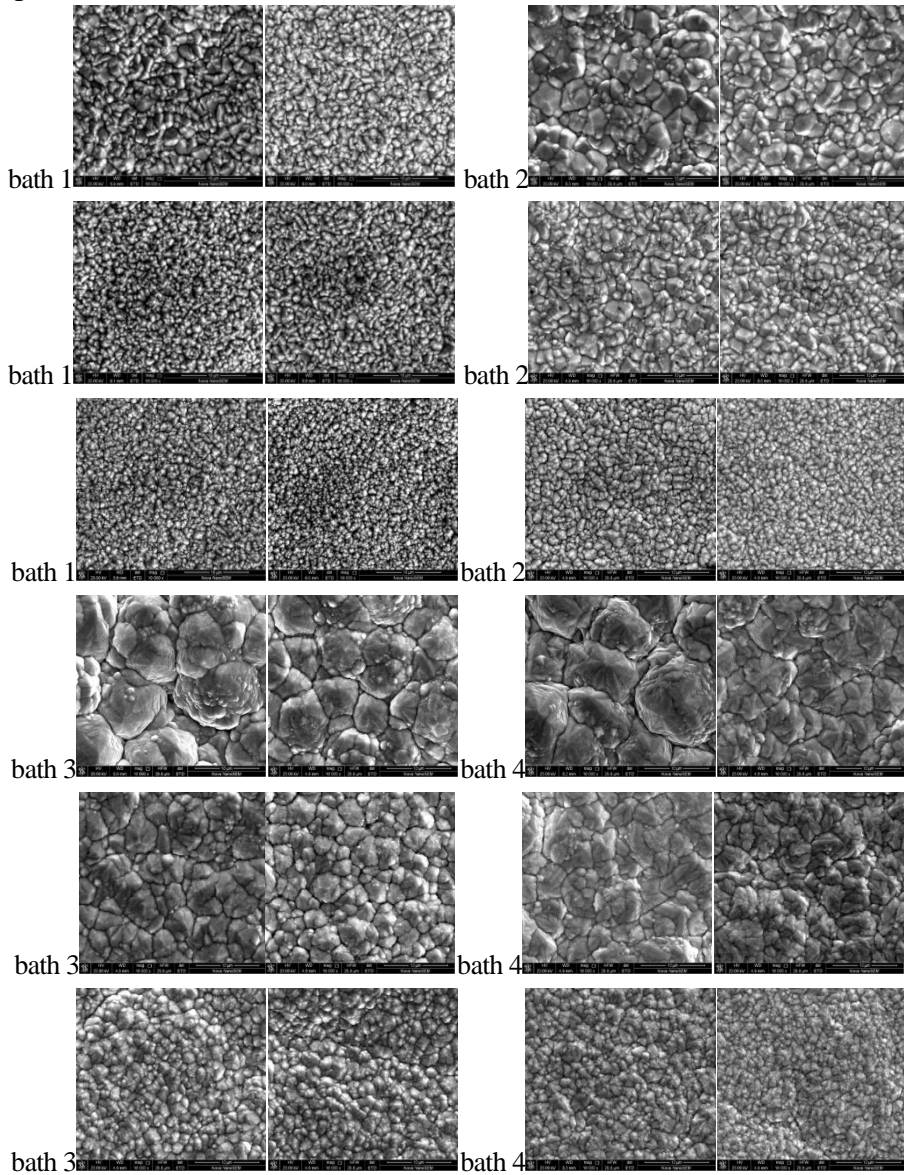


Fig.3 Effect on surface morphology

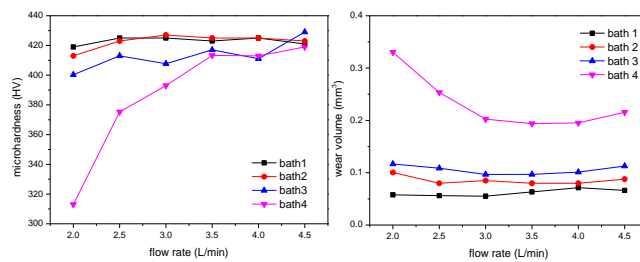


Fig.4 Effect on microhardness and wear volume

Wear behavior of ceramic coatings formed by microarc oxidation on 7N01 aluminium alloy

Ailian Bao, Wanhui Liu, Jianxin Zhang, Zhongyuan Wei, Yunxiao Fang

(Department of Chemistry and Material Engineering, Changshu Institute of Technology, Changshu, China)

liuwh@cslg.edu.cn

Abstract: In this paper, wear resistant coatings were prepared on 7N01 Al alloy by micro-arc oxidation (MAO) technique in alkaline sodium aluminate solution. The microstructure characterization of MAO-treated samples were carried out by scanning electron microscopy (SEM). Fig.1 shows SEM morphology of coatings formed on 7N01 Al alloy samples at different concentrations of NaAlO₂. The tribological behavior of the coatings was investigated under dry sliding condition using linearly reciprocating ball-on-flat wear test. The results showed that the MAO coatings exhibited a friction coefficient of about 0.5 against the GCr15 steel ball as the friction partner (Fig.3). After MAO treatment the wear rate of coating was only 1/12 of 7N01 Al substrate. Worn surfaces indicated slightly abrasive wear combined with adhesive wear for the coatings. The surface of the specimens exhibited a transfer steel layer after the wear test (Fig.4).

Keywords: wear, 7N01 aluminium alloy, microarc oxidation, ceramic coatings

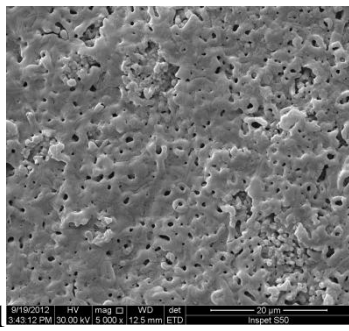


Fig.1

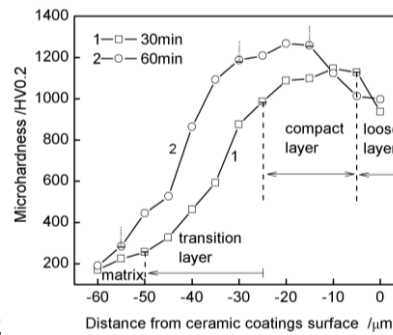


Fig.2

Fig.1 SEM morphology of MAO coatings

Fig.2 Microhardness curve of MAO ceramic coatings

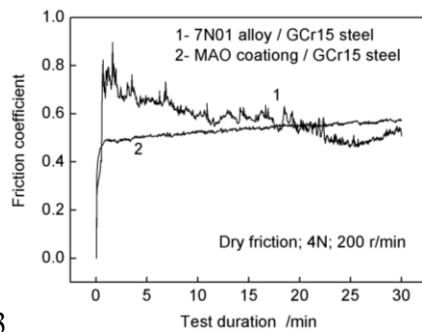


Fig.3

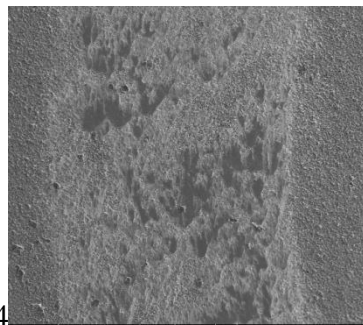


Fig.4

Fig.3 Friction coefficient curves of MAO coatings

Fig.4 The wear scars on surface of MAO ceramic coatings

Seed-mediated growth of the conductive yet transparent anatase Nb-TiO₂ films

Cuiqing Jiang, Shu Xiao, Liangliang Liu, Zhongzhen Wu

(School of Advanced Materials, Peking University Shenzhen Graduate School)

wuzz@pkusz.edu.cn

Abstract: Transparent Conducting materials with low cost, good etching property and durability compared to indium tin oxide (ITO) are needed in a broad range of application, such as solar cells, organic light emission diode (OLED), etc. Here we show a potential alternative, Nb-TiO₂ (NTO) oxide films comprising pure anatase phase deposited by seed-mediated growth on soda-lime glass instead of epitaxial growth on valuable sapphire. In order to control the crystal orientation of TiO₂, two-step preparation is described. An amorphous NTO film is first prepared on the economical soda-lime glass substrate by low-energy magnetron sputtering and then annealed in Ar with 5at% H₂ at 400 °C. To probe the phase structure and orientation, XRD were performed. And to validate the evolution of the phase transition during the process of the post-annealing, the whole real time transition process from room temperature to 500 °C were observed by in situ variable temperature transmission electron microscopy. Since resistivity and transmittance of NTO films are highly related to crystal phase and crystalline orientation, these properties were also characterized to demonstrate the effect of phase structure. The amorphous NTO films with (004) orientated seed crystal was fabricated by low-energy magnetron sputtering precisely controlling the annealing temperature. The XRD pattern shows that the amorphous NTO films could form excellent crystallized anatase NTO phase without the appearance of rutile. The TEM result validate the evolution of the phase transition during the process of the post-annealing : the crystals mainly growing with the seed crystals when the temperature is below 400 °C. Continuing raising the temperature, some seed crystals are nucleation and growth.

Moreover, we demonstrate their excellent conductivity, which achieve a low resistivity of $7.4 \times 10^{-4} \Omega \cdot \text{cm}$. By the processing of reducing reflection, the transmittance could reach 90% in visible wavelengths. High purity anatase NTO films were fabricated by seed-mediated growth. These films obtain good conductivity and transmittance, and can be found widespread applicability in solar cells and OLED devices.

Keywords: NTO films, magnetron sputtering, phase structure, resistivity, transmittance

Increasing recoverable energy storage in PZT films using low dielectric constant layer

Ying Zhou, Wen Wang

(Institute for Advanced Ceramics, School of Materials Science and Engineering, Harbin Institute of Technology, Harbin Heilongjiang 150080, China)

wangwen@hit.edu.cn

Abstract: Ceramic film capacitors with high dielectric constant and high breakdown strength hold special promise for applications demanding high power density. The lead zirconium titanate film thin films have attracted extensive attention due to their high piezoelectric coefficient and electromechanical coupling coefficient. However, the high residual polarization intensity and low breakdown electric field limit the further enhancement of the films energy storage density. In this paper, we mainly improved the $\text{PbZr}_{0.52}\text{Ti}_{0.48}\text{O}_3$ bilayer films energy storage density with two aspects by increasing electric breakdown strength and decreasing remanent polarization. Firstly, ferroelectric $\text{PbZr}_{0.52}\text{Ti}_{0.48}\text{O}_3$ films with a thickness of about 300 μm were successfully fabricated on $\text{Si}/\text{SiO}_2/\text{Ti}/\text{Pt}$ substrates by chemical solution deposition. The $\text{PbZr}_{0.52}\text{Ti}_{0.48}\text{O}_3$ films with LaNiO_3 (LNO) buffer demonstrate more highly (111) – oriented by XRD analysis. The films with LNO buffer also exhibit higher maximal polarization (P_{max}) when compared to the films without LNO buffer, which shows the crystallographic orientation enhances the polarization of $\text{PbZr}_{0.52}\text{Ti}_{0.48}\text{O}_3$ thin films. The following results were measured on films with and without LNO buffer: remanent polarization (P_r) values of 47.8 and 31.4 $\mu\text{C}/\text{cm}^2$, P_{max} of values of 93.4 and 68.2 $\mu\text{C}/\text{cm}^2$, respectively. A recoverable energy storage density of 11.9 and 8.9 J/cm^3 at 1200 kV/cm have been obtained for the $\text{PbZr}_{0.52}\text{Ti}_{0.48}\text{O}_3$ films with and without LNO buffer. Based on this work, sandwich structured ($\text{PbZr}_{0.52}\text{Ti}_{0.48}\text{O}_3/\text{PbZrO}_3/\text{PbZr}_{0.52}\text{Ti}_{0.48}\text{O}_3$) thin films consisting of two $\text{PbZr}_{0.52}\text{Ti}_{0.48}\text{O}_3$ films and inner PbZrO_3 films with low dielectric constant were proposed because PbZrO_3 films possessed very small residual polarization intensity and improved the breakdown electric field of the films. All the composite films show lower remanent polarization intensity and larger electric breakdown strength compared cure $\text{PbZr}_{0.52}\text{Ti}_{0.48}\text{O}_3$ films when the thickness of PbZrO_3 films is 60, 120, 180, 240 nm. The most greatly improved electric breakdown strength value of 1867 kV/cm and ($P_{\text{max}}-P_r$) value of 51.9 $\mu\text{C}/\text{cm}^2$ have been obtained when the thickness of PbZrO_3 films is 180 nm. The enhanced energy storage density of 17.9 J/cm^3 at 1676 kV/cm has been achieved in $\text{PbZr}_{0.52}\text{Ti}_{0.48}\text{O}_3/\text{PbZrO}_3/\text{PbZr}_{0.52}\text{Ti}_{0.48}\text{O}_3$ bilayer films at room temperature, which is higher than that of individual $\text{PbZr}_{0.52}\text{Ti}_{0.48}\text{O}_3$ films (11.9 J/cm^3). Otherwise, electric breakdown strength of antiferroelectric/ferroelectric films is strengthened and then weakened with the increasing of the thickness of PbZrO_3 layer because of the result of mutual influence of the PbZrO_3 layer's sharing the external voltage and the large lattice mismatch between the PbZrO_3 layer and $\text{PbZr}_{0.52}\text{Ti}_{0.48}\text{O}_3$ films. Our results indicate that the design of $\text{PbZr}_{0.52}\text{Ti}_{0.48}\text{O}_3/\text{PbZrO}_3/\text{PbZr}_{0.52}\text{Ti}_{0.48}\text{O}_3$ bilayer films may be an effective way for enhancing energy storage density.

Keywords: (111)-oriented, low dielectric constant layer

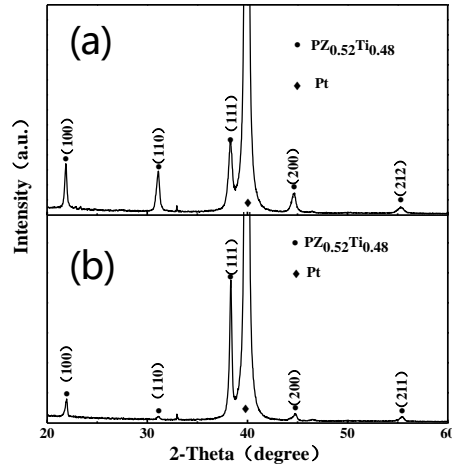


Fig.1 X-ray diffraction pattern of (a) Si/SiO₂/Ti/Pt/PZT and (b) Si/SiO₂/Ti/Pt/LNO/PZT films

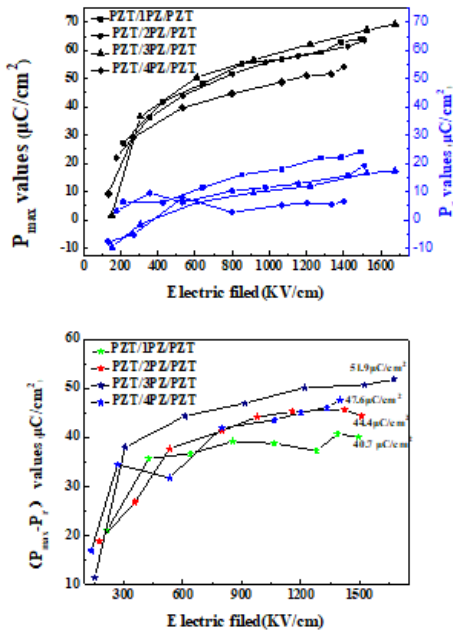


Fig.2

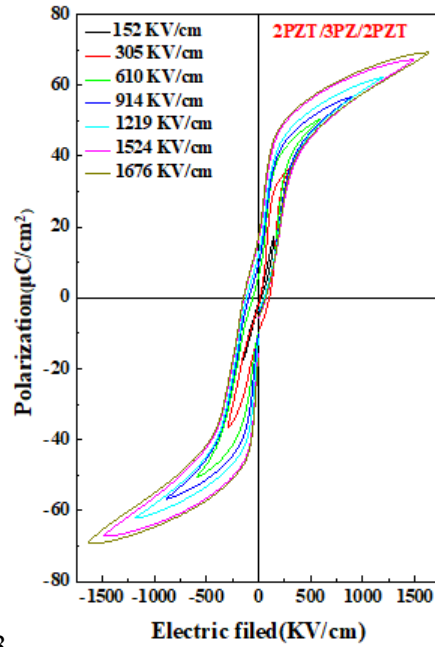


Fig.3

Fig.2 The picture of (C), (D) shows the P_m, P_r, and (P_{max}-P_r) values at different electric field respectively

Fig.3 The P-E loops of PZT/PZ (180nm)/PZT bilayer films under different electric field

Preparation of nanocrystalline coating on Ti alloy by cathodic plasma electrolytic deposition and its catalytic activity toward oxygen evolution reaction

Zhongping Yao¹, Jiankang Wang^{1,2}, Pengcheng Dai¹, Qixing Xia¹, Zhaohua Jiang¹

(1. School of Chemistry and Chemical Engineering, State Key Laboratory of Urban Water Resource and Environment, Harbin Institute of Technology, Harbin, 150001, China;

2. Chongqing Key Laboratory of Extraordinary Bond Engineering and Advanced Materials Technology (EBEAM), Yangtze Normal University, Chongqing 408100, China)

yaozhongping@hit.edu.cn

Abstract: Monolithic nanocrystalline coating on Ti alloy was successfully prepared by cathodic plasma electrolytic deposition and was used as binder-free OER catalyst. SEM characterization indicated that approx. 300 nm nanocrystalline was aggregated into great particles with micron size and then deposited on Ti alloy. OER performance measured in 0.1 M KOH solution revealed that the overpotential at 10 mA/cm² was 330 mV. This result suggested that the obtained coating exhibited decent OER catalytic activity and had potential application in water splitting.

Energy crisis and environmental issues caused by traditional fossil fuels urged us to pursue eco-friendly and highly efficient energy. Hydrogen energy with high energy density and zero carbon emission has been considered as a saviour to solve these problems. Electrochemical water splitting has potential application prospect for hydrogen generation. During electrochemical water splitting, oxygen evolution reaction (OER) involved in four-proton coupled electron transfer which endowed it with sluggish kinetics process. So far, great efforts have been devoted to decrease OER overpotential for increasing H₂ generation efficiency. However, the traditional OER catalysts in powder often needed nafion binder to prevent them from peeling off from the collector, which will sacrifice their electro-conductivity and also has the tendency to fall out during continuous bubbling. Nanocrystalline coating on Ti alloy as OER catalyst with strong adhesion to substrate prepared by cathodic plasma electrolytic deposition was seldom reported.

Nanocrystalline coating on Ti alloy was prepared by cathodic plasma electrolytic deposition. Typically, the polished Ti alloy and stainless electrolyzer were employed as cathode and anode, respectively. The electrolyte was comprised of triethanolamine, urea and ammonium nitrate. This deposition process was operated at constant potential of 200 V, duty ratio of 40 %, frequency of 1000 Hz and reaction was designed to be 15 min. The obtained coating was washed and dried for OER measurement.

Electrochemical measurement was performed on electrochemical workstation CHI660D at ambient temperature. The as-prepared coating was utilized as working electrode and Pt wire, saturated calomel electrode (SCE) were used as counter and reference electrode, separately. All potentials measured were calibrated to RHE using the following equation: $E_{RHE} = E_{SCE} + 0.241 \text{ V} + 0.059 \times \text{pH}$.

Monolithic nanocrystalline coating on Ti alloy was successfully prepared by cathodic plasma electrolytic deposition and was used as binder-free OER catalyst. SEM characterization shown in Fig.1 indicated that approx. 300 nm T nanocrystalline was aggregated into great particles with micron size and then deposited on Ti alloy. As for the composition and elemental valent state of as-obtained coating, we will study them in our future work by XRD and XPS measurement. OER performance measured in 1.0 M KoH solution in Fig.2 revealed that the overpotential (η) at 10 mA/cm² was 330 mV. Faradic efficiency measured by gas chromatography at $\eta=330$ mV reached 90 % after 100 min reaction. This result suggested that the obtained coating exhibited decent OER catalytic activity and had potential application in water splitting.

Keywords: cathodic plasma electrolytic deposition, nanocrystalline coating, Ti alloy, water splitting, oxygen evolution reaction

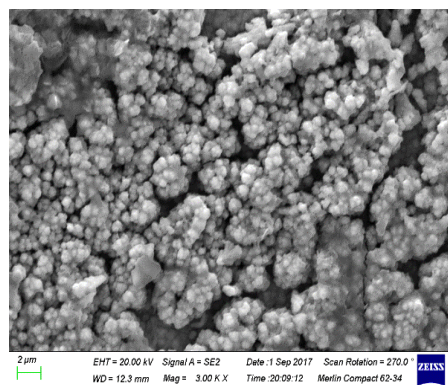


Fig.1 SEM images of as-prepared coating

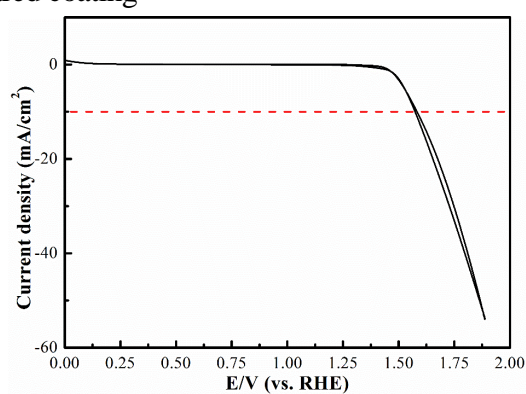


Fig.2 Cyclic voltammetry (CV) curves of as-prepared coating measured at 1.0 M KOH with the scan rate of 50 mV/s

Spontaneous escape behavior of silver from carbon and titanium nitride coating and its inhibition mechanism

Wenting Shao¹, Xinyu Zhang¹, Bailing Jiang², Yongpeng Qiao²
(1.Nanjing Tech University; 2. Xi'an University of Technology)
15251834625@126.com, jiangbail@vip.163.com

Abstract: A series of silver-doped carbon and titanium nitride coatings were prepared on the surface of aluminum alloy using the magnetron sputtering method. The differences of spontaneous escape behavior of silver from carbon and titanium nitride coatings were studied, and its inhibition mechanism was proposed. The results showed that for silver doped carbon coating, when the sample prepared with a 0.01 A current on the silver target was placed in an atmospheric environment for 0.5 h, an apparent silver escape phenomenon could be observed. When the current on the silver target increased to 0.05 A, a 150 nm-thick silver layer was formed on the surface of the coating even for samples placed in the atmosphere for 180 h. Moreover, for the same thickness of silver doped titanium nitride coating, even the current on the silver target increased to 0.10 A, no more than 15% of the surface was covered by silver particles for samples placed in an atmospheric environment for 180 h; Further increased the current on the silver target to 0.20 A, 200 nm sized silver particles can be observed on the cluster interface after the 1000 h exposure to an atmospheric environment, far from the attainment of crystalline layers distribution state. The results indicated that the spontaneous escape rate of silver from titanium nitride coating is far less than amorphous carbon coatings. Also, 700 nm pure carbon coating coverage silver doped carbon coating that prepared under the silver target current of 0.05 A, a few silver particles could be observed on the carbon cluster interface after the 2000 h exposure to an atmospheric environment. However, 470 nm pure titanium nitride coating coverage silver doped titanium nitride coating that prepared under the silver target current of 0.20 A, no silver escape phenomenon was observed after 2000 h of exposure in an atmospheric environment. About 500 nm pure titanium nitride coating coverage on the surface could permanent retention of silver in the silver doped titanium nitride coating. With TEM observation of carbon and titanium nitride coating clusters interface found that, compared with the smooth level off clusters interface of amorphous carbon coating, the clusters interface of titanium nitride coating is mutual crisscross dendritic network structure. Such dendritic network structure blocked the silver spontaneous escape, permanent retention of silver in titanium nitride coating.

Keywords: silver doping, carbon coating, titanium nitride coating, spontaneous escape, inhibition mechanism

Photocatalytic water decomposition for hydrogen production on TiO₂ loaded on foam nickel

Yanli Jiang¹, Yingxi Zhu², Xianjin Hou², Mei Tian¹, Lijuan Yang¹, Zhaohua Jiang²

(1. Department of Chemistry, Harbin University, Harbin, 150086, China;

2. School of Chemistry and Chemical Engineering, State Key Laboratory of Urban Water Resource and Environment, Harbin Institute of Technology, Harbin 150001, China)

519214930@qq.com

Abstract: The nano-size TiO₂ powder is easy to lose in gas-phase photocatalytic reaction and difficult to be collected after the reaction, which disturbs the recycle of photocatalyst and hampers the practical applications of nano-size TiO₂ powder. The immobilization of nano-size TiO₂ overcomes the difficulties in separation and recycle of photocatalyst and restrains aggregation and deactivation of the catalyst particles. The immobilized nano-size TiO₂ is an ideal material to design photocatalytic reactor by combining the functions of the photocatalyst and the support. The TiO₂ film was prepared by sol-gel method. The crystalline phases of the products were determined by X-ray diffractometer. The optical properties were analyzed by UV-V is diffuse reflectance spectrometer (UV 2401). The photocatalytic reactions were carried out at room temperature under normal pressure in a closed circulation system using a Hg-arc lamp (125 W) X-ray photon spectroscopy (XPS) measurements of Cu2p, Ti2p and O1s were recorded with a ESCA 2000 (VZ MicroTech, Oxford, UK) system, equipped with a non-monochromatic AlK (1486.6 eV) X-ray source. The rate of hydrogen production was measured from an aqueous solution containing 0.1 M Na₂S and 0.02 M Na₂SO₃ as sacrificial reagents under a Hg-arc lamp (125 W).

In system with the existence of foam nickel, the bubble produce smoothly because the froth nickel has provided the massive concaves and the convex. The bubble also could be generation continuously when there is no other carrier part in the system. Fig.1 shows that repeated coating improves the amount of TiO₂ loaded on foam nickel, but the photocatalytic activity of TiO₂ can not increase continuously by repeated coating. So, the optimum dipping cycles for TiO₂ films on foam nickel is three. XPS analysis reveals TiO₂ photocatalyst showed a sharp edge at 500 nm, while that of TiO₂ was observed at 390 nm. The Ni²⁺ ion transfers from the foam nickel substrate to TiO₂ films during the high-temperature treatment and results in the formation of nickel-doped TiO₂ films on foam nickel substrate. The absorption edges of nickel-doped TiO₂ films shift from UV region to visible light region ($\lambda < 520$ nm). The nickel-doped TiO₂ films display high photocatalytic activity under visible light irradiation. XRD analysis shows that NiO on the surface are formed in the process of the pre-oxidation, which increases the roughness of the surface. The roughness is crucial to photocatalytic hydrogen production. Because the existence of NiO can prevent the transfer of electron to Ni, which avails photocatalytic hydrogen production.

In summary, foam nickel has the inimitable advantage in the field of photocatalytic hydrogen production because of its high mechanical performance, small opening, stability, which can be made to multifarious figures at discretion. Furthermore, H₂ can be separated out rapidly from the aqueous solution due to high small opening. The hydrogen production was measured from an aqueous solution containing 0.1 M Na₂S and 0.02 M Na₂SO₃ as sacrificial reagents under a Hg-arc lamp (125 W). Besides, the hydrogen production activity of the TiO₂ film on foam nickel are also increased through the pre-oxidation.

Keywords: TiO₂ films, foam nickel, hydrogen production, pre-oxidation

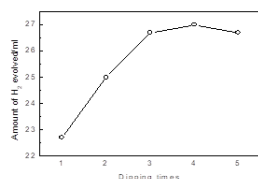


Fig.1

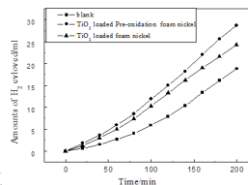


Fig.2

Fig.1 Effects of dipping times on the photocatalytic hydrogen production activity of TiO₂ films

Fig.2 The effects of pre-oxidation to hydrogen production activity of the TiO₂

Rapid preparation of alumina thin films by high-power density reaction magnetron sputtering

Tielei Shao¹, Zhongzhen Wu^{1,2}, Liangliang Liu¹, Xiaokai An¹, Shu Xiao¹, Hai Lin¹, Xiubo Tian¹, Paul K. Chu², Feng Pan¹

(1. School of Advanced Materials, Peking University Shenzhen Graduate School, Shenzhen, China;

2. Department of Physics and Materials Science, City University of Hong Kong, Tat Chee Avenue, Kowloon, Hong Kong, China)

wuzz@pkusz.edu.cn

Abstract: Al₂O₃ thin films have been widely used in optical, microelectronics, mechanical and other fields because of its excellent optical properties, high mechanical strength, and corrosion resistance [1-2]. At present, many methods have been applied to prepare Al₂O₃ thin films, such as reaction magnetron sputtering, chemical vapor deposition (CVD), sol-gel process, Micro-arc oxidation (MAO), atomic layer deposition (ALD), pulsed laser deposition (PLD) and so on [3-5]. Reaction magnetron sputtering is a simple, scalable, and relative low temperature way, while, it is limited by the deposition rate and the film quality due to the activity and poison of the Al target.

In this study, a magnetron-sputtering cathode with excellent cooling system (up to 200 W/cm² power density) is developed and the deposition window without target poison is broadened. The results show that with the increase of average power density the deposition rate are increased (Fig.2(a)), meanwhile the structure of the films changed observed from the section images (Fig.1), which formed a kind of denser columnar microstructure due to the high Particle energy. It improved the performance of the films, including the transmittance (Fig.2(b)), the breakdown voltage. The test by ellipsometer also proved the high quality of the Al₂O₃ thin films. The deposition rate of Al₂O₃ thin films reaches 148 nm/min when the distance between the substrate and the target is $d_{s-t}=45$ cm, which is more efficient than 20-40 nm/min of normal reaction magnetron sputtering.

Keywords: Al₂O₃, high-power density, deposition rate, optical properties

Reference:

- [1] Sridharan M, Sillassen M, Bottiger J, Chevallier J, Birkedal H. Pulsed DC magnetron sputtered Al₂O₃ films and their hardness. *Surface & Coatings Technology*. 2007, 202(4-7):920-924.
- [2] Voigt M, Sokolowski M. Electrical properties of thin RF sputtered aluminum oxide films. *Materials Science and Engineering B-Solid State Materials for Advanced Technology*. 2004, 109(1-3):99-103.
- [3] Gao M, Ito A, Goto T. Preparation of gamma-Al₂O₃ films by laser chemical vapor deposition. *Applied Surface Science*. 2015, 340:160-165.
- [4] Chiba Y, Abe Y, Kawamura M, Sasaki K. Formation process of Al₂O₃ thin film by reactive sputtering. *Vacuum*. 2008, 83(3):483-485.
- [5] Simon DK, Jordan PM, Dirnstorfer I, Benner F, Richter C, Mikolajick T. Symmetrical Al₂O₃-based passivation layers for p- and n-type silicon. *Solar Energy Materials and Solar Cells*, 2014, 131:72-76.

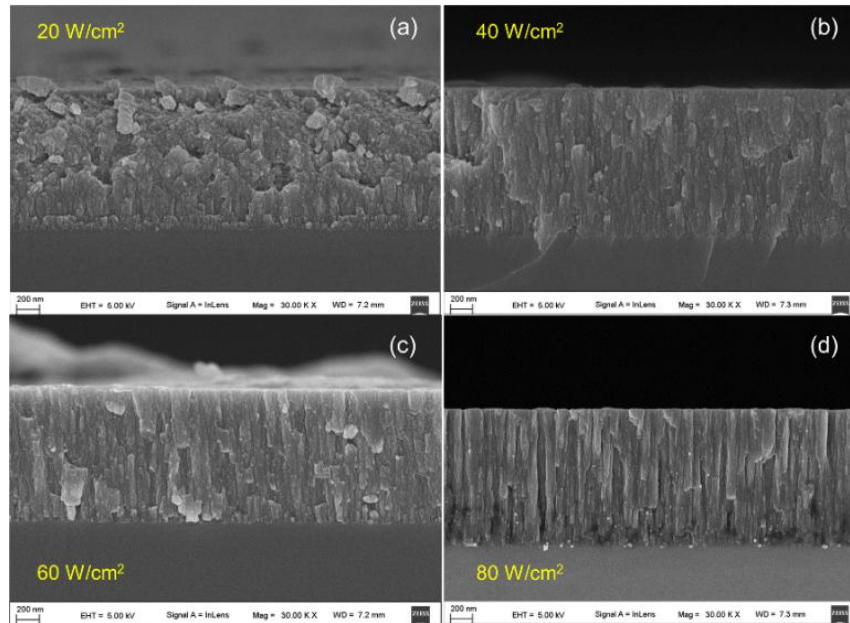


Fig.1 SEM images of Al₂O₃ films at different power densities, the thickness is about 1 μm

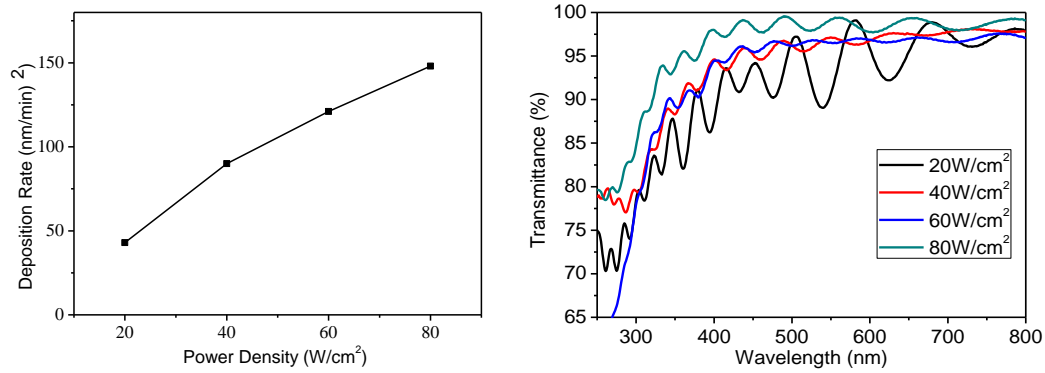


Fig.2 The deposition rate (a) and transmittance (b) of Al₂O₃ films at different power densities

Effects of anodization-assisted electrodeposition conditions on the fabrication of Cu coatings on nanoporous stainless steel

Hefeng Wang^{1,2}, Jiaojiao Zhang¹, Zhi Yuan¹, Xuefeng Shu³, Xiaomin Jin¹

(1. College of Mechanics, Taiyuan University of Technology, Taiyuan 030024, China;

2. Department of Chemical and Materials Engineering, University of Alberta, Edmonton, Alberta, Canada;

3. Institute of Applied Mechanics and Biomedical Engineering, Taiyuan University of Technology, Taiyuan 030024, China)

wanghefeng@tyut.edu.cn

Abstract: Cu coatings were prepared on 316L nanoporous stainless steel (NPSS) by anodization-assisted electrodeposition for applications in antibacterial materials. The present study investigated influences of HClO₄ concentration, reaction temperature and load voltage on the morphology, structure and composition of the coatings were discussed. The microstructure of the NPSS and Cu coatings prepared on NPSS (Cu/NPSS) were determined using X-ray diffraction (XRD), scanning electron microscopy (SEM) and energy dispersive X-ray spectroscopy (EDX). It reveals that the Cu/NPSS is mainly composed of Cu₂O and CuO phases. After anodization-assisted electrodeposition, the Cu coatings can be successfully formed on NPSS. The EDX result indicates the Cu and O embedded on the as-prepared Cu/NPSS.

Keywords: nanoporous stainless steel, electrodeposition, anodization, copper

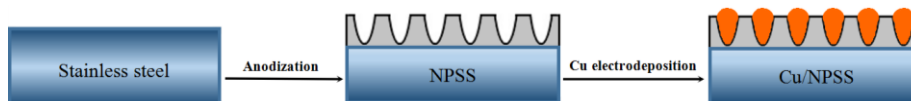


Fig.1 Schematic illustration of the procedure for preparing Cu/NPSS

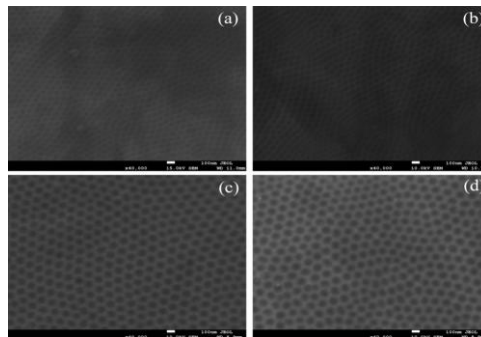


Fig.2 SEM images of stainless steel samples anodized under different load voltage (a: 20 V, b: 30 V, c: 40 V and d: 50 V)

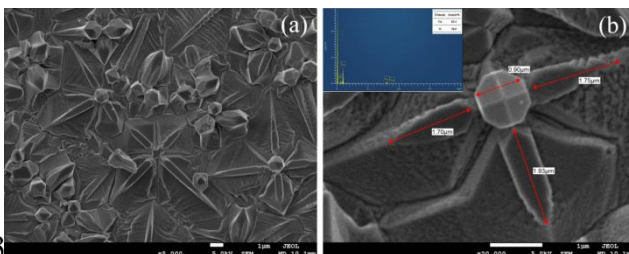


Fig.3

Fig.4

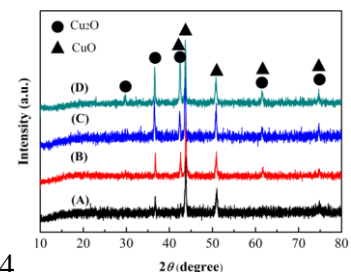


Fig.3 SEM images of electrodeposition of Cu film on NPSS under D, The inset shows the corresponding elemental atomic ratios

Fig.4 XRD spectra of the Cu/NPSS

Fabrication and characterization of dense Cr₂O₃-Al₂O₃ double coatings by electrochemical technique

Jiao Di, Lihong Xue

(Huazhong University of Science and Technology)

xuelh@hust.edu.cn

Abstract: Tritium permeation barrier (TPB) is regarded as one of the most effective methods to minimize tritium permeation through structural materials to environment. Cr₂O₃ ceramic has been studied as a promising TPB because of its thermostability, chemical inertness and small permeability of hydrogen isotopes. However, the practical permeation reduction performance of Cr₂O₃ ceramic coatings is much lower than the calculated performance values, which is due to the microcrack and porous microstructure in the coating by the difference of thermal expansion between the ceramic coating and substrate metals and lower sintering temperatures. Thus, in this study, a dense Al₂O₃ sealing layer was prepared on the surface of Cr₂O₃ coating to prevent microcrack and seal open pores.

Firstly, the Cr layer were electrodeposited in the electrolytic solution containing 220 g/L chromic acid (CrO₃) and 2.2 g/L sulfuric acid (H₂SO₄). During the electroplating, the electrolyte was stirred by a magnetic bar and maintained at 72 °C. A pure Pt plate was used as anode, and the 321 steel substrate was used as cathode. Distance between two electrodes was fixed to 40 mm and the electrodeposition was conducted at current density of 0.3 A/cm² for 80 min. Then the as-deposited Cr layer was heat treated in air for 4 h at 700 °C and the heating rate was 4 °C/min.

Then, a Al₂O₃ capping layer was fabricated on the surface of Cr₂O₃ coating in 0.1 mol/L Al(NO₃)₃ · 9H₂O ethanol solution. The Cr₂O₃ coating specimen acted as cathode, and pure Pt plate was used as anode. The distance between the anode and cathode was 15 mm. The electrolytic deposition was carried out at 10 A/m² for 10 min, and subsequent drying process at 150 °C for 20 min. Finally, the specimens were heated at different temperatures in air for 1 h after two times repeating of electrolytic deposition and drying processes.

Processing parameters were optimized to obtain crack-free coatings. A dense Cr₂O₃/Al₂O₃ double coatings without pores and cracks is prepared when the electroplating current density is 10 A/m² and heat treatment temperature is 750 °C after two times repeating of electrolytic deposition and drying processes. The double coatings sample oxidized at 750 °C exhibits a good resistance to corrosion. And the Vickers hardness of the Al₂O₃/Cr₂O₃ coating specimen oxidized at 750 °C is 220 N/mm², which is higher than the specimens oxidized at 650 °C and 700 °C. The bond strength of the sample oxidized at 750 °C reaches a maximum value and it exceed that of the conventional Al₂O₃ coating.

Keywords: Cr₂O₃-Al₂O₃, electrodeposition, double coatings, vickers hardness, corrosion resistance

Wear resistance of Al₂O₃ /WC-Co/epoxy coatings on

TC18(Ti-5Al-5Mo-5V-1Cr-1Fe) alloy

Yuqin Yan¹, Shuqin Li¹, Dongbo Wei¹, Shiyuan Wang¹, Fengkun Li¹, Feng Ding¹, Baozhang Duan¹,
Zhangzhong Wang², Pingze Zhang¹

(1. Nanjing University of Aeronautics and Astronautics; 2. Nanjing Institute of Technology)
shuqli@nuaa.edu.cn

Abstract: This study investigates the effects of adding Nano filler Al₂O₃ and WC-Co particle in the epoxy resin coating on dry sliding under ambient temperature. Al₂O₃ and WC-Co reinforced epoxy resin coatings were fabricated by air spraying process on the surface of TC18 alloy. Al₂O₃ and WC-Co enhance hardness of epoxy coating while maintaining toughness. The wear behaviours of the base alloy and coatings were comparatively studied. The addition of ceramic particles led to an enhancement of wear resistance of 64.7%-69% and 59.4%-62% in epoxy/Al₂O₃ and epoxy/WC-Co coatings respectively compared with that of the substrate. TC18 abases alloy mainly showed abrasive wear, while epoxy/Al₂O₃ and epoxy/WC-Co coatings showed adhesive wear. The resin in the coating will soften or even carbonized in the friction state, so as to play a role in lubrication, but a long time of reciprocating friction made the friction contact surface delamination.

Keywords: epoxy/ Al₂O₃ coating, epoxy/WC-Co coating, friction and wear, TC18 alloy

A combined experimental and first-principle study on the oxidation

behavior of plasma surface Ta-W alloyed γ -TiAl

Dongbo Wei¹, Yuqin Yan¹, Shuqin Li¹, Shiyuan Wang¹, Fengkun Li¹, Feng Ding¹,
Pingze Zhang¹, Zhangzhong Wang²

(1. Nanjing University of Aeronautics and Astronautics; 2. Nanjing Institute of Technology)
qinyanyu@nuaa.edu.cn

Abstract: A γ -TiAl alloy (Ti-46.5Alwt%) was plasma surface modified with Ta-W elements by double glow discharge to improve the surface oxidation resistance at 900 °C. The obtained Ta-W modified layer was composed of a dense deposited layer and a boat diffusion layer. Isothermal oxidation experiment of the samples with the as-prepared Ta-W alloying layer at 900 °C in static air for 100 h shows that the oxygen inward diffusion can be effectively suppressed to a low level. Based on the first-principle methods, the geometry, oxygen adsorption energies and electronic structure of TaW-doped γ -TiAl are investigated to reveal the mechanisms. Doping Ta and W alloying elements can inhibit the oxidation of Ti in the inner layer, which is beneficial to reduce the formation of harmful oxide TiO₂. At the same time, Ta, W and Ti, Al will bind each other to form new intermetallic compounds, thus reducing the Ti-Al bond.

Keywords: γ -TiAl, oxidation, Ta-W alloying, first principles

Erosion behaviour of laser clad FeCoCrNiTi high-entropy alloy coating at elevated temperature

Shiyi Zhang

(China University of Petroleum)

zsy4141@126.com

Abstract: A FeCoCrNiTi high-entropy alloy coating and Co-based alloy coating were prepared by laser cladding on 304L stainless steel substrates. The coating composition and microstructure were characterized by energy dispersive X-ray spectra, X-ray diffraction and scanning electron microscope. The high temperature erosion properties of FeCoCrNiTi high-entropy alloy coating and Co-based alloy coating were determined at different impact angles and environmental temperatures, respectively. The results show that the phase of FeCoCrNiTi high-entropy alloy coating consists of FCC and (Cr, Fe) solid solution, which are not easy to decompose, making the high entropy coating has good thermal stability. Compared with the Co-based coating, FeCoCrNiTi high-entropy alloy coating has lower erosion rate than Co-based alloy coating at wide erosion angles. Many erosion particles were inlaid into the Co-based alloy coatings at small erosion angles leading the Co-based alloy coating erosion rate decreased. The FeCoCrNiTi high-entropy alloy coating presents itself as a potential protective coating for resisting particles erosion at elevated temperature.

Keywords: high-entropy alloy, high temperature erosion

Influence of current density at glow-arc discharge transitional section on microstructure and properties of TiN films

Juan Hao

(School of Materials Science and Engineering, Xi'an University of Technology)

haojuan19901207@163.com

Abstract: The volt-ampere characteristics of gas discharge was introduced into the glow-arc discharge transitional section using an adjustable pulse power control mode and TiN films were deposited at different current densities. The influences of target current density on the microstructure, hardness and bonding strength of the films were investigated by XRD, SEM, TEM, nano indentation tester and coating adhesion automatic scratch tester. The results show that the leave-target mechanism of plating material particles transforms from collide leave-target in sputtering condition to collide enhance heat emission leave-target and the deposition particles have a higher density, high ionization and high energy with the increase of current density. The films have better surface quality and density degree, and the hardness and membrane-binding strength are upgraded from 13.4 GPa to 24.7 GPa and from 2.4 N to 21.6 N, respectively.

Keywords: glow-arc discharge transitional section, leave-target mechanism, current density, TiN films

The structure and properties of TiN films deposited using dc, modulated pulse power magnetron sputtering and arc ion plating

Chao Yang
(Xi'an University of Technology)
yangch@xaut.edu.cn

Abstract: Continuous dc magnetron sputtering (dcMS) TiN film exhibits a porous columnar structure with low mechanical properties and corrosion resistance due to the low ionization rate and energy of the deposited particles. Another arc ion plating (AIP) technique can deposit dense TiN film because of the high ion flux and ion energy from the deposited particles, but high-energy arc discharge easily induces molten metal particles with diameter in micron scale onto the film surface, which causes AIP TiN film possessing a rough surface and poor corrosion resistance. In order to overcome shortcomings of the dcMS and AIP techniques, a new modulated pulse power magnetron sputtering (MPPMS) deposition technique has been developed that overcomes the molten macroparticles problem while still achieving a high ionization rate of the deposited particles. In our study, nanocrystalline TiN films were deposited using the dcMS, AIP and MPPMS at the same average target power respectively. It was found that the MPPMS TiN film exhibited a dense columnar structure and enhanced mechanical properties comparing with the dcMS, and also possessed smooth surface and improved corrosion resistance than AIP TiN film.

Keywords: dc magnetron sputtering, modulated pulse power magnetron sputtering, arc ion plating

Effect of target power density on tribological properties of graphite-like carbon films deposited by pulsed dc magnetron sputtering

Dan Dong
(Xi'an University of Technology)
dd307071519@126.com

Abstract: In order to improve the film-substrate adhesion and tribological performance, a series of graphite-like carbon (GLC) films with different graphite target power densities were prepared by pulsed dc magnetron sputtering. The valence bond and microstructure of films were characterized by AFM, TEM, XPS and Raman spectra. The variation of mechanical and tribological properties with graphite target power density was analyzed. The results showed that with the increase of pulse power density, the deposition rate and the ratio of sp² bond increased obviously. The hardness firstly increased and then decreased with the increase of pulse power density, whilst the friction coefficient and the specific wear rate increased slightly after a decrease with the increasing pulse power density. The friction coefficient and the specific wear rate were the lowest when the graphite target power density was 31.1 W/cm².

Keywords: pulsed dc magnetron sputtering, graphite-like carbon films, target power density, tribological performance, structure

The effect of N ion implantation on the properties of W18Cr4V based

TiAlN/Al₂O₃ coatings

Miao Hu, Liuhe Li

(School of Mechanical Engineering and Automation, Beihang University)

liliuhe@buaa.edu.cn

Abstract: TiAlN nanocomposite coatings were deposited onto high-speed steel (W18Cr4V) substrates by reactive direct current magnetron sputtering (DCMS). Al₂O₃ films were prepared using self-assembled atomic layer deposition (ALD) systems on the surface of TiAlN coatings. Between them, N ions were implanted. The effect of N ions implantation doses on elements concentration, high temperature oxidation resistance, microstructure, surface/cross-sectional morphology, hardness and adhesion strength of coatings were studied with energy dispersive spectroscopy (EDS) together with scanning electron microscopy (SEM), X-ray diffraction (XRD), atomic force microscopy (AFM), Nano-indentation and Rockwell indentation tester.

Atomic layer deposition (ALD) is a thin film deposition technique that is able to deposit ultrathin, uniform, and conformal layers. The ALD process, consisting of two sequential, self-limiting surface chemical reactions, has been shown to provide the desired coating in a variety of systems on planar substrates and into high-aspect-ratio structures. TiAlN is a very promising material for high temperature corrosion and oxidation resistance coatings resulting in high hardness and wear resistance. Many researchers have investigated TiAlN or ALD coatings about corrosion and oxidation resistance and made significant progress. However, the influence related to ion implantation on TiAlN coatings encapsulated by ALD Al₂O₃ film still remains vacant.

In this paper, the hardness as well as high temperature oxidation resistance of TiN films coated Al₂O₃ by ALD in different N ion implantation doses were mainly analyzed.

Keywords: TiAlN, DCMS, ALD, ion implantation, hardness, high temperature oxidation resistance

Corrosion properties of steel sheet with zinc-base alloyed coatings

Guangrui Jiang

(Shougang Research Institute of Technology)

guangrui82@qq.com

Abstract: Steel sheets with three kinds of zinc alloyed coatings, that is pure zinc coating, Galfan coating and Zn-Al-Mg coating, were hot-dipping galvanized by a hot-dip process simulator (HDPS). Alloying elements content as mass percent in the three coatings are Zn-0.2%Al, Zn-5%Al and Zn-2%Al-2%Mg, respectively. Corrosion behavior of the steel sheets with zinc-base alloyed coating was studied by total immersion test. Corrosion resistance of the zinc-base alloyed coatings dipped with different time was analyzed by means of electrochemical measurement and scanning electron microscope (SEM) analysis. The results show that the Zn-Al-Mg coating has the largest corrosion current density at the early stage of immersion. Along with increasing immersing time, corrosion current density of the Zn-Al-Mg decreases but that of the pure zinc coating and the Galfan coating increase. For the Galfan coating, diffusion characteristics could be found for the Nyquist curve, which means higher corrosion rate. However, for the Zn-Al-Mg coating, limited diffusion characteristics could be found for the Nyquist curve, which means corrosion product covered the surface enhances the corrosion resistance.

Keywords: Zn-Al-Mg coating, corrosion resistance, Galfan coating

Influence of different nanoparticles for the wear resistance on the surface of anodized AZ31

Liang Wu¹, Xingxing Ding², Zhicheng Zheng², Aitao Tang¹, Gen Zhang², Lei Liu², Fusheng Pan²

(1. College of Materials Science and Engineering, Chongqing University, Chongqing, China;

2. National Engineering Research Center for Magnesium Alloys, Chongqing University, Chongqing, China)

wuliang@cqu.edu.cn

Abstract: In this paper, the anodizing process was used to prepare uniform and dense anodic oxide films on the surface of AZ31 magnesium alloy, which was including sodium aluminate and sodium hydroxide. Then, MgAl-layered double hydroxide (LDH) films were prepared by using this anodic film as a source of cations, without the introduction of any kinds of trivalent metal salts. After that, the holes of the LDHs were sealed by different nanoparticles (Al_2O_3 , ZrO_2) through electrochemical deposition process. X-ray diffraction, scanning electron microscopy and energy dispersive spectrometer were used to characterize different films. The electrochemical tests, friction and wear tests, hardness tests and binding tests were used to evaluate the corrosion resistance and other aspects of the performance of comparative study, and then the different nanoparticles for the film performance were analyzed. Through the friction and wear test as well as the electron microscopy analysis of the wear marks, it can be seen that the nano-particles in the composite LDH film will play a better role in wear debris and improve the wear resistance of the substrate. Finally, according to the experimental results, the wear-resistant mechanism of the composite LDH films was established.

Keywords: LDHs, corrosion, Mg alloy, nanoparticles, wear-resistance

Friction and wear characteristics of TiN coatings in ethanol

Yufeng Li¹, Sasaki Shinya²

(1. School of Materials Science and Engineering, Shenzhen Graduate School, Harbin Institute of Technology;

2. Department of Mechanical Engineering, Tokyo University of Science)

yfli@hit.edu.cn

Abstract: In recent years, bioethanol has recently attracted much attention in the automotive industry because CO_2 emissions can be reduced by using it as a fuel. Higher performance and longer durability of engine materials will become increasingly important with the use of alter-native fuels. Therefore, improved lubricants and advanced coatings are required in today's modern technology engines. TiN coatings are considered as promising coatings for wear protection of engine components. However, the tribological properties of TiN coatings have not yet been investigated sufficiently when the lubricant is ethanol. In this paper, the friction and wear characteristics of TiN coating prepared by PVD method have been evaluated with a ball-on-disk tribometer against ASTM 52100 steel, Al_2O_3 and Si_3N_4 balls under ethanol condition. The TiN coatings exhibit a friction coefficient of 0.19-0.32 and a wear rate of 2.7×10^{-8} to 1.8×10^{-6} mm^3/Nm , depending on the counter materials. The TiN/ Si_3N_4 ball pair shows more excellent tribological properties than the others. Due to the friction-induced-temperature-rise, the Si_3N_4 ball is easy to react with water in the ethanol to form SiO_2 firstly. Subsequently, the SiO_2 will further react with water to form hydrated silica. The hydrated silica accumulated between the contacting surfaces and formed discontinuous lubricating film on the worn surface, which result in the low friction coefficient and wear rate.

Keywords: TiN coating, ethanol, friction, wear

Study on corrosion resistance of a DLC film coated titanium and stainless steel by magnetron sputtering

Arachi Uozumi¹, Beibei Han¹, Huijun Zhao², Dongying Ju¹

(1. Saitama Institute of Technology; 2. Hangzhou Dianzi University)

dyju_mgcenter@163.com

Abstract: In recent years, fuel cell vehicles equipped with hydrogen fuel cells in the automobile industry have attracted attention. The bipolar plates are the most bulky and also one of the most expensive to manufacture among the components. Hence the reduction of the cost, mass, and volume of these bipolar plates is critical to the development of fuel cells. In this study, a diamond-like carbon (DLC) film was deposited on different metal substrates with the conditions of 500 V, 0.9 A and 50 Pa for 6 h using a carbon target (99.9% in purity) by magnetron sputtering. The characterizations and corrosion behaviors of the DLC film coated titanium, initial stainless steel and stainless steel with flow channels were investigated and evaluated. The carbon bonding microstructure and proportion of the DLC films were confirmed by Raman spectroscopy and X-ray photoelectron spectroscopy (XPS). The surface micromorphology and roughness of the films were observed and analyzed by scanning electron microscope (SEM) and atomic force microscopy (AFM). The DLC films coated titanium, initial stainless steel and stainless steel with flow channels were corroded by potentiostatic polarizations in a 0.5 mol/L sulfuric acid solution at 90 °C for 168 h. The metal ions in sulfuric acid corrosion solution were detected by inductively coupled plasma (ICP) atomic emission spectroscopy. The Raman spectroscopy and XPS results indicate that the DLC films have been successfully deposited on metal substrates. The DLC film deposited on the titanium showed the lowest Ra of the surface morphology. The metal ions concentration of DLC film on titanium is obviously lower than that of DLC film on stainless steel. Compared with stainless steel, titanium exhibits a higher corrosion resistance, particularly suitable for fuel cells.

Keywords: diamond-like carbon, titanium, stainless steel, corrosion resistance

Effects of additives on the corrosion resistance of chromium-free zinc-aluminum coatings

Junfeng Gou

(Guangdong University of Technology, School of Electromechanical Engineering, Guangzhou, China)

junfenggouhit@163.com

Abstract: Effects of different additives including sodium phosphomolybdate and coupling agent KH560 on the corrosion resistance of the chromium-free zinc-aluminum coatings were studied, which acted as functional coatings. The morphologies of the coatings before and after the corrosion tests were observed by a scanning electron microscope. The composition of the coatings was studied by an energy dispersive spectrometer. Polarization tests and immersion tests were used to study the corrosion resistance of the coatings. The results showed that both of the additives increased the stability of the coating and improved its corrosion resistance. Sodium phosphomolybdate and KH560 could decreased the corrosion current of the coatings obviously. The corrosion potential of the coating with KH560 increased more than 140 mV than that of the coating without additives. The failure time of the coating without additives in the 5% NaCl solution was 23 days. But the failure time of the coatings with sodium phosphomolybdate and KH560 in the 5% NaCl solution could reach 34 days and 52 days.

Keywords: chromium-free zinc-aluminum coatings, additives

Fabrication and characterization of HVOF sprayed NiCoCrAlYCe coatings on K417G nickle-based superalloy

Feifei Zhou¹, You Wang¹, Min Liu², Chunming Deng², Xiaofeng Zhang², Yaming Wang¹, Liang Wang³

(1. School of Materials Science and Engineering, Harbin Institute of Technology;

2. National Engineering Laboratory for Modern Materials Surface Engineering Technology, Guangdong Institute of New Materials;

3. Key Laboratory of Inorganic Coating Materials CAS, Shanghai Institute of Ceramics, Chinese Academy of Sciences)

wangyou@hit.edu.cn, liumin_gz@163.net

Abstract: MCrAlY (M=Ni or/and Co) coatings are widely used as bond coatings in thermal barrier coatings system and overlay coatings alone. The characteristics of MCrAlY feedstocks directly determine the performance of thermal sprayed coatings. In this work, the spherical NiCoCrAlY feedstocks modified by rare earth Ce (NiCoCrAlYCe) have been investigated.

The phase composition of NiCoCrAlYCe feedstocks consists of γ -Ni, β -NiAl and Cr. The NiCoCrAlYCe coatings with 200 μm thick were fabricated on K417G nickle-based superalloy by high velocity oxygen fuel (HVOF) spraying. The microstructure and the mechanical properties of NiCoCrAlYCe coatings were characterized. The NiCoCrAlYCe coatings are composed of γ' -Ni₃Al, γ -Ni, β -NiAl and Cr, which indicates that the reaction $\gamma\text{-Ni} + \beta\text{-NiAl} \rightarrow \gamma'\text{-Ni}_3\text{Al} + \text{Cr}$ happens during HVOF spraying. The elastic modulus and nanohardness are 110.748 ± 1.951 GPa and 5.440 ± 0.684 GPa, respectively. The average tensile strength is 56.5 MPa and the fracture failure has been analysed in detail.

AUTHOR INDEX

Keywords: NiCoCrAlYCe coatings, HVOF spraying, characterization, tensile strength

Preparation and characterization of tetrahedral amorphous carbon thin films with high strength and high toughness on YG6 cemented carbide

Yuting Li¹, Mingjiang Dai¹, Hong Li², Songsheng Lin², Qian Shi², Yifan Su²

(1. College of Materials and Energy, Guangdong University of Technology;

2. Guangdong Institute of New Materials)

2403673759@qq.com

Abstract: The vacuum cathode multi-arc ion plating technique was used to fabricate tetrahedral amorphous carbon (ta-c) thin films on single crystal polished silicon substrates and YG6 cemented carbides with thickness of 0.5 μm . Scanning electron microscopy (SEM) and 3D profilometer were used to characterize the surface, cross-section morphology, thickness and roughness of the films. The mechanical properties of the films were measured by nano-indentation instrument. The content of sp³ bond and sp² bond were calibrated by Raman spectroscopy and XPS. The results show that the roughness of tetrahedral amorphous carbon film on cemented carbide surface is 0.13 μm , the content of sp³ bond is 70%, the adhesion between the film and the substrate is 60 N, the modulus of elasticity is 469.9 GPa, the hardness is 45.9 GPa, and the fracture toughness is 71.8 MPa m^{1/2}. The tetrahedral amorphous carbon (ta-c) film has high strength and toughness and has a wide application prospect in wear-resistant parts.

Keywords: cemented carbides, tetrahedral amorphous carbon

Melt expulsion and ablation effects of the laser nanocrystallization on the surface of Al₂O₃/ZrO₂ eutectic ceramic

Zhigang Wang, Jiahu Ouyang
(Harbin Institute of Technology)

zhigang_imut@163.com, ouyangjh@hit.edu.cn

Abstract: Laser processing is one of the current prevailing approaches offering the possibilities to modify the microstructure, phases, composition, and the topography of the surfaces of engineering materials via a range of laser-material interactions including heating, melting, surface vaporization, ablation, and shock peening et al. In the present work, nanostructured surface layers of eutectic oxide ceramic were produced on the surfaces of conventionally sintered Al₂O₃/ZrO₂ ceramic via the laser beam induced rapid solidification process. The evolution of molten pool profile, microstructure and phase composition were characterized by surface profilometer, scanning electron microscopy (SEM), X-ray diffraction (XRD) and Raman spectroscopy.

The molten pool depth and width were quantitatively investigated as a function of laser beam power densities of 8-30 kW/cm² and velocities of 0.1-2 mm/s, respectively. When the power is set too high, the formation of a key-hole can be observed, together with evaporation of material. The melt pool had a circular shape at low velocities and tended to lengthen at higher velocities. It is noted that the center of molten pool presented a marvelous spontaneously nucleated cellular eutectic microstructure, and was consisted of α -Al₂O₃, m-ZrO₂ and t-ZrO₂ phases, where t-ZrO₂ was the dominant phase. The laser ablation effects have been explored, and further analysis showed that the tracks mainly ablated in the manner of liquid evaporation. In the melting pool, the ablation mechanism presented a combined effects of melting and the thermomechanical shear-induced damage.

Keywords: Al₂O₃/ZrO₂ eutectic, melt expulsion, surface layer, ablation effects, laser

The corrosion resistance of hot dip galvanized steel pretreated with silanes modified with nano silicon carbide

Yan Zhang¹, Fang Gong¹, Junhui Huang²

(1. Nanjing Institute of Technology; 2. Nanjing Institutr of Technology)

zhangyan3@njit.edu.cn

Abstract: The hot dip galvanized (HDG) steel has been extensively used in mechanical, automobile and transmission and transformation infrastructure industries. In order to improve corrosion resistance, inorganic compounds and organic compounds passivation process has been adopted. Chromate passivation process has been replaced by molybdate, silicate, titanium salt and so on. Organic Compounds passivation process mainly uses phytic acid, tannic acid, silane and so on. But both of the effects are not very satisfactory. Thus, it is highly desired to have simple, Environment-friendly, and effective passivation process. The present work aims at assessing the corrosion behaviour of HDG steel pretreated with silane and titanium salt composite solutions modified with particles of nanoSiC. The component and morphology of the films formed on the galvanized steel substrate were characterized by X-Ray spectrometry and scanning electron microscope. The results show that the passivation process can improve corrosion protection when immersing in NaCl solutions compared to conventional Chromate and silane.

Keywords: hot dip galvanized (HDG) steel, passivation process, nano SiC, corrosion resistance

Hydrogen permeation resistance property and characterization of

zircon coatings on the surface of zirconium hydride alloy

Zhigang Wang¹, Weidong Chen², Shufang Yan², Wen Ma², Jiahu Ouyang¹

(1. Harbin Institute of Technology; 2. Inner Mongolia University of Technology)

zhigang_imut@163.com, wdchen@imut.edu.cn

Abstract: Zirconium hydride has been recognized as one of the most ideal moderators for nuclear reactors. However, the problem of hydrogen losses for zirconium hydride moderator at the working temperatures has not been solved satisfactorily. To fabricate hydrogen permeation barriers on the surface of zirconium hydride has been considered as a practical solution to restrict hydrogen losses for long-term performance. The present investigation aims to develop a zirconia coating prepared by micro-arc oxidizing to improve the superior hydrogen permeation resistance of zirconium hydride alloys. The microstructure, chemical composition and phase composition of the as-prepared ZrO₂ coating were investigated by means of scanning electron microscopy (SEM), energy dispersive spectrometry (EDS) and X-ray diffraction (XRD), respectively. The hydrogen permeation resistance property of the coating was characterized by vacuum dehydrogenation experiment and thermal desorption spectroscopy (TDS). The results showed that the as-prepared ZrO₂ coating consisted of a compact and uniform inner layer and a porous outer layer. The coating was mainly composed of m-ZrO₂, t-ZrO₂ and a trace of c-ZrO₂. The quantitative analysis suggested an increased amount of m-ZrO₂ phase towards the coating surface and an increased amount of t-ZrO₂ phase towards the interface between oxide and zirconium hydride. Hydrogen permeation resistance property of the substrate was significantly improved by the as-prepared ZrO₂ coating. Hydrogen desorption starting at 500 °C for zirconium hydride, while it delays decomposition to relatively higher temperature of 660 °C in the presence of ZrO₂ coating. Permeation Reduction Factor (PRF) value improved by nearly 13 times compared with the uncoated zirconium hydride.

Keywords: hydrogen permeation barrier, zirconium hydride, zircon coating, micro-arc oxidizing

Research on the correlation between corrosion properties and electron work

function of the Al₂O₃/TiO₂ coatings modified by nano graphite

Qiwen Zhang¹, Junsheng Meng², You Wang¹, Junfeng Gou¹, Feifei Zhou¹, Zhenguo Zhang¹

(1. School of Materials Science and Engineering, Harbin Institute of Technology, Harbin, China;

2. Naval Architecture & Marine Engineering College, Shandong Jiao Tong University Weihai Campus, China)

wangyou@hit.edu.cn

Abstract: The nano materials of Al₂O₃/TiO₂ were used as raw materials with addition of nano graphite particles to fabricate feedstocks used in the thermal spray by ball milling. The ceramic coatings with different amounts of nano-graphite were deposited on the substrate of 316L stainless steel by plasma spray. The effect of corrosive behaviors on surface morphology and EWF of the nano-graphite modified Al₂O₃/TiO₂ coatings was comparatively investigated in 3.5% NaCl solution using a scanning electron microscopy and a scanning Kelvin probe. The microstructure and properties of the feedstocks and coatings affected by nano-graphite particles were researched in detail. The results showed that the EWF of the modified coatings would trend to decrease after increase with the increasing of the nano graphite, and it is the best when the graphite content is 9%. With the increase of corrosion time, the EWF was firstly decreased and then kept stable. The corrosion resistance and bonding strength of the nano graphite modified coating is the best when the graphite content is 9%.

Keywords: plasma spray, nano graphite, Al₂O₃/TiO₂ ceramic coating, EWF

Solidification and epitaxial growth of nanostructured Al₂O₃/ZrO₂ eutectic surface layers formed by high energy laser or oxyacetylene flame

Zhigang Wang, Jiahu Ouyang
(Harbin Institute of Technology)

zhigang_imut@163.com, ouyangjh@hit.edu.cn

Abstract: Surface layer nanocrystallization is one of the current prevailing approaches offering the possibility of improving the mechanical properties, wear- and corrosion-resistances of engineering materials with precise and complex geometries, which are difficult or even impossible to be realized by conventional manufacturing techniques. In the present work, nanostructured surface layers of eutectic oxide ceramic were produced on the surfaces of conventionally sintered Al₂O₃/ZrO₂ ceramic via the laser beam or oxyacetylene flame induced rapid solidification process. The morphology, microstructure and growth mechanisms of nanostructured surface layers were characterized by surface profilometer, X-ray diffraction (XRD), Raman spectroscopy, scanning electron microscopy (SEM) and transmission electron microscopy (TEM). The mechanical properties were evaluated using Vickers micro-hardness and nanoindentation testers. Nanostructured eutectic colony-enhanced surface layers with the graded microstructure are obtained by laser radiation at a power density of 17 kW/cm² and traveling speeds of 0.1-1 mm/s, and are composed of (i) an outermost layer of ultrafine eutectic conolies and (ii) a coarse irregular eutectic layer with faceted feature. The outermost layer composed of spherical colonies with an average interlamellar or inter-rod spacing of about 200 nm was obtained at a growth rate of about 275 μm/s. It is noted that the initial eutectic growth follows against the heat flow direction, and gradually tends to be parallel to the crystallographic preferred orientation. The nanostructured surface layers consist of α-Al₂O₃, m-ZrO₂ and t-ZrO₂ phases, where t-ZrO₂ is the dominant phase. The measured maximum Vickers hardness on the transverse cross-section of eutectic surface layers reaches 18 GPa. In addition, the nucleation and epitaxial growth mechanisms of highly textured Al₂O₃-ZrO₂ nanoeutectics induced by rapid solidification of oxyacetylene flame are proposed. Consequently, rapid solidification by high energy density beam melting is beneficial to the fabrication of new materials with ultrafine eutectic microstructure and improved mechanical properties.

Keywords: nanostructured Al₂O₃/ZrO₂, epitaxial growth, surface layer, laser, oxyacetylene flame

Effects of vacuum heat treatment on composition, microstructure and thermal cycling life of thermal barrier coatings by EB-PVD

Zaoyu Shen, Limin He, Zhenhua Xu, Rende Mu
(Beijing Institute of Aeronautical Materials)

shenzaoyu@163.com

Abstract: A TBC system with NiCrAlYSi and 8YSZ is developed by means of arc ion-plating PVD and EB-PVD techniques. Considerable inter-diffusion occurs between NiCrAlYSi layer and substrate due to the vacuum heat treatment at different temperatures. The element interdiffusion behaviors and microstructural evolution of NiCrAlYSi layer play an important role in the performance of TBCs. After vacuum heat treatment at 870 °C and 3 h for bond coat, TBCs exhibits the highest thermal cycling life (average about 1134 cycles). The possible mechanism of improved thermal cycling life relates to the relatively low TGO growth rate induced by properly controlling the diffusion rate of Al within NiCrAlYSi layer.

Keywords: thermal barrier coatings, EB-PVD

Effect of graphene on the properties of plasma electrolytic oxidation coating on the biodegradable ZK60 magnesium alloy

Zhaozhong Qiu, Changhai Zhou, Ailian Liu, Hong Tian, Zhizhong Zhu, Xuewei Li
(Heilongjiang University of Science and Technology)
qzhzh11@163.com

Abstract: Few-layer graphene has been prepared by electrochemical intercalation of graphite cathode using H_2O_2 and $(NH_4)SO_4/NaOH$ complexes as intercalation agent. Graphene sheets with good dispersion in solvents can be prepared at moderate temperatures without the need for acidic media. X-ray photoelectron spectra and Raman spectra indicate that the graphene material has lower content of defects and oxygen functional groups compared with that obtained by chemically reducing graphene oxide. The adsorption of graphene provided an insight into the interactions between the carbon atoms and the magnesium surface. The adsorption behavior of graphene on Mg (002) surface has been investigated by using molecular dynamics simulations. The influence of graphene on the morphology, composition and corrosion resistance of magnesium alloys during the plasma electrolytic oxidation process has been also studied. Experimental studies show good agreement with the theoretical prediction that graphene could improve the quality of coating effectively. Furthermore, the graphene surface could significantly improve the corrosion resistance compared with the pristine magnesium alloy in 3.5wt% NaCl solution.

Keywords: graphene, plasma electrolytic oxidation, magnesium alloy, graphene, plasma electrolytic oxidation, magnesium alloy

Effect of W coating on the microstructure and corrosion properties of NiTi alloys deposited by SLM

Ailian Liu¹, Dongyang Li², Jiawen Xu¹, Xiaolong Pang¹
(1. Heilongjiang University of Science and Technology; 2. University of Alberta)
laleileen@hotmail.com

Abstract: NiTi shape memory alloys are widely applied in many fields such as electronics, aerospace, mechanical and medical fields due to their unique shape memory effect, pseudoelasticity and excellent biocompatibility. However due to the high content of Ni atoms (around 50at%), much more attention has been focused on the surface modification of NiTi SMAs.

In our paper, W coating were deposited on the surface of NiTi alloys by Selective Laser Melting(SLM). The surface morphology, corrosion properties in Hank's solution and mechanical properties are investigated by SEM, XRD, atomic absorption spectroscopy, potentiodynamic anodic polarization and tensile tests. The results show that the solubility of W is very low and the excessive tungsten forms fine precipitates and W-rich compounds. The thickness of W coating increases with the increase of laser power, and the thickness is about 100-300 μm . W coating can prevent the release of Ni^{2+} from the alloy obviously and when the laser power is 300 W, the concentration of Ni^{2+} in Hank's solution decreases about 50% compared with that of the NiTi binary alloy. The corrosion potential increases slightly with the laser power increases and the i_{corr} of the NiTi alloy with W coating decreases two orders of magnitude compared with that of NiTi alloys. When the power is 300 W, the i_{corr} of the experimental alloy is only $2.13E^{-8}$. Therefore W coating can improve the corrosion properties of NiTi alloys.

Keywords: NiTi alloys, W coating, SLM, corrosion behavior

Surface modification of tools by application of tungsten compounds coatings in high-frequency discharge

Larisa Petrova, Vladimir Aleksandrov, Aleksey Perekrestov, Aleksandra Sergeeva
(MADI)

petrova_madi@mail.ru

Abstract: The paper presents the results of investigation of surface modification of tools made of high speed steels and of steels with low content of tungsten. The purpose of the study consists in examination of structure and properties of modified layers in tool steels after low-temperature gas nitriding with previously formed tungsten oxide coating.

Surface modification of tool steels was carried out by deposition of tungsten oxide coating in electrodeless high-frequency discharge with subsequent nitriding. The first stage of a process consisted in formation of tungsten trioxide powder layer at steel surface by sputtering of a tungsten electrode in an oxygen-containing atmosphere. At the second stage tungsten oxytetrachloride was formed by heating in chlorine-containing atmosphere. Nitriding of tools in mixtures of ammonia and acetone vapor was the final stage of the process. As a result of chemical reactions, coatings based on tungsten nitride are formed. For various steels, coatings' structure and hardness were experimentally studied; as well as the resistance tests were made. Examination of nitrided modified layers has shown that morphology and phase composition of layers, their thickness and microhardness depend on chemical composition of substrate steel. The highest resistance is observed for cutters made of HSS R6M5 steel with nitride coating. Comparative tests determined that cutters with strengthened removable blades made of X40CrMoV5-1 steel have the resistance 20%...30% higher than the resistance of no strengthened blades from HSS R6M5 steel. The processes of surface modification with forming of tungsten nitride coatings give the opportunity to strengthen cutting tools made of low-tungsten and of tungsten-free steels. Increase of resistance of such steels with coatings creates preconditions for HSS substitution in manufacturing of removable blades.

Keywords: tool steel, surface modification, nitriding, high-frequency discharge

Current advances in solid lubricant coatings

Zhmud Boris¹, Chao Xia²

(1. Applied Nano Surfaces; 2. Sweden)

boris.zhmud@appliednanosurfaces.com

Abstract: In recent years, significant progress has been made in the development of solid lubricant coatings. Nowadays, such coatings can be found in a wide range of automotive and industrial applications. Recent advances in the field include self-lubricating hard coatings and nanoparticle-fortified bonded coating systems offering improved performance and durability. Water-borne coatings are another hot topic due to growing environmental concerns. The present communication overviews recent developments in solid lubricant coatings, elaborate on lubrication mechanisms and discuss common application challenges. A special emphasis is made onto the tribology of thermoset polymer-bonded solid lubricant and polymer-free thermo-induced solid lubricant coating systems, and the use of nanoparticles as structural fortifiers therein.

Keywords: solid lubricant coating, nanoparticle

Microstructure and tribological properties of low-pressure plasmasprayed

Mo-Cu-WC coatings at elevated temperatures

Jiahu Ouyang, Zhanguo Liu, Yaming Wang, Yujin Wang
(Harbin Institute of Technology, School of Materials Science and Engineering)
ouyangjh@hit.edu.cn

Abstract: For automobile applications, molybdenum coatings are widely used in production of piston rings for internal combustion engines, which can withstand elevated temperatures and reduce friction. Plasma-sprayed coatings such as Mo alloys or cermets (Mo-MoO₂, MoCr₃C₂) coatings are studied to meet the demands of heavy-duty truck and marine diesel engines or other advanced low heat rejection engines instead of traditional hard chrome plating and TiN coating. In this paper, Mo-Cu-WC coatings were low-pressure plasmasprayed on AISI 304 steel for applications as next-generation ring-face coatings. The prealloyed composite powders consisted of fine agglomerated powders (2-4 μm in particle size) of Mo, Cu and WC. Spray parameters such as powder feed rate, primary gas pressure and spraying distance were optimized to produce less porous and strongly adherent coatings with a thickness of 0.2 mm. The composite coating exhibited a typical lamellar structure of Mo and Cu constituents, together with uniformly distributed fine WC particles. The wear tests were performed on a standard SRV friction and wear tester with reciprocating motion. The coatings were tested against a bearing-steel ball under boundary-lubricated conditions. The wear parameters under boundary-lubricated condition are 20 and 50 N load, 50 Hz frequency, 1 mm stroke, 1 h test duration and temperatures from 50 to 150 °C. The Mo-Cu-WC coatings exhibit low friction coefficients of 0.06 to 0.11 and small wear rates in the order of 10⁻⁶ mm³/Nm, depending on load and temperature. Increasing the test temperature reduces the coefficient of friction and, however, increases the wear rate of MoCu-WC coatings. The wear mechanisms of Mo-Cu-WC coating under boundary lubricated conditions were proposed to obtain a better understanding on the wear performance.

Keywords: Mo-Cu-WC coatings, tribological properties at elevated temperatures

Effect of different working layer on wear and cutting performance of

AlCrSiN coatings

Ying Gao¹, Wei Fang¹, Yi Zhao¹, Sidra Iram¹, Fei Cai¹, Shihong Zhang¹, Qimin Wang²
(1. AHUT; 2. GDUT)
tougaoyouxiang206@163.com

Abstract: In this paper, AlCrSiN coatings with different working layer were deposited on M42 high speed steel substrates by multi arc ion plating technology. Transmission electron microscope (TEM), Scanning electron microscopy (SEM) and X-ray diffractometer (XRD) were employed to examine the chemical composition, microstructure and surface morphology. Mechanical properties, friction and wear behavior and cutting performance of the coatings were also investigated. The results showed that the thickness of working layer increased from 0.8 μm to 2.5 μm. The phase structure of the coatings included fcc-CrN phase and fccAlN phase. Si₃N₄ phase could also be observed from the TEM results. The AlCrSiN coatings with 0.8 μm working layer had the minimum particles and droplets on the surface, the lowest surface roughness (Sa: about 1795.9 Å), the best adhesion strength between the substrates (Lc₂: about 35 N) and the maximum cutting life (14.04 m).

Keywords: AlCrSiN coatings, working layer, microstructure, friction and wear behavior, cutting performance

Fabrication and high temperature properties of plasma-sprayed nanostructured yttria stabilized zirconia thermal barrier coatings

Jiahu Ouyang, Zhanguo Liu, Hongzhi Liu, Yaming Wang, Yujin Wang
(Harbin Institute of Technology, School of Materials Science and Engineering)
ouyangjh@hit.edu.cn, wlhit@126.com

Abstract: In order to improve thermal efficiency and performance, Thermal barrier coatings (TBCs) are broadly used in hot-section components of advanced gas-turbines to meet severe requirements so that they can operate under extreme environments, such as elevated temperature, thermal stress, thermal shock and hot corrosion. In the present work, nanostructured yttria-stabilized zirconia feedstocks have been prepared by spray drying to produce a ceramic top coat. Thermal barrier coatings, composed of a NiCoCrAlYTb bond coat and a 8wt% Y_2O_3 - ZrO_2 nanostructured ceramic top coat, were deposited on a GH4099 super-alloy substrate by an atmospheric plasma spraying using Sulzer Metco plasma spraying unit with a 9 MB plasma gun. Crystal structure, morphologies, bond strength, thermalshock resistance and thermal emissivity of nanostructured coatings were investigated. The adhesive strength of ceramic coatings to the substrate was tested by a direct pull-off method, and reaches up to 58 ± 5 MPa. The thermal cycling numbers of nanostructured YSZ coatings are 102 cycles and 50 cycles, while it was heated to the desired surface temperature of 1000 and 1100 °C, respectively. During thermal cycling, the tetragonal-prime phase transforms to tetragonal and cubic phase at temperatures of both 1000 and 1200 °C. The thermal shock failure of nanostructured TBCs coatings mainly occurs at the interface between YSZ and bond coat. Normal spectral emissivity of nickel-based superalloy is about 0.2 over the whole wavelength range of 3-14 μm , however, the emissivity of nanostructured YSZ coatings is about 0.7 at short wavelengths and above 0.9 in the wavelength range of 7-14 μm .

Keywords: nanostructured thermal barrier coatings, thermal emissivity

Improved adhesion of TiAlSiN nanocomposite coatings on cemented carbide substrate by pre-implantation

Lei Wang, Lihue Li, Guodong Li, Quansheng Ma
(Beihang University)
Liliuhe@buaa.edu.cn

Abstract: The TiAlSiN coatings, by using a plasma immersion ion implantation & deposition (PIII&D) system, were deposited on YT15 cemented carbide substrate by reactive direct current magnetron sputtering (DCMS). The pre-implantation step and the coating deposition were carried out with the same experimental setup. In this article the effects of pre-implantation of several different elements (N, C, O) were investigated. The adhesion strength, hardness, micro-structure, element concentration, depth profile and the formation of coatings after PIII experiments were characterized by a wide variety of techniques such as Rockwell indentation, scratch test, nano-indentation measurement, X-ray diffraction, energy dispersive spectroscopy, Auger electron spectroscopy and X-ray photoelectron spectroscopy. The results showed that the adhesive strength of TiAlSiN coatings was significantly improved on the samples pre-implanted with N and O whereas slightly improved with preimplantation of C. Additionally, the microstructure and mechanical properties of the TiAlSiN coatings also altered through pre-implantation. The improved adhesion could be explained by the grain refinement and surface energy enhancement of substrate by preimplantation.

Keywords: pre-treatment, TiAlSiN, lasma immersion ion implantation & deposition (PIII&D), adhesive strength

Influence of Al₂O₃ addition in NaAlO₂ electrolyte on microstructure and high-temperature properties of plasma electrolytic oxidation ceramic coatings formed on Ti₂AlNb alloy

Zhaoying Ding¹, Yuanhong Wang¹, Jiahu Ouyang², Zhanguo Liu², Yaming Wang², Yujin Wang²
(1. Key Laboratory of Advanced Structural-Functional Integration Materials & Green;
2. School of Materials Science and Engineering, Harbin Institute of Technology)
ouyangjh@hit.edu.cn

Abstract: Plasma electrolytic oxidation (PEO) has become an effective surface modification method to form ceramic coatings on orthorhombic Ti₂AlNb alloy due to the characteristics of high productivity, economic efficiency and ecological friendliness. In the present work, different contents of Al₂O₃ additives were introduced into a NaAlO₂ basic electrolyte with the aim of improving the high-temperature properties of the as prepared PEO ceramic coatings on Ti₂AlNb alloy. The influence of Al₂O₃ addition in NaAlO₂ electrolyte on microstructure, adhesion and hardness, isothermal oxidation behavior and tribological properties of PEO coatings at elevated temperatures were investigated by means of X-ray diffraction, scanning electron microscopy, the pull-off method, micro-hardness tests, isothermal oxidation tests as well as ball-on-disc friction and wear tests. The introduction of Al₂O₃ into basic electrolyte promotes the formation of Al₂TiO₅ phase in the PEO coatings, and results in a large number of micropores at the interfaces between the coating and substrate. Isothermal oxidation tests at 800 °C up to 150 h showed that PEO coatings prepared with Al₂O₃ addition exhibit better oxidation resistance than those formed in the basic electrolyte. The PEO coating formed in the electrolyte with 4 g L⁻¹ Al₂O₃ additive exhibits the least mass gain of 1.33 mg cm⁻². The micro-hardness of the PEO coatings prepared with Al₂O₃ additive is improved due to the presence of Al₂TiO₅ phase, however, the adhesive strength of PEO coating is slightly weakened due to the formation of defects inside ceramic coating. The friction coefficient and wear rate of the PEO coating prepared with Al₂O₃ additive is comparable to those formed in the basic electrolyte at both room temperature and 600 °C.

Keywords: plasma electrolytic oxidation, Ti₂AlNb alloy, Al₂O₃ addition, oxidation resistance, tribological properties

Influence of thermo-hydrogen treatment on microstructure and superplastic properties of Ti6Al4V alloy

Hongzhi Liu
(Institute of Electronic Engineering, China Academy of Engineering Physics)
liuhongzhi-1983@163.com

Abstract: Ti6Al4V alloys with different hydrogen contents (0, 0.1, 0.2, 0.3, 0.4, 0.5wt%) were prepared by thermo-hydrogen treatment method. The microstructure and superplastic properties of these alloys were studied by the X-ray diffraction, optical microscopy, scanning electron microscopy, and high-temperature tensile measurements. All Ti6Al4V alloys consist of α phase and β phase, and the volume fraction of β phase in the alloys increases with the increase of hydrogen content. The hydrogenation of Ti6Al4V alloy results in a decrease in flow stress and an increase in elongation as compared with unhydrogenated alloy at 750 °C and an initial strain rate of 10⁻³ s. Ti6Al4V alloy with 0.4wt% hydrogen has the lowest flow stress value of 47 MPa, and the alloy with 0.1wt% hydrogen has the highest elongation value of 726%.

Keywords: Ti6Al4V, thermo-hydrogen treatment, microstructure, superplastic properties

Microstructure evolution and impedance analysis of 7YSZ thermal barrier coating during gas thermal-shock

Wenlong Chen¹, Min Liu², Jifu Zhang², Xiaoling Xiao¹, Weixue Tang¹

(1. Guangdong Industrial Analysis and Testing Center; 2. Guangdong Institute of New Materials)
15521377719@163.com

Abstract: Gas thermal-shock experiment of thermal barrier coating (TBCs) was carried out in air up to 1250 °C in order to simulate the thermal cycling process of the engine blades during the start heating and shut cooling. The growth of thermal growth oxide (TGO) layer and microstructure evolution of YSZ layer during thermal cycling process were investigated systematically by electrochemical impedance spectroscopy testing and SEM. The results show that the thickness of TGO layer increases when increasing the frequency of thermal cycling, and the impedance response of middle frequencies is more and more remarkable. Meanwhile, initiation and growth of micro-cracks occur in YSZ layer during the gas thermal-shock experiment. The corresponding impedance characterization of YSZ layer after 100 cycles is similar to the as-sprayed sample, meaning that micro-cracks in short time could heal since the YSZ micro-cracks sinter at high temperature. But after 300 cycles, the impedance spectroscopy of YSZ layer is quite different to the as-sprayed sample, with the corresponding impedance of particle-gap of YSZ more and more remarkable when prolonging the thermal-shock times, indicating that un-healing micro-cracks form in the YSZ layer, which may be the main reason to induce the failure of YSZ layer.

Keywords: thermal barrier coating, microstructure evolution, impedance analysis, gas thermal-shock

Plasma etching pretreatment effect on adhesion of carbon-based film

Zhendong Li¹, Ruijun Wang², Hua Zhan³

(1. Chinese Academy of Agricultural Mechanization Sciences;
2. Surface Engineering and Technology Institute; 3. Beijing Golden Wheel Special Machine Co., Ltd.)
zhanhua1101@163.com

Abstract: In order to improve the adhesion strength between the substrate and the film, the samples were treated by plasma etching pretreatment. Anode-layer ion source was used for treating the M50 steel samples with different ion source power and processing time. Also, tungsten doped DLC film was prepared on processed samples' surface. The morphology of samples' surface processed by plasma etching was studied by atomic force microscope. The Raman spectroscopy was used for analyzing the microstructure of the film. The adhesion strength between the film and the substrate was tested by the scratch tester. The results showed that different ion source power and plasma etching time could lead to different micro surface roughness of the substrate. The D peak and the G peak value of Tungsten doped DLC film were near 1350 cm⁻¹ and 1580 cm⁻¹, respectively. And it was the typical diamond like carbon structure. The value of ID/IG was about 1.5. The adhesion strength between film and the substrate without plasma etching pretreatment was 23 N, in contrast, the adhesion of the samples with pretreatment increased to 69 N, where the best ion source and etching time was 2 kW and 60 min, respectively. Plasma etching pretreatment can effectively improve the adhesion strength between the film and the substrate.

Keywords: plasma etching, anode-layer ion source, M50 steel, Tungsten doped DLC, ion source power

Stable electrochromic polyamide films containing flexible chains: preparation, electrochemical, fluorescence and memory properties

Rongrong Zheng¹, Xu Zhang¹, Zhipeng Zhang¹, Haijun Niu¹, Cheng Wang², Wen Wang³
(1. Heilongjiang University; 2. haijunniu@hotmail.com; 3. Harbin Institute of Technology)
haijunniu@hotmail.com, wangc_93@163.com

Abstract: A series of electroactive polyamides (PAs) containing alkyl chains and triarylamine unit serving as functional group. They were synthesized via polymer condensation reaction of N1-(2-Aminoethyl)-N1-(4-carbazol-9-yl-phenyl)-ethane-1,2-diamine, hydrobromide (3) with various cyclohexane binary acids. The structures of monomers and polymers were confirmed by fourier transform infrared (FT-IR), the nuclear magnetic resonance (NMR) techniques, and gas chromatography and mass spectrometry (GC-MS). All polymers were readily soluble in polar organic solvents and high thermal stability which could be solution cast into tough and flexible films. They exhibited well defined and reversible redox couples together with multielectrochromic behaviors. And they exhibited excellent fluorescence. PAs showed memory property.

Keywords: electrochromic, electrochemical, memory property, fluorescence, alkyl chains, triphenylamine

Controllable electrodeposition and mechanism research of nanostructured Bi₂Te₃ thin films with high thermoelectric properties

Xin Bo, Aiyue Tang, Meiling Dou, Zhilin Li, Feng Wang
(Beijing University of Chemical Technology)
lizl@mail.buct.edu.cn, wangf@mail.buct.edu.cn

Abstract: Nanostructured Bi₂Te₃ thin films were electrodeposited in the electrolyte of TeO₂ and Bi(NO₃)₃·5H₂O without any additive. CV, LSV and EDS tests proved that Bi³⁺ was reduced to Bi firstly, which induce the reduction of HTeO²⁺ to fulfill the co-position. The stoichiometric ratio of Bi₂Te₃ was controlled by adjustment of the depositing duration under suitable deposition potential. The EIS results illustrated that the rate of stable growth of the films was determined by the applied potential. The nucleation of Bi₂Te₃ was a progressive process, during which all the nuclei formed uniformly. The subsequent stable growth of the Bi₂Te₃ thin films was controlled by Nernst diffusion process at a suitable depositing rate. The uniform nucleation and growth caused the ideal (110) texture. The HER reaction and the over growth was avoided, so that the compact rice-like nanostructure could be obtained. The Bi₂Te₃ thin films were controlled to a state of stoichiometry composition, single phase structure, compact rice-like nanomorphology and (110) texture. Their electrical conductivity reached as high as 1.240×10⁵ s·m⁻¹, which caused the maximum PF of 5.234×10⁻⁴ W·m⁻¹·K². This facile synthetic approach is promising for the preparation of nanostructured Bi₂Te₃ thin films as the thermoelectric materials.

Keywords: thermoelectric thin film, Bi₂Te₃, electrodeposition, morphology, texture